CRWMS/M&O

Controlled Document Instructions

Complete only applicable items.

DATE
08/02/93

TO	COPY NO.	LOCATION
FRIDLEY SUSAN	102067.0	US NRC WASHINGTON

Description of Document(s)

TITLE	DOCUMENT IDENTIFIER	EFFECTIVE DATE	NO. OF SHEETS
B00000000-01717-2200-00010 Rev. 0 A COMPARATIVE APPLICATION OF THE REPOSITORY INTEGRATION PROGRAM (RIP) TO TOTAL SYSTEM PERFORMANCE ASSESSMENT - 1991		07/16/93	

Instructions/Remarks

ISSUANCE OF:

A COMPARATIVE APPLICATION OF THE REPOSITORY INTEGRATION PROGRAM (RIP) TO TOTAL SYSTEM PERFORMANCE ASSESSMENT - 1991

YOU ARE NOW ON "MANAGED" DISTRIBUTION FOR THIS DOCUMENT

*** New issue - no obsolete material ***

see enclosure on shelf.

102.8 WM-11 D
NH03/1

DUE BY: N/A

Receipt Acknowledgement

NAME	SIGNATURE	DATE

Contact the Document Center staff member named below with any questions regarding these instructions.

BY	LOCATION	PHONE
DCC LAS VEGAS	TES3/423	(702) 794-5312

rec'd with letter dtd 7/16/93

WBS: 1.2.5.4.1
QA: N/A

Civilian Radioactive Waste Management System
Management & Operating Contractor

A COMPARATIVE APPLICATION OF THE REPOSITORY INTEGRATION PROGRAM (RIP) TO TOTAL SYSTEM PERFORMANCE ASSESSMENT - 1991

Document No. B00000000-01717-2200-00010-00

July 16, 1993

Prepared for:

U.S. Department of Energy
Yucca Mountain Site Characterization Project Office
P.O. Box 98608
Las Vegas, Nevada 89193-8608

Prepared by:

INTERA Inc.
101 Convention Center Drive
Las Vegas, Nevada 89109

Under Contract Number
DE-AC01-91RW00134

1028

ACKNOWLEDGEMENT

The Total System Performance Assessment (TSPA) analyses generated using the Repository Integration Program (RIP) were conducted by the staff of the Civilian Radioactive Waste Management System (CRWMS), Management and Operating (M&O) Contractor, Performance Assessment group, including (in alphabetical order) Carl Bruch, Tim Dale, Jerry McNeish, and B.S. RamaRao under the direction of Robert Andrews. Additional analyses of unsaturated zone flow and transport using Total System Performance Assessment Code (TOSPAC) and TRACR3D were performed by Noreen Baker with support from Mark Reeves. Reviews of this document have been performed by Suresh Pahwa and Abe Van Luik.

The results presented in this document reflect a comparison of the RIP methodology for total system performance with that used by Sandia National Laboratories (SNL) and its contractors in TSPA-1991 (Barnard et al., 1992). Preliminary results were presented to SNL staff in January 1993. Helpful comments were received from Mike Wilson, Rally Barnard, Holly Dockery, Felton Bingham (all SNL) and Jack Gauthier (Spectra) during this meeting. Several upgrades to RIP have been generated over the past months by Golder Associates Inc. staff including Ian Miller, Rick Kossik, and Joe Hachey. In addition, the Golder staff has been helpful in identifying approaches to more efficiently utilize RIP.

The work presented in this document was funded under WBS 1.2.5.4.1--Total System Performance Assessment by the U.S. Department of Energy (DOE) Office of Civilian Radioactive Waste Management--Yucca Mountain Project Office under contract #DE-AC01-91RW00134. The DOE Branch Chief responsible for this work is Jeremy Boak. The M&O Office Manager responsible for this work is Jean Younker. The support of these individuals and organizations is gratefully acknowledged.

EXECUTIVE SUMMARY

During Fiscal Year (FY) 1991 and FY 1992, SNL and Battelle Pacific Northwest Laboratory were assigned the responsibility to generate initial TSPAs of the Yucca Mountain site. The analyses performed by these organizations (called TSPA-1991) are reported in Barnard et al. (1992) and Eslinger et al. (1993). During this same time period, Golder Associates Inc. was assigned the task of generating a model capable of analyzing the total system performance of a high-level radioactive waste repository. The developed model, called RIP, is documented in Kossik and Hachey (1993), Miller et al. (1993), and Golder Associates Inc. (1993).

In FY 1993, the CRWMS M&O Contractor was assigned the responsibility to plan, coordinate, and contribute to the second iteration of TSPA-2. Prior to initiating the next TSPA iteration, it was decided that it would be valuable to evaluate the applicability of RIP for use in this iteration. Therefore, analyses were conducted to compare the results generated by RIP to those reported in TSPA-1991. In particular, the aim was to generate a RIP input data set as equivalent as possible to that documented in Barnard et al. (1992) and to analyze the total system performance (as well as the performance of the individual subsystem components of the waste package/Engineered Barrier System (EBS), unsaturated gaseous flow and transport, unsaturated aqueous flow and transport, saturated flow and transport, and disruptive processes/events). The performance measure for comparison with the results of TSPA-1991 is the cumulative release of radionuclides to the accessible environment over a 10,000-year period following closure normalized to the U.S. Environmental Protection Agency (EPA) release limits specified in 40 CFR 191.

While the main goal of this study is to "test" the ability of RIP to be used for future total system performance assessment iterations, it has the added benefit of "testing" the results presented in TSPA-1991 (Barnard et al., 1992). The approach used to approximate the individual subsystem components in RIP is sufficiently different from that used in TSPA-1991 (in particular, for the waste package/EBS and unsaturated aqueous flow and transport), that exercising RIP produces an independent "verification" of the TSPA-1991 results given the same conceptualizations and input data assumptions are used.

We have based our abstraction on the TSPA-1991 document prepared by SNL staff and contractors (Barnard et al., 1992). We have chosen the representations presented in TSPA-1991 because they describe the broad spectrum of domains likely to be required in any assessment of total system performance. As a result of the abstracted nature of the TSPA-1991 conceptual models and parameters, developing an equivalent RIP data set proved to be relatively straightforward. Once an initial RIP data set was created from the conceptual descriptions and parameter values provided in the TSPA-1991 document, we "tested" each individual domain to determine our ability to reproduce the TSPA-1991 results. In some instances this was a direct comparison with conditional Complementary Cumulative Distribution Functions (CCDFs) or some other measure of domain performance. In other cases, we ran expected values from the parameter distributions and compared time releases (in Ci/yr) at particular boundaries of the system (for example, the host rock at the edge of the EBS). Following the "test" of each domain, we conducted additional sensitivity analyses on individual domains as well as the combination of domains. These sensitivity analyses consisted of one-at-a-time sampling from parameter

distributions and conceptual model variations to determine the impact on the results. In order to gain additional insights on system and domain behavior, we also created scatter plots of the sampled input parameter versus the dependent variable (generally, the cumulative release to some boundary).

The principal differences between TSPA-1991 and our implementation of the same data set using RIP are enumerated below:

- RIP input has to be simplified to mimic the treatment of radionuclide inventories and solubilities adopted in TSPA-1991. RIP allows complete chains to be specified and tracked and allows for partitioning between radionuclides which compete for solubility-limited releases.

- Diffusive releases in RIP are assumed to be steady-state.

- RIP can approximate fracture-matrix coupling by a Markovian process, which requires definition of a Markov transition rate. Such an approach does not reproduce dispersive mass transport.

- Future states are simulated directly in RIP. We have conducted conditional simulations for comparison to TSPA-1991 by using the importance sampling option in RIP.

The following items summarize the principal results of the comparison between RIP and TSPA-1991:

- RIP has been successfully used to approximate the relevant processes in TSPA-1991, including the waste package failure rate, waste form alteration, radionuclide release and radionuclide transport to the accessible environment.

- The TSPA-1991 results for release from the waste package are higher than RIP for solubility-limited radionuclides and lower for alteration-limited radionuclides.

- The TSPA-1991 CCDF for release from the EBS is slightly higher than calculated by RIP. This discrepancy may be due to slight differences in the waste package failure distribution and solubilities used in RIP and TSPA-1991.

- Slight differences in RIP and TSPA-1991 results for gaseous releases to the accessible environment are likely due to small differences in the waste package failure distribution and the time-stepping algorithm used in RIP to approximate the breakthrough curve.

- Differences between RIP and TSPA-1991 exist in the analysis of aqueous releases from the unsaturated zone when the Markovian multi-mode transport algorithm is used. For representative Markov transition rates (about 1/L, where L is the layer thickness), good agreement exists. When the matrix flow layers are treated as single-mode transport units in RIP, good agreement also exists.

- RIP reproduces the saturated zone radionuclide transport presented in TSPA-1991.
- RIP reproduces the volcanic and human intrusion scenarios presented in TSPA-1991.

Based on the experience gained in this study, we feel confident that the RIP approach is a viable method for use in future iterations of total system performance assessment. Its advantages (notably, flexibility in handling numerous types of functional relationships) far outweigh the simple representations required to make the model efficient for multiple realizations (in particular, the Markovian approximation of multi-mode transport and the temporal approximation of theoretical breakthrough curves). The flexibility of the RIP approach should be used to advantage in the next TSPA iteration (TSPA-II) to account for temperature dependencies on water contact mode, waste package failure, waste form alteration and dissolution, radionuclide mobilization (solubility), the percent of water in contact with the waste, and the gaseous and aqueous phase velocities. These dependencies should be derived from expert judgment or more detailed process-oriented modeling.

TABLE OF CONTENTS

Page

TABLE OF CONTENTS (Continued)

Page

LIST OF FIGURES

LIST OF FIGURES (Continued)

LIST OF FIGURES (Continued)

LIST OF FIGURES (Continued)

LIST OF FIGURES (Continued)

LIST OF FIGURES (Continued)

LIST OF FIGURES (Continued)

LIST OF FIGURES (Continued)

LIST OF FIGURES (Continued)

LIST OF FIGURES (Continued)

LIST OF FIGURES (Continued)

LIST OF TABLES

LIST OF TABLES (Continued)

LIST OF TABLES (Continued)

1. INTRODUCTION

Yucca Mountain, Nevada is currently being characterized to determine its suitability as a potential site for a mined geologic repository for the permanent disposal of high-level radioactive waste. An important component in the determination of the suitability of Yucca Mountain is the prediction of the ability of the geologic and engineered barriers to contain and isolate the radioactive wastes. Performance Assessments (PAs) are conducted to evaluate the ability of the site as well as the repository and waste package designs to meet regulatory criteria. The post-closure regulatory criteria include the cumulative radionuclide release from the total system specified by the U.S. Environmental Protection Agency (EPA) in 40 CFR Part 191[1], and the Nuclear Regulatory Commission (NRC) criteria for the geologic setting (10 CFR 60.113 (a)(2)), the Engineered Barrier System (EBS) (10 CFR 60.113 (a)(1)(ii)(B)), and the waste package (10 CFR 60.113 (a)(1)(ii)(A)). The total system performance assessment combines the effects of the waste package, other engineered barriers, and the site to determine the release of radionuclides to the accessible environment due to all significant processes and events.

Several Total System Performance Assessments (TSPAs) have been conducted to provide preliminary indications of the likelihood that the proposed Yucca Mountain site and designs proposed for this site will meet the EPA regulatory requirements. The NRC staff completed a Phase 1 Iterative Performance Assessment in 1990. Electrical Power Research Institute (EPRI) completed a Phase 1 Total System PA in 1990 and a Phase 2 evaluation in 1992. Pacific National Laboratories (PNL) completed an initial assessment in 1988 (Doctor et al., 1992). Recent assessments have been performed by Sandia National Laboratories (SNL) (Barnard et al., 1992) and PNL (Eslinger et al., 1993). The recent assessment by SNL is called Total System Performance Assessment -1991 (TSPA-1991). These analyses use different levels of detail to describe the processes that affect total system performance.

Beginning in Fiscal Year 1993, the Management and Operating Contractor (M&O) for the Civilian Radioactive Waste Management System (CRWMS) was given the responsibility to plan, coordinate, and manage the next iteration of total system performance assessment for the Yucca Mountain Project Office (YMPO) of the Office of Civilian Radioactive Waste Management (OCRWM). This responsibility includes defining the scope of activities required to enhance the analyses conducted to date. The M&O responsibility also includes conducting a portion of the total system PA to complement the analyses being performed by other participants (principally SNL).

---

[1]Section 801 of the Comprehensive National Energy Policy Act of 1992 specifies that the EPA Standards promulgated under 40 CFR Part 191 do not apply to Yucca Mountain. This Act directed EPA to have the National Academy of Sciences (NAS) conduct a study to determine the reasonableness of different types of standards (notably, individual dose) to protect human health. Based on the NAS recommendations, EPA is directed to promulgate a new standard for Yucca Mountain and NRC is to modify 10 CFR Part 60 to be consistent with the revised EPA standard. Although the EPA standard is no longer directly applicable to Yucca Mountain, it is still a useful measure of total system performance and can be used as a surrogate for the suitability of the geologic disposal system until such time as a new standard is promulgated.

Before initiating the second total system performance assessment iteration (TSPA-II), it is prudent to review the applicability/representativeness of the conceptual models and parameters used in the analyses to date and to independently compare the results from different TSPA models to determine whether different approaches can be used to generate analogous results. In the following chapters we present a comparison of the TSPA results generated with the Repository Integration Program (RIP) developed by Golder Associates Inc. with those previously generated by SNL in their TSPA-1991, using, to the extent practicable, the same data set as was used in TSPA-1991.

RIP is a performance-assessment and site-characterization strategy-evaluation software developed by Golder Associates Inc. under contract to OCRWM in 1991 and 1992. RIP is a very flexible tool that allows the user to describe the different compartments affecting release of radionuclides to the accessible environment. RIP was designed to be at the top of the performance assessment "pyramid" of analyses in that it describes the system and incorporates as many of the system interdependencies as the user chooses to specify, but it does not explain the behavior of the physical-chemical processes acting in the system. More detailed process models are required to develop the physical understanding, while RIP can be used to describe this understanding and its impact on total system performance.

1.1 OBJECTIVES

The objective of the comparison of the TSPA results generated using RIP with those reported by SNL in TSPA-1991 (Barnard et al., 1992) is to evaluate the ability to abstract the parameters and functional relationships required in RIP from the data set presented in TSPA-1991. A related objective is to test the reasonableness of the results presented in TSPA-1991 by determining whether an abstract representation of the relevant processes (as contained in RIP) can be used to reproduce the CCDFS presented by Barnard et al. (1992). In essence, we are simultaneously testing the utility of RIP to be used in subsequent iterations of TSPA as well as the ability of an independent analysis group to reproduce the results presented in TSPA-1991.

In addition to the above principal objectives, we have a goal to extend the analyses presented to date by (1) conducting additional uncertainty analyses on some parameters believed to be important to the prediction of cumulative radionuclide release, and (2) evaluating the sensitivity of TSPA performance measures to variability in selected parameters.

1.2 APPROACH

The approach taken in this study was first to generate an initial input data set for RIP based on an abstraction from the information presented in TSPA-1991.

We have chosen RIP for this assessment because it uses a "top-down" TSPA approach which allows the user to incorporate varying levels of detail to describe the processes which occur within the different domains of the geologic disposal system (the waste packages/EBS, the unsaturated zone, the saturated zone, and external events and processes such as magmatism, tectonism, and human intrusion). RIP directly calculates the CCDF for cumulative release by propagating the uncertainty in parameters and processes through the abstract representations of

the system behavior. RIP is designed in a very flexible manner which allows the user to incorporate as much or as little detail as desired.

We have based our abstraction on the TSPA-1991 document prepared by SNL staff and contractors (Barnard et al., 1992). This document presents descriptions and justifications of the processes, conceptual models, and parameter values used to generate total system cumulative releases. We have chosen the representations presented in TSPA-1991 because they describe the broad spectrum of domains likely to be required in any assessment of total system performance. The conceptual models and parameter values used to describe the system represent the culmination of years of effort by SNL staff and contractors, including earlier PA exercises such as COVE-2a and PACE-90 as well as the development of waste package/EBS models by Lawrence Livermore National Laboratory (LLNL).

The data set presented in TSPA-1991 is somewhat abstracted already. The detailed chemical-physical processes which occur within the waste package domain are approximated by simplified time periods (rewetting, container breach, waste alteration, release concentration build-up and fall-off). The unsaturated zone (UZ) aqueous flow and transport is represented by a one-dimensional composite porosity model. The UZ gaseous flow and transport is derived by a one-dimensional representation of the gas phase travel time distributions generated by Ross et al. (1992). The treatment of volcanic and human intrusion events is based on simple geometric arguments. As a result of the abstracted nature of the TSPA-1991 conceptual models and parameters, developing an equivalent RIP data set proved to be relatively straightforward.

Once an initial RIP data set was created from the conceptual descriptions and parameter values provided in the TSPA-1991 document, we "tested" each individual domain to determine our ability to reproduce the TSPA-1991 results. In some instances this was a direct comparison with conditional CCDFs or some other measure of domain performance. In other cases, we ran expected values from the parameter distributions and compared time releases (in Ci/yr) at particular boundaries of the system (for example, the host rock at the edge of the EBS).

Following the "test" of each domain, we conducted additional sensitivity analyses on individual domains as well as the combination of domains. These sensitivity analyses consisted of one-at-a-time sampling from parameter distributions and conceptual model variations to determine the impact on the results. In order to gain additional insights on system and domain behavior we also created scatter plots of the sampled input parameter versus the dependent variable (generally the cumulative release to some boundary).

1.3 GENERAL DESCRIPTION OF RIP

The RIP repository performance assessment and strategy model is a computational tool for conducting probabilistic integrated total system performance assessments for geologic repositories. It is not a model in the normal sense of the word in that it does not explain the behavior of the system or its components but it attempts to describe the behavior. The description of the system is left entirely for the user to define by the use of simple or complex algebraic functional relationships. In a sense, the RIP program is similar to a spreadsheet. While the current version contains a large amount of built-in logic and calculational capabilities, the problem solved is

entirely defined by the user. The theory and capability of RIP are described in Miller et al., (1993). A user's guide for RIP has been published by Kossik and Hachey (1993).

The overall structure of RIP consists of a front-end, a back-end, and a post-processor. The front-end is where the parameter values and functional relationships are defined and sampled using a Monte Carlo-type sampling algorithm. The back-end is where the actual computation occurs. The back-end is run for each sampled realization created in the front end. The post-processor is used to display the results (whether as time histories or CCDFs) and conduct simple sensitivity analyses (one-and two-dimensional scatter plots and simple parameter correlations).

The computation part of RIP used in this report is divided into three primary domains: the waste package/EBS radionuclide release model, the near and far field radionuclide transport model, and the disruptive events model. These models are briefly described below.

1.3.1 Waste Package/EBS Radionuclide Release Model

The waste package/EBS component of RIP can be used to describe several processes which, if they occur, could lead to radionuclide releases to the geosphere. These include container failure, exposure of rapid release and bound radionuclides, and the mass transfer of radionuclides from the waste package to the host rock. Each of these processes may be dependent on the environmental parameters in the near field; in particular the temperature, geochemistry, and hydrology.

RIP allows the user to define multiple modes of container failure. These failure modes may be temperature or time dependent or dependent on the water contact mode adjacent to the waste package. The primary (container) and secondary (cladding or pour canister) containers may fail either sequentially or simultaneously.

Once the containers (primary and secondary) fail, the radionuclide inventory is exposed. RIP allows three inventories, a free inventory which is released instantaneously once the primary container fails, a gap inventory which is released instantaneously once the secondary container fails, and a matrix (i.e., bound) inventory which is released as the matrix is altered and dissolved. The exposure of bound radionuclides in the fuel or glass matrix is a function of the dissolution rate, the surface area exposed and the percent of surface area in contact with water.

Once radionuclides have been dissolved, they may be transferred to the host rock by advective transport, diffusive transport or a combination of advective-diffusive transport. Advective releases apply to all gaseous radionuclides. Aqueous-phase advective releases are a function of the radionuclide concentration in contact with the waste (which may or may not be solubility limited) and the flux past each waste package. Diffusive releases are a function of the radionuclide concentration, the effective diffusion coefficient and a geometric factor which embodies the effective cross-sectional area of the container surface through which diffusive releases may occur and the length of the diffusive path. Only steady-state diffusive releases can be handled in RIP. The release from the waste package is not dependent on the ability of the geosphere to transport the radionuclides.

1.3.2 Far Field Flow and Radionuclide Transport Model

RIP allows for a simplified description of radionuclide transport through the geosphere. The geosphere may be "discretized" into multiple pathways that are combined either in parallel or in series. These pathways may represent different flow regimes (aqueous vs gaseous), different flow domains (saturated or unsaturated zone), or different cross-sections of the repository. In addition, different flow modes may be applied to each pathway. A single-flow mode may be used to represent an equivalent porous media, while a multiple mode pathway may be used to describe fracture-matrix coupling in a dual porosity-dual permeability media. For single mode pathways, RIP uses an analytical solution to the one-dimensional advection-dispersion equation. For multiple mode pathways, RIP uses a modified Markovian process algorithm to predict the transition between the two modes. The details of the flow and transport solution schemes are described in Miller et al. (1993).

1.3.3 Disruptive Events Model

RIP assumes all disruptive events can be simulated as a Poisson process. The user simply defines the annual probability of the event occurring (as well as a description of the effects of the event on the other domains if it occurs), and RIP randomly determines if that event occurs during a particular time step of any given realization.

Once the event occurs, the effects may be either direct or indirect. Direct effects may include moving a certain percentage of the inventory (determined by geometric consideration such as interception ratios) either directly to the accessible environment (i.e., the surface) or to another pathway (i.e., the saturated zone). Indirect effects may include modifying the behavior and characteristics of the waste package or radionuclide transport pathways.

RIP allows for a particular sampling algorithm (called importance sampling) to increase the possibility of sampling infrequent events in a particular simulation. When importance sampling is used, all other realizations are weighted to account for the actual probability of occurrence.

1.4 EPA SUM

The remanded EPA standard (EPA, 1985) specifies probabilities that cumulative releases of radionuclides to the accessible environment shall not exceed certain levels within 10,000 years. The EPA sum is the sum of the ratios of the cumulative release of a radionuclide and the EPA-prescribed limit for that radionuclide, as given below:

$$M = \sum_i \frac{Q_i}{L_i} \qquad (1\text{-}1)$$

where M is the normalized cumulative release (the EPA sum), Q_i is the cumulative radioactivity of the *i*th radionuclide released to the accessible environment within 10,000 years, and L_i is the EPA limit for the *i*th radionuclide. The quotient Q_i/L_i is known as the EPA ratio for radionuclide i.

The EPA sum relates only to releases to the accessible environment. Accordingly, releases from EBS and unsaturated zones are not EPA sums.

1.5 PRESENTATION OF STOCHASTIC OUTPUT

The methodology used in this study to address the parameter uncertainty involves sampling parameter values from their probability distributions. Corresponding to one realization of such input parameters, obtained by sampling, the system is simulated and a measure of system performance is derived. For example, an important system performance measure in this study is the EPA sum, which is the normalized release to the accessible environment, explained in Section 1.4.

If a thousand Monte Carlo simulations of the system are performed, corresponding to a thousand realizations of the input vector, there would be one thousand results for the desired system performance, such as the EPA sum.

There are three alternative (and equivalent) options available to display such stochastic results. They are: (1) the Probability Density Function (PDF); (2) the Cumulative Distribution Function (CDF); and (3) the Complementary Cumulative Distribution Function (CCDF). The relationship between the three alternative forms of display is explained here.

The probability density function corresponds to a "histogram" for continuous variables. Figure 1-1a shows a PDF. The area under the PDF gives the probability. For example, the probability that a variable lies between X_1 and X_2 is given by the area under the PDF between X_1 and X_2 (Figure 1-1a). The total area under the PDF equals unity, denoting the certainty that the variable must lie between its lowest and highest limits.

If one defines the probability that the variable x is less than X, i.e. $P(x \leq X)$, it is evidently given by

$$F(X) = P(x \leq X) = \int_0^X p(x)dx \qquad (1\text{-}2)$$

(Negative values for x are not feasible here.) F(x) is called the CDF. Since total area under the PDF is unity, F(x) varies between zero and one. Figure 1-1b presents an example CDF, and shows that the probability that x (e.g., EPA sum) is less than or equal to a stated value X_1, is F_1.

The most popular form of presenting the stochastic results in the performance assessment context is by a CCDF, $F^*(x)$, defined simply by $F^*(x) = 1 - F(x)$. It denotes the probability that a variable x is greater than a stated value X, and may be called the probability of exceedance. Figure 1-1c presents an example CCDF and shows that the probability of x exceeding X_1 is given by F_1^* $(= 1 - F_1)$.

The complementary cumulative distribution function is chosen in this report as the most desirable form of displaying the output.

1.6 TYPES OF INPUT PARAMETER DISTRIBUTIONS

The stochastic input parameters are defined by their assumed probability density function. Some of the parameters are defined by normal, uniform, and log-uniform distributions. However, most of the stochastic input parameters in this study are defined by beta distributions. As the beta distribution is not as commonly known as the other distributions, the expression for this distribution is given below.

$$p(x) = c(x - a)^{\alpha} (b - x)^{\beta} \qquad (1\text{-}3)$$

where $p(x)$ = probability density
c = normalizing constant
x = value of the random variable (input parameter)
a = min [x]
b = max [x]
α,β = exponents

The exponents α, β in Equation (1-3) can be calculated based on the mean, standard deviation, and the minimum and maximum values of the distribution.

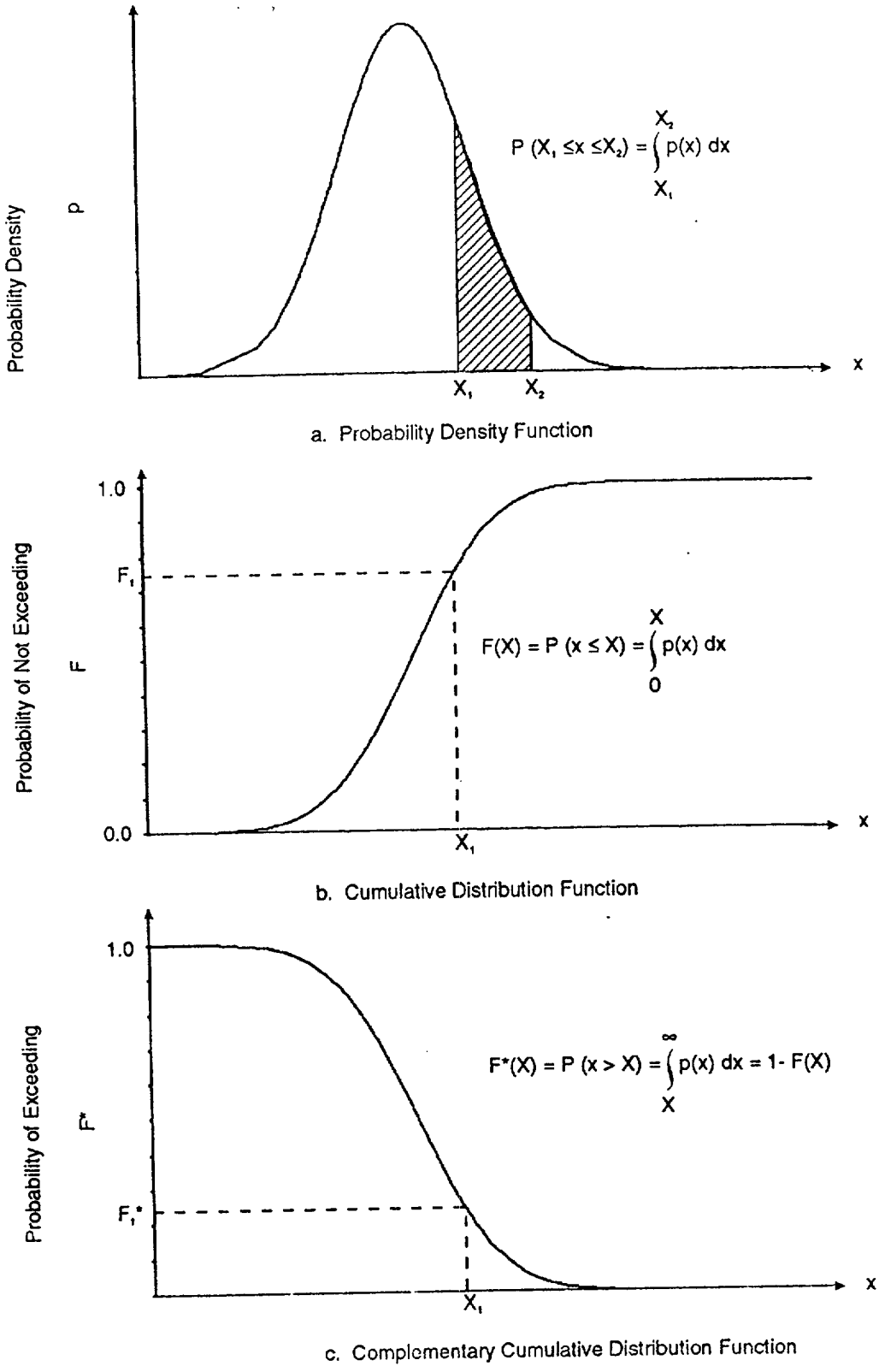

Figure 1-1. Presentation of Stochastic Input and Output

2. WASTE PACKAGE

The source term for all subsequent analyses of radionuclide release to the accessible environment is derived from the waste package/engineered barrier system. Thus, the accuracy of the total release to the accessible environment and any dose calculations are initially dependent on the appropriateness of the conceptualization of the waste package/engineered barrier system (WP/EBS).

The following discussion of the WP/EBS includes:

- Description of the TSPA-1991 conceptual model and parameter distribution
- Description of the RIP conceptual model and parameter distribution
- Comparison of CCDF results from TSPA-1991 and RIP
- Comparison of individual radionuclide release from TSPA-1991 and RIP
- Sensitivity of the radionuclide release to various WP features.

2.1 TSPA-1991 APPROACH TO WASTE PACKAGE

As noted, TSPA-1991 included a simplified waste package release model which assumed the reference container and repository layout as defined in the Yucca Mountain Site Characterization Plan (SCP) (DOE, 1988) and the Site Characterization Plan Conceptual Design Report (MacDougall et al., 1987). A schematic of the TSPA-1991 waste package (Barnard et al., 1992) is presented in Figure 2-1. The individual waste containers were assumed to be vertically emplaced with a 3 cm air gap separating the containers from the host rock. (MacDougall et al. (1987) used a 3.8 cm air gap). The effect of the cladding on the exposure of the fuel matrix was not considered in this conceptualization.

The radionuclide inventory used for the source term was dependent on the analyses conducted. For aqueous release analyses, 9 radionuclides were included; for volcanic events and human intrusion 39 radionuclides were included; and for gaseous release only ^{14}C was included. The volcanic events and human intrusion analyses simulate direct release to the surface, so all significant radionuclides are included. On the other hand, the aqueous release contains additional considerations such as velocity, retardation, and release rate. Some radionuclides are very insoluble and highly retarded, and thus provide a negligible contribution to total release. These are disregarded in the analyses. A summary of the radionuclides included in aqueous and gaseous release analyses is presented in Table 2-1.

For the aqueous release analyses, significant ingrowth of radionuclides was calculated up-front and included in the initial inventory of parent radionuclides. In particular, the initial inventories for ^{234}U and ^{237}Np were increased to account for their parents (notably ^{238}Pu, ^{241}Pu, and ^{241}Am) which were not simulated.

The 33,300 containers in the waste inventory were divided into two major categories based on data in the SCP (DOE, 1988): 60 percent pressurized-water-reactor (PWR) spent fuel and 40 percent boiling-water-reactor (BWR) spent fuel. TSPA-1991 assumed 2.1 metric tons of heavy metal per container, based on Apted et al. (1990). The only distinction between the two groups

was the assumed burnup value which was 33,000 megawatt-days per metric ton of heavy metal (MWd/MTHM) for PWR, and 27,500 MWd/MTHM for BWR. These values are used to calculate the "EPA ratio," the ratio of a radionuclide's release (radionuclide-specific cumulative release limit of 40 CFR Part 191 (EPA, 1985) (see Section 3.5.1, below)). A total repository of 70,000 MTHM of waste was assumed.

The processes included in the TSPA-1991 waste package/engineered barrier system included container wetting after the thermal dryout period, container failure, radionuclide mobilization, and radionuclide transport out of the container.

Rewetting: Rewetting means the re-occurrence of liquid-phase water into the host rock after the thermal period. It does not mean that saturated conditions are expected or will occur. There are two parts to the TSPA-1991 repository rewetting: (1) the actual time of wetting the waste packages being contacted by liquid water after the thermal pulse, and (2) the procedure to determine how many waste packages are contacted by liquid water. The system was assumed to be dry initially due to heat released from the waste. No thermal calculations were included. No waste was released during this time period. Container wetting was assumed to occur gradually, starting 300 years after emplacement and reaching equilibrium, with all packages "rewet," 1000 years later.

TSPA-1991 divided the waste packages into four categories depending on the water saturation of the waste packages. The saturation was directly related to the release mode of radionuclides from the containers. Four different modes of release were included: (1) advective only, (2) diffusive only, (3) advective and diffusive, and (4) none. Advective releases were assumed to occur if a waste package was in a locally wet (seepage area) part of the repository. A simple flow-through model was assumed in calculating the advective releases. Diffusive releases were assumed to occur if the air gap was partially filled with rubble. The height of the rubble in the air gap was assumed to be the same as the height of the water in the container, thus simplifying the estimate of the fraction of the spent fuel in a given container that contributes to diffusive releases. Advective and diffusive releases occurred when the containers were in locally wet areas and had rubble in the air gap. A fraction of the waste packages potentially were in dry areas with an intact air gap, and no release occurred from these packages.

The relative number of waste packages in each category was determined in the following manner. The fraction of containers in seepage areas is denoted by f_s and the fraction of containers with rubble filling at least part of the air gap is denoted f_r. The f_s fraction covers those containers experiencing advective releases, and the f_r fraction covers those containers with a failed air gap. The f_r fraction was a user supplied value. In TSPA-1991, half of the containers were assumed to be in the f_r fraction. The fraction of containers in the f_s fraction was calculated from the following equation:

$$f_s = P[q > q_0] = 0.5 \cdot \mathrm{erfc}\left(\frac{\ln q_o - u}{\sqrt{2}\,\sigma}\right) \qquad (2\text{-}1)$$

where: erfc = complementary error function (see Appendix A)
u = mean of the spatial flux distribution in log space
σ = standard deviation of the spatial flux distribution in log space
q = percolation rate
q_0 = flux carried by porous matrix (assumed equal to the saturated matrix hydraulic conductivity of the Topopah Springs (K_0), a tuff unit of Yucca Mountain that is the potential repository host rock).

The average flux for those containers subjected to seepage flow is given by:

$$q' = q \cdot f_s^{-1} \cdot 0.5 \cdot \text{erfc}\left(\frac{\ln q_0 - u - \sigma^2}{\sqrt{2}\,\sigma}\right) \qquad (2\text{-}2)$$

It is assumed that q_0 of that flux is carried by the porous matrix, so that the average flux available for seepage flow is given by:

$$q_s = q' - q_0 \qquad (2\text{-}3)$$

Figures 2-2 through 2-5 illustrate histograms of q, K_0, f_s, and q_s, respectively, generated with @RISK. It can be seen that f_s has a large number of values close to 0.0 (corresponding to no advective releases) and 1.0 (corresponding to advective releases). It bears noting that if f_s=0.5, then 25 percent of the waste packages would be in each of the four water contact and release modes.

Container Failure: The container failure distribution used in TSPA-1991 was based on the rewetting period and a time to failure given the repository is rewet with an assumed log-uniform distribution from 500 to 10,000 years. For a particular realization, a time was sampled from the distribution, and all containers were failed by the sampled time. If failures could not occur until 500 years after the container was wet, the initial releases should not occur until at least 800 years. However, a review of the individual radionuclide release curves (Barnard et al., 1992, Figure 4-47) shows that releases occurred starting at 300 years. (NOTE: There is some uncertainty regarding the interpretation of failure distributions used in TSPA-1991. We have used three different assumptions that are described in Section 2.3.1 below).

Radionuclide Mobilization: Before the radionuclides can be transported from the repository, the container must fail and the waste must be altered and mobilized. Alteration refers to chemical alteration (oxidation) of the UO_2 fuel matrix which frees the radionuclide for possible dissolution. The waste inventory was divided into alteration-limited (high solubility) and solubility-limited radionuclides. In TSPA-1991, 2 percent of the high-solubility radionuclide inventory (^{135}Cs, ^{129}I, ^{79}Se, and ^{99}Tc) was available for quick release once the container failed. This prompt inventory fraction is at the upper end of the values suggested, and the SCP goal is to achieve less than 0.02 (DOE, 1988). The matrix alteration rate (a_m), prompt alteration rate (a_p), and fraction of the

waste-form surface area wetted (f_{ws}) are included in the calculation of waste mobilized for advective releases. These are all input parameters in TSPA-1991 analyses. The matrix alteration is assumed to proceed at a certain rate, but only part of the waste is contacted by water and is releasing its waste to the water. The TSPA-1991 matrix alteration rate upper bound was based on laboratory experiments of spent fuel leaching (Apted et al., 1990). The lower bound was arbitrarily selected as 20 times lower to reflect the uncertainty in the parameter (Barnard et al., 1992). The prompt alteration rate was simply a small number to spread the release over 2 years, but is insignificant relative to the other time scales in the analyses (Barnard et al., 1992). The fraction of the waste form surface area wetted was simply set to the middle of the possible range (Barnard et al., 1992). For diffusive releases, f_{wd} is the fraction of the waste-form surface area wetted and participating in diffusive releases. This parameter was also set to the middle of the possible range (Barnard et al., 1992).

Radionuclide Transport: After the radionuclides have been mobilized, they are available for transport out of the waste containers. The TSPA-1991 calculation of advective release is different than that of diffusive release. Also, the treatment of transport of alteration-limited radionuclides is different from that of solubility-limited radionuclides.

For the advective-release model, TSPA-1991 assumed that water flows into the container at the top, and exits at the bottom. The time scale for this process is given by the volume of water in the container divided by the rate at which water flows through the container. The volume of water inside the waste container is given by:

$$V_1 = A \cdot d_{film} \cdot f_{ws} \tag{2-4}$$

where A = total surface area of the spent fuel rods in a container, d_{film} = thickness of the water film on the wetted part of the spent-fuel surface, and f_{ws} is the fraction of the waste-form surface area wetted.

The volume rate at which water flows through the container is given by:

$$V_2 = A_c \cdot f_{in} \cdot q_s \tag{2-5}$$

where A_c = the area around a waste container where water flux is gathered and funneled into the container (the "effective catchment area"), f_{in} = fraction of the flux through A_{cross} that actually gets into the waste package, and q_s is the average seepage flux in the vicinity of containers that have seepage flux.

For advective solubility-limited releases, the rate at which radionuclides are released is given by the rate of flow through the container multiplied by the maximum solubility of the radionuclide.

For diffusive releases across the rubble, two values of the diffusion coefficient were used, one for a wet container environment, and one for a moist container environment. Also, the diffusion time scales differ because the radionuclides have different retardation values. Combination advective-diffusive transport is handled differently for alteration-limited and solubility-limited cases. For alteration-limited radionuclide mobilization, the advective and wet-diffusive time scales are combined. The fastest process will dominate the mobilization. For solubility-limited

radionuclide mobilization, the advective and wet-diffusive releases are calculated separately, then added together.

TSPA-1991 results used for comparison purposes with RIP waste package results are presented in Figures 2-6 and 2-7. The CCDF of release from the WP/EBS is shown in Figure 2-6. Note that Figure 2-6 applies the EPA standard at the EBS/host-rock interface rather than at the accessible environment boundary as specified in the EPA's 40 CFR Part 191. This was done for ease of computation and for illustrative purposes only. Individual radionuclide release curves are presented in Figure 2-7 in terms of the ratios of their calculated release rates to the allowable release rates specified in the NRC's 10 CFR Part 60.

2.2 RIP APPROACH TO WASTE PACKAGE/ENGINEERED BARRIER SYSTEM

The RIP software is capable of simulating the primary concepts included in the TSPA-1991 waste package analyses. The following discussion divides the waste package concepts into five categories: container data, inventory, exposure of radionuclides to liquid water, transport of radionuclides, and air gap. Where appropriate, direct comparison of TSPA-1991 data with the RIP conceptualization are included in tables. Figure 2-8 shows a schematic of the processes which may be included in RIP waste package modeling.

Container Data: The container data used in RIP are directly comparable to the TSPA-1991. Table 2-2 details the comparison. Note that the RIP case of 2.1 MTHM/container only results in 69,930 MTHM in the repository, slightly less than the TSPA-1991 value of 70,000 MTHM.

Inventory: The waste inventory defined in TSPA-1991 can also be implemented within RIP, after units conversion. Table 2-3 shows the TSPA-1991 inventory for aqueous release analyses and the comparable RIP inventory. The RIP inventory was input as Ci/container, converted from Ci/MTHM as 2.1 MTHM/container. Prompt release fractions were included in the RIP data set as gap inventory, essentially free inventory within the secondary container. This is discussed in more detail in the "Exposure of Inventory" section. TSPA-1991 prompt alteration rate (calculated to take 2 years) is not included as such in RIP. RIP includes such release as rapid, or instantaneous release once the container fails. The TSPA-1991 prompt release time period is so small relative to the 10,000 year analysis period that it is insignificant.

Solubilities for the RIP data set were converted from TSPA-1991 moles/liter to g/m^3 according to the following formula:

$$\left(\frac{\text{mole}}{\text{liters}}\right) \cdot \left(\frac{\text{g}}{\text{mole}}\right) \cdot \left(\frac{1{,}000 \text{ liters}}{\text{m}^3}\right) = \frac{\text{g}}{\text{m}^3} \text{ of radionuclide} \qquad (2\text{-}6)$$

TSPA-1991 did not specify the solubilities for the alteration-limited radionuclides, essentially setting them to infinity (Wilson, 1993). In RIP, the solubilities for these radionuclides were set to values large enough to allow alteration rather than solubility to control the release rate.

Mobilization of Inventory: There are two aspects to mobilization of the radionuclides prior to transport. The inventory must be altered and the containers must fail. Table 2-4 lists the WP failure parameters. The TSPA-1991 rewetting time parameter values are based on thermal modeling of the spatial array of waste packages (Johnson and Montan, 1990). The 9,500-year range for container lifetime distribution was chosen for TSPA-1991 to reflect the significant uncertainty in container performance (Barnard et al., 1992). Table 2-5 lists the various parameters important to mobilization of the radionuclides. The TSPA-1991 fractions for containers with rubble in the air gap, fuel wet with seepage, and fuel wet and diffusing, were simply set to the middle of the possible range (Barnard et al., 1992). The source of TSPA-1991 matrix alteration rate and prompt alteration rate was discussed in Section 2.1. The TSPA-1991 value for spent fuel surface area per package was taken from design data tabulated in the SCP (DOE, 1988). The water film thickness on a spent fuel surface under unsaturated conditions is unknown, but will probably depend on surface roughness, capillarity, and water surface tension (Barnard et al., 1992). Many of the TSPA-1991 parameters are shown graphically on Figure 2-1.

The TSPA-1991 waste package failure distribution is described in Section 2.1. RIP simulation of WP failure requires the use of both container failures (primary and secondary) to adequately represent the TSPA-1991 WP failure. Resaturation was simulated by a uniform primary container failure of 800 - 1800 years. Once a package was contacted by liquid-phase water, the simulation of WP failure was initiated.

WP failure was simulated using the secondary container failure feature of RIP. To mimic the TSPA-1991 log-uniform distribution, the distribution used initially was a Weibull distribution. (*Note:* Initially, RIP did not allow for a log-uniform failure distribution. This was modified in subsequent versions of the software.) Other WP failure distributions are included in Table 2-4.

Within TSPA-1991, the fraction of seepage entering the container is combined with the water collection area. In RIP, these parameters are combined into an effective catchment area. The effective catchment area is only activated for the two water contact modes that have advective release (modes 1 and 2).

Many of the parameters in Table 2-5 help define the number of waste packages in each water contact mode. Within TSPA-1991, diffusive releases occur only in containers that have rubble in the air gap. Advective releases occur in containers that have fuel wet with seepage. Some containers have both diffusive and advective releases when fuel is wet and diffusing. The dry containers have no release.

RIP used the same four water contact modes defined in TSPA-1991, although with a different nomenclature. The advective-only release mode is called *wet-drip* in RIP. The advective and diffusive release mode is called *wet-feet* in RIP. The diffusive-only release mode is called *moist-continuous* in RIP. The no release mode is called *nominal* in RIP. Wet-drip and wet-feet occur when the fraction of containers in seepage areas (f_s) is equal to 1. Moist-continuous and nominal releases occur when f_s=0.0. When f_s=0.5, then 25 percent of the waste packages will be in each of the four water contact modes. It bears noting that for advective releases, only advective parameters are required (such as effective catchment area, seepage flux, and fraction of waste wet); for diffusive releases, only diffusive parameters are required (such as diffusion coefficient, geometric factor for diffusion, and the fraction of waste wet); while for the combined advective-

diffusive release both sets of parameters are required. It also bears noting that the diffusion coefficients for moist-continuous release is less than that for wet-feet releases due to the differences in tortuosity and effective area available for release when the media is partially saturated (see Conca, 1990).

Transport Parameters: The transport of exposed radionuclides is dependent on numerous parameters. Transport may be divided into advective and diffusive transport. Diffusive transport is further subdivided into moist and wet diffusion. Within RIP, the different diffusion coefficients are implemented by simulating release from each of the water contact modes differently. For water contact modes 1 and 2, the wet diffusion coefficient is used. For water contact mode 3, the moist diffusion coefficient is used. For water contact mode 4, no diffusive release is allowed. These parameters are detailed in Table 2-6. The TSPA-1991 diffusion coefficients are based on modifying the typical diffusion coefficient in water (3.0×10^{-2} m^2/yr) (Travis et al., 1984) to account for tortuosity and constrictivity effects. Also, under wet conditions the diffusion coefficient might be as high as it is in water (Barnard et al., 1992), but under moist conditions the effective diffusion coefficient is reduced by several orders of magnitude (Conca, 1990). The TSPA-1991 distribution of "wet" diffusion coefficients is a small range about the far-field value of 3.16×10^{-3} m^2/yr; the "moist" diffusion coefficient distribution is broader and its maximum is below the minimum wet values (Barnard et al., 1992).

The TSPA-1991 percolation rate distribution is based on distributions used in prior performance assessment analyses (PACE-90; SCP; Sinnock et al., 1984) and an exponential distribution was chosen to weight the range toward the low end of the distribution.

The TSPA-1991 effective diffusion area is equal to the waste container surface area reduced by the product of the effective porosity and the saturation of the rubble (Barnard et al., 1992).

The TSPA-1991 water collection area is subjective, based on expected drainage area for a single container. The fraction of seepage through the water collection area was set at the midpoint of the possible range (Barnard et al., 1992).

The TSPA-1991 rubble thickness is assumed to be 3 cm, based on Apted et al. (1990) and Ueng and O'Connell (1992).

Diffusive Release: RIP models diffusive releases through the waste package as a steady state process, with the transfer rate equal to the product of the effective diffusion coefficient, the concentration of the radionuclide in contact with the waste matrix, and a geometric factor. Several formulations of the geometric factor for diffusive mass transfer (w) exist. Assuming a spherical waste form of radius R, Chambre et al. (1985) define the geometric factor as

$$w = 4 \cdot \pi \cdot R \cdot n \cdot f \qquad (2\text{-}7)$$

where n = effective porosity of the degraded package, and f = percent of the waste in contact with a diffusive pathway. Assuming R = 0.9 m, n = 0.2 and f = 0.5, yields a geometric factor for diffusive mass transfer of about 1.0.

Air Gap: The TSPA-1991 air gap is implemented in RIP as a pathway, with an assigned transport velocity that is based on the arrival time for the 50 percent mass breakthrough given a diffusive release. The pathway is only accessed for releases from waste packages in water contact mode 3. The velocity is calculated as:

$$vel = D_{eff}/L \tag{2-8}$$

where D_{eff} = the effective diffusion coefficient and L = path length.

Additional Capabilities: RIP has additional capabilities not demonstrated in TSPA-1991 which increase the ability to simulate process complexity. These additional capabilities are primarily in the source term, decay, and effective solubility of radionuclides.

Source Term: RIP has three potential fractions of the source term (Free, Gap, and Bound) versus only two for TSPA-1991 (Prompt and Bound). This allows RIP to directly incorporate the effects of the cladding failure rate if the primary and secondary container failure modes are modeled as the sequential failure of the container and cladding. This was not done in this exercise.

Decay: RIP handles decay of radionuclides as the decay occurs. On the other hand, TSPA-1991 pre-calculated decay and then introduced the decay components into the source term. The RIP implementation produces a release inventory consistent with analytical calculations of decay products from the initial repository radionuclide inventory.

Effective Solubility: Another issue where RIP is more complex than TSPA-1991 involves the concept of effective solubilities. TSPA-1991 pre-calculates the impact of isotopes on solubility and partitions the solubility for particular isotopes. RIP calculates the effective solubility as additional isotopes are created due to radioactive decay. For example, in RIP the concept causes a decrease in the ^{234}U release relative to the TSPA-1991 ^{234}U release values, due to competing solubilities with other Uranium isotopes (e.g., ^{235}U). Figure 2-9 shows the result of including the effective uranium solubility in the calculation of release for ^{234}U. The ^{234}U plot in TSPA-1991 which does not include effective solubility reaches a plateau, while the RIP simulation shows that ^{234}U peaks and then declines as other uranium isotopes are produced due to radioactive decay and begin competing with the ^{234}U for solubility (Figure 2-10). Similar effects are seen for other radionuclides which have more than one isotope in the inventory.

2.3 RESULTS OF WASTE PACKAGE/ENGINEERED BARRIER SYSTEM ANALYSES

The RIP analyses of the waste package release involved incorporating increasing complexity into the conceptual model to obtain a waste package similar to the conceptual model of the waste package in TSPA-1991. The modifications dealt with:

- Waste package failure distribution
- Radionuclide inventory
- Solubility of radionuclides
- Infiltration-dependent water contact distribution
- Air gap around waste packages.

Table 2-7 indicates the primary differences between the RIP simulations. The initial case, RUN 2.1, was developed to simulate conditions contained within the TSPA-1991 waste package. The container failure distribution was a Weibull distribution, for gradual container failure beginning 500 years after container wetting and continuing for 9500 years. The inventory included the nine TSPA-1991 radionuclides along with their most significant decay products. The inventory for the daughter products was 0 Ci/container. However, within RIP, when radionuclides are present in the initial radionuclide list table, the possibility exists for ingrowth of the radionuclide. The solubility for alteration-limited radionuclides was initially taken to be the same distribution as in Golder Associates Inc. (1993) because the TSPA-1991 did not list actual solubilities for these radionuclides. The waste packages were divided evenly into 4 water contact modes, as identified in Section 2.2. Finally, the initial case did not include a diffusion gap for the 3 cm air gap simulated in TSPA-1991.

2.3.1 Sensitivity of CCDF to Waste Package Failure

The RIP initial waste package was set up to simulate failure of the waste packages with a Weibull distribution intended to mimic a log-uniform waste package failure distribution of 9,500 years. The Weibull distribution and the log-uniform distribution are shown in Figures 2-11 and 2-12. The Weibull distribution has more containers failing at early times than the log-uniform distribution. The CCDF for 1000 realizations using these two distributions demonstrates as expected that the Weibull failure distribution causes greater release than the log-uniform distribution. A CCDF of the WP case with the Weibull failure distribution is presented in Figure 2-13. A recent upgrade to RIP allowed use of a log-uniform distribution for WP failure. Figure 2-14 presents the CCDF for this case. Comparison of the 1.0, 0.1, 0.01, and 0.001 probability values on the CCDF show that the case with the log-uniform distribution consistently has lower release than the case with the Weibull distribution. These and other CCDF figures in this section should be compared to Figure 2-6, the TSPA-1991 composite porosity release from the EBS.

2.3.2 Sensitivity of CCDF to Inventory

As noted previously, the TSPA-1991 inventory for aqueous release included only nine radionuclides, and these radionuclides decayed but the decay products were not tracked. The initial RIP waste package (which included decay) was set up for 16 radionuclides (Table 2-1) which included the most significant daughter products from the nine TSPA-1991 radionuclides. The results of the initial case simulation with 16 radionuclides are included in Figures 2-13 and 2-14. Later RIP simulations reduced the inventory to nine radionuclides, not allowing any production of daughter products, but still calculating decay. This caused a significant decrease (a factor of 2) in the simulated release from the waste packages. The CCDF results for the reduced number of radionuclides are presented in Figure 2-15. The results are consistently lower than the case with 16 radionuclides primarily because daughter product production (especially ^{210}Pb and ^{226}Ra) does not occur in the case with nine radionuclides.

2.3.3 Sensitivity of CCDF to Waste Alteration

Solubility of Radionuclides: One parameter not specified in TSPA-1991 (Barnard et al., 1992) is the solubility of alteration-limited radionuclides such as ^{99}Tc. Wilson (1993) indicated the

solubilities were effectively infinite (>1000 kg/m^3). Solubility values were varied in RIP to find the value above which no additional release occurs. RIP solubilities for the alteration-limited radionuclides were then specified as greater than these values in the simulations presented in Figure 2-16. ^{99}Tc and ^{135}Cs were the only radionuclides given the high solubility values. The results indicate a slightly larger total release when essentially infinite solubilities are used for ^{99}Tc and ^{135}Cs.

2.3.4 Sensitivity of CCDF to Waste Package Release

Failure Time per Realization: TSPA-1991 waste package failures occurred according to the distribution described in Section 2.1. All previously presented RIP simulations failed the waste packages gradually through time for the duration of the 9500-year failure period. Figure 2-17 presents the results of simulations which implemented the TSPA-1991 failure characterization. This caused an increase in the release from the waste packages as shown on the CCDF, primarily because the waste package failures occurred earlier in time and were completed earlier than for the previous distribution (which had failure of all packages at 10,300 years).

Implementation of Relationship between Infiltration and Saturated Matrix Hydraulic Conductivity: Thus far, the number of waste packages in each water contact mode was equal to one quarter (25 percent) of the total number of waste packages. As noted in Section 2.1, TSPA-1991 used a functional relationship between infiltration and the saturated matrix hydraulic conductivity of the Topopah Springs to determine the number of waste packages in each of the water contact modes. In this waste package simulation, the f_s implementation described in Section 2.1 was simulated. Figure 2-18 shows the CCDF for this conceptualization. Comparison with the TSPA-1991 CCDF (Figure 2-6) shows that the RIP release is less than the TSPA-1991 release.

Air Gap: An additional factor in TSPA-1991 was the implementation of a 3-cm air gap at the edge of the waste packages. Within RIP, this was simulated as a 3-cm pathway that was only activated if releases were from the moist continuous waste packages and the diffusion coefficient value was the same as the moist diffusion coefficient. The dispersivity, a parameter required for a pathway in RIP, was arbitrarily selected as 1 m. Additional details are found in Appendix A. The results of adding the air gap to these simulations, which provide a waste package conceptual model very similar to the TSPA-1991 waste package are presented in Figure 2-19. Compared to Figure 2-18, the results are only slightly reduced. The air gap has the effect of delaying the release of the diffused radionuclides, leading to lower overall release.

Implementation of Average Flux Available for Seepage Flow: A final factor which TSPA-1991 included was an evaluation of whether or not the infiltration rate would cause fracture flow. In the cases where the flux is greater than the saturated matrix hydraulic conductivity of the Topopah Springs, fracture flow is assumed to be initiated. Only when fracture flow exists is there any possibility for waste packages to experience *wet-feet* or *wet-drip* water contact modes and the corresponding advective releases from the EBS. This q_s evaluation was included in RIP for the final waste package analysis to more precisely mimic the TSPA-1991 conceptualization. Results are shown in Figure 2-20. In general, as with the addition of the air gap to the conceptual model, the results show slightly lower releases than the previous simulations.

Additional CCDFs showing the results for individual radionuclide release are provided in Figures 2-21 through 2-25. These CCDFs present results for ^{99}Tc, ^{129}I, ^{239}Pu, ^{79}Se, and ^{234}U, respectively. Note the high ^{239}Pu release. It is to be noted again that all these CCDFs for WP/EBS releases are not calculations of the EPA standard's performance measure at the accessible environment boundary. These calculations apply that performance measure to the EBS-rock interface for illustrative purposes only.

2.3.5 Comparison of Individual Radionuclide Release from TSPA-1991 and RIP

The individual radionuclide release curves for the expected values of TSPA-1991 are presented in NRC-normalized form in Figure 2-7. The non-normalized results are presented in Figure 2-26. The peak values for TSPA-1991 and some of the RIP simulations are presented in Table-2-8. As noted in Section 2.1, the treatment of alteration-limited radionuclide release was different from solubility-limited release in TSPA-1991. In RIP, the radionuclides are treated identically, except that the solubility limit for a particular radionuclide will affect whether that nuclide has solubility-limited or alteration-limited release.

The TSPA-1991 peak values for the solubility-limited radionuclides are generally slightly higher than those from the RIP simulations. The expected value from the given TSPA-1991 solubility distribution is slightly lower when implemented in RIP for ^{243}Am, ^{237}Np, and ^{234}U. This difference, while slight, would cause a difference in the release for these radionuclides.

TSPA-1991 used partitioning of isotope solubility limits rather than calculate solubility limits as they changed through time. The partitioning factors at 10,000 years were used to adjust the solubility limits since they are higher than the ones at early time. RIP simulations used the same solubilities as TSPA-1991 over all times.

The TSPA-1991 peak values for the alteration-limited radionuclides are generally lower than those from the RIP simulations. The RIP results for the RUN 2.4 case alteration-limited radionuclides are very close to the TSPA-1991 values. Note the RUN 2.4 WP failure distribution produces less release at early time than the failure distribution in RUN 2.5 and RUN 2.8 because the WP failures in RUN 2.4 are spread out over 9,500 years after rewetting, while the WP failures in RUNs 2.5 and 2.8 are spread out from the time of rewetting to a value sampled from the log-uniform distribution of 0-9,500 years (mean of 3,170 years).

The description of TSPA-1991 individual radionuclide release indicates that rewetting starts at 300 years, continues uniformly for 1000 years, and no release occurs until at least 500 years after a container is wet (at least 800 years from waste emplacement). However, Wilson (1993) clarified that while the rewetting period was as we expected, the failure distribution was as follows. A maximum time of failure was sampled from a log-uniform distribution from 500 to 10,000 years. The expected value of this distribution is 3,170 years. The failure then was assumed to be uniform from 0 years after rewetting to the maximum failure time.

An additional RIP simulation was conducted to evaluate the impact of using 300 years as the start time for release. These CCDF results are presented in Figure 2-27. The release is slightly higher than Figure 2-20, the CCDF results for the RIP data set that resembles TSPA-1991 most closely. The individual radionuclide release curves are presented for a few of the radionuclides

(^{99}Tc and ^{239}Pu) in Figures 2-28 and 2-29. As expected, the release start time matches TSPA-1991 and the time of peak arrival occurs earlier than in Figure 2-20 and closer to the TSPA-1991 peak arrival.

2.3.6 Scatter Plots for Selected Parameters from CCDF Analyses

Limited sensitivity analyses were conducted to evaluate the importance of selected parameters on the release of certain radionuclides. These scatter plots were developed based on RUN 2.8. The effect of the dissolution value on ^{99}Tc release (1,000 realizations) is presented in Figure 2-30. Increasing the dissolution has a direct effect on the total ^{99}Tc release. The ^{239}Pu release as a function of the effective catchment area and geometric diffusion factor (100 realizations each) are shown in Figures 2-31 and 2-32. The release of ^{239}Pu is not directly affected by the effective catchment area value, while an increase in the geometric diffusion factor increases the total ^{239}Pu release. Finally, the effect of the diffusion coefficient on ^{135}Cs release (100 realizations) is presented in Figure 2-33. There is no apparent correlation between the increase in diffusion coefficient and ^{135}Cs release.

2.4 PARAMETER SENSITIVITY ANALYSIS

The release from the different waste packages is dependent on many variables. In an attempt to determine the sensitivity of the release to these parameters, we started with a base case with all the parameters set constant, usually to their expected values. The base case was a product of the comparison with TSPA-1991 discussed earlier. Multiple-realization runs were made with RIP varying one parameter at a time. This way, we were able to observe the effect of the various parameters without the stronger effects obscuring the more subtle effects.

Subsequently, simulations were made varying many parameters simultaneously. These combined runs allowed us to determine the relative importance of the different parameters to the release of radionuclides.

The release of radionuclides that we analyze falls into two categories: low-solubility (solubility-limited) and high-solubility (alteration-limited). The radionuclides ^{243}Am, ^{237}Np, ^{239}Pu, ^{126}Sn, and ^{234}U are in the former category, while ^{135}Cs, ^{129}I, ^{79}Se, and ^{99}Tc are in the latter category. The elements within each group have similar sensitivities, and for simplicity we present the results for ^{99}Tc and ^{239}Pu as being representative of high- and low-solubility radionuclides, respectively. Where there is variation within a category of radionuclides and it is not appropriate to consider a single "representative" radionuclide, the range of behaviors is discussed.

Four water contact modes were considered: wet-feet, moist-continuous, wet-drip, and nominal. The inventory was assumed to be divided equally among the four modes, but post-processing allowed us to independently analyze the waste packages in the different water contact modes. As there is no water contact for the nominal mode, no release occurs for these waste packages. Thus, none of the parameters of interest will affect the release of radionuclides from these containers, and we will not further discuss the nominal case.

2.4.1 Sensitivity of Waste Package to Waste Alteration Parameters

We first considered waste alteration parameters, including the matrix dissolution rate, the fraction of waste wetted, and the solubility of the radionuclides. The results for high- and low-solubility radionuclides are shown in Tables 2-9 and 2-10, respectively. These tables contain the parameter description, the range of the parameter analyzed, the expected value of the parameter, the sensitivity exhibited by the parameter (e.g., none, linear, or log-like), and the water contact modes responsible for the sensitivity. When the sensitivity was linear, the slope was represented by m, the standard convention (y=mx+b). In some cases, the sensitivity curve consisted of linear segments, each of different slope. For these cases, the slopes were designated by m_1 , m_2 , ... , from left to right for the respective segments. For simplicity, the water contact modes are abbreviated WF, WD, and MC for wet-feet, wet-drip, and moist-continuous, respectively.

It is seen that the high-solubility radionuclides are dependent on all the waste alteration parameters analyzed, exhibiting log-like behavior for the matrix dissolution rate (R_{dis}) and the fraction of waste wetted (f_w) (Figures 2-34 and 2-35) and linear behavior for the solubility. For all three cases, the wet-feet, wet-drip, and moist-continuous water contact modes are sensitive to changes in the waste alteration parameters.

The sensitivity curve for the solubility of ^{99}Tc is qualitatively different from the sensitivity curves discussed above (see Figures 2-36 and 2-37). For extremely low solubilities, the release increases linearly with great slope as the solubility increases. For a technetium solubility (S_{Tc}) of approximately 100, the slope of the sensitivity curve changes and the release then increases slowly, but linearly, as the solubility increases. Finally, at S_{Tc} approximately 9,000, there is another change in the slope of the sensitivity curve, and the release is constant with further increases in solubility. This behavior is simply explained. For a particular water contact mode, a low solubility means that the release is solubility-limited. As the solubility increases, the release increases until a critical solubility is reached. At this point, the release becomes alteration-limited and no increase in solubility can increase the release. The wet-feet and wet-drip water contact modes have approximately the same critical solubilities, while the moist-continuous mode has a significantly higher solubility. The sensitivity curve is a superposition of all the modes. In the first region, the releases from the wet-feet, wet-drip, and moist-continuous modes are increasing. In the second region, the releases from the wet-feet and wet-drip modes have plateaued, but the release from the moist-continuous mode is still increasing. In the third region, the release from the moist-continuous mode has plateaued, and the total release is constant.

Generally, the low-solubility radionuclides are not sensitive to the matrix dissolution rate or the fraction of waste wetted. For instance, only ^{126}Sn exhibits any sensitivity to changes in the matrix dissolution rate (Figure 2-38). In this case, the release rises linearly until it becomes constant. However, the increase is slight and considered insignificant. For the fraction of waste wetted, the releases of ^{234}U and ^{126}Sn rise linearly and become constant early in the sensitivity curve. This behavior is not very significant because of the low value at which the release becomes alteration-limited, and the magnitude of the overall increases (0.1% and 0.7% for ^{234}U and ^{126}Sn, respectively). Changes in solubility linearly affect the release of low-solubility radionuclides, as may be expected from our experience with the high-solubility radionuclides (at low solubilities, the release increases linearly).

2.4.2 Sensitivity of Waste Package to Release Parameters

The release parameters examined with sensitivity analyses are the repository infiltration rate, the volume of water contacting the matrix, the moist-continuous and wet-feet diffusion coefficients, the geometric factor for diffusion, and the effective catchment area. The results for the high- and low-solubility radionuclides are shown in Tables 2-11 and 2-12, respectively. As for Tables 2-9 and 2-10, these tables include the parameter description, the range over which the parameter was sampled, the expected value of the parameter, any sensitivities exhibited during the variation, and the water contact modes that were the cause for the sensitivities. In one case, the sensitivity was the "left-most point." This is in essence a linear rise followed by a constant region. However, because only the realization with the lowest parameter value (the left-most point on the curve) had a lower value for the release than the rest of the realizations that all had the same value, it was not possible to obtain a slope for the region of linear increase. For these cases, high-solubility radionuclides other than ^{99}Tc had different sensitivity curves. Some were always rising linearly, some increased linearly before they became constant, and some were always constant.

For both the geometric factor for diffusion (w) and the effective catchment area (A_c), the expected value is zero. This is because these variables are dependent on the water contact mode. For the former, w is zero for the wet-drip water contact mode, and it is non-zero for the moist-continuous and wet-feet water contact modes. For the latter, A_c is zero for the moist-continuous water contact mode, and it is non-zero for the wet-feet and wet-drip water contact modes. For the high-solubility radionuclides, the moist-continuous waste packages are sensitive to changes in w and the wet-drip waste packages are sensitive to changes in A_c.

The high-solubility radionuclides exhibited little or no sensitivity to the release parameters. The general pattern, exhibited by all but the wet-feet diffusion coefficient and the water volume contacting the matrix, was that of linear increase until the release was constant with further parameter increase (e.g., Figure 2-39). The point at which the transition occurs depends on the parameter and on the radionuclide. For a given parameter, there is usually a range of transition points corresponding to the different radionuclides. As an example, consider the repository infiltration rate (q_{inf}): ^{135}Cs has the transition point at 0.0002, so that there are enough points left of the transition that the linear behavior is apparent. ^{99}Tc has a lower transition point, so that there are fewer points showing on the plot. ^{129}I and ^{79}Se have the transition even lower, so that the only points plotted are above the transition--only the plateau is shown. The regions where the releases are sensitive to variations in q_{inf} are significantly less than the expected value of q_{inf}. Thus, near the expected values, the release of high-solubility radionuclides is insensitive to changes in the release parameters.

Whereas all the other sensitivity curves increase monotonically (or are constant), the dependence exhibited by the volume of water contacting the matrix is that of monotonic decrease. For high-solubility radionuclides ^{79}Se and ^{99}Tc, the curves are constantly decreasing. The shape of these curves indicates that the release is inversely related to the volume: release $\propto V^{-1}$ (Figure 2-40). For ^{135}Cs, the sensitivity curve was constant for volumes less than 0.11, and decreasing for greater volumes in a different manner than the other two high-solubility radionuclides discussed above (Figure 2-41). The behavior is due to the waste packages in the wet-feet, wet-drip, and moist-continuous water contact mode. The decrease is due to a change of the effective

concentration C(n) of the radionuclide in the water in contact with the matrix (Golder Associates Inc., 1993, p. 62). This concentration is defined as:

$$C(n) = \min\left[\frac{M_p(n)}{V}, C_s(n)\right] \qquad (2\text{-}9)$$

where $M_p(n)$ is the average amount of exposed mass of radionuclide n in a failed waste package; V is the volume of water contacting the matrix; and $C_s(n)$ is the saturation concentration of radionuclide n. For small volumes of water contacting the matrix, the effective concentration is the saturation concentration. For sufficiently large volumes of water, the effective concentration is not controlled by solubility considerations ("i.e., the solubility is high and the concentration is determined by how much mass has been exposed and the volume of water into which it has dissolved" (Golder Associates Inc., 1993, p. 63).

The low-solubility radionuclides exhibited linear, non-trivial dependence on all the release parameters (Table 2-12) except the water volume contacting the matrix. These sensitivity curves were straight-forward and did not introduce any new insights. The sensitivity curves of the water volume contacting the matrix were, with one exception, expected. For ^{239}Pu and ^{237}Np, the release is insensitive to changes in the volume. For sufficiently large values of the water volume, the releases of ^{234}U and ^{243}Am decreased as the volume increased. This behavior is explained in the same fashion as in the discussion relating to Equation 2-9. The only irregularity was the sensitivity curve for ^{126}Sn: it has much more structure than any of the other sensitivity curves for the water volume contacting the matrix (Figure 2-42). This structure is exhibited by the wet-feet, wet-drip, and moist-continuous water contact modes. At this time, we do not have an explanation for the behavior of this sensitivity curve.

As we mentioned above, some simulations were made with multiple parameter variations. The coefficients of the correlation matrix were generated and analyzed. A negative correlation coefficient implies that as the parameter increases, the release decreases; a zero correlation coefficient means that there is no correlation between the release and a particular parameter; and a positive correlation coefficient means that as the parameter increases, the release increases. The larger the magnitude of the coefficient, the greater the correlation between a parameter and the release. Thus, when many parameters are varied, the parameters with the largest correlation coefficients have the most influence on the release of the radionuclides.

In the first multiple-parameter RIP RUN (RUN 2.9) we varied the moist-continuous diffusion coefficient ($D_{eff,mc}$), the matrix dissolution rate (R_{dis}), the fraction of waste wetted (f_w), and the solubility of technetium (S_{Tc}). The correlation coefficients for the 1000-realization run are shown in Table 2-13. Based on our discussion above, we conclude that for low-solubility radionuclides,

$$D_{eff,mc} >> R_{dis}\ ,\ f_w >> S_{Tc}\ .$$

By this, we mean that the effects from varying the moist-continuous diffusion coefficient ($D_{eff,mc}$) overwhelm any effects seen by varying R_{dis} or f_w , which in turn overwhelm any effects seen by varying S_{Tc} . Comparing with Tables 2-10 and 2-12, we see that this behavior

is consistent with our earlier results. Using the same nomenclature for high-solubility radionuclides,

$$R_{dis} > f_w > D_{eff,mc} ,$$

and for ^{99}Tc, in particular,

$$R_{dis} > f_w > S_{Tc} > D_{eff,mc} .$$

In the second multiple-parameter RIP RUN (RUN 2.10), we varied the moist-continuous diffusion coefficient ($D_{eff,mc}$), the wet-feet diffusion coefficient ($D_{eff,wf}$), the effective catchment area (A_c), the geometric factor for diffusion (w), the repository infiltration rate (q_{inf}), and the solubility of plutonium (S_{Pu}). The correlation coefficients for this 1,000-realization run are shown in Table 2-14. For the low-solubility radionuclides, the sensitivities are

$$w > D_{eff,wf} > A_c > q_{inf} >> D_{eff,mc} ,$$

and for ^{239}Pu, in particular,

$$S_{Pu} > w > D_{eff,wf} > A_c > q_{inf} >> D_{eff,mc} .$$

The high-solubility radionuclides do not exhibit as uniform behavior. ^{129}I and ^{79}Se have near-zero coefficients for all parameters in this run. ^{135}Cs has the following sensitivity:

$$D_{eff,mc} , w > q_{inf} > A_c >> S_{Pu} , D_{eff,wf} .$$

^{99}Tc has similar behavior:

$$D_{eff,mc} , w > q_{inf} > A_c , S_{Pu} , D_{eff,wf} .$$

We may combine the relations above to obtain series of relations which describe the relative importance of the different parameters for release of ^{239}Pu and ^{99}Tc. For ^{239}Pu,

$$S_{Pu} > w > D_{eff,wf} > A_c > q_{inf} >> D_{eff,mc} >> R_{dis} , f_w$$

For ^{99}Tc,

$$R_{dis} > f_w > S_{Tc} > D_{eff,mc} , w > q_{inf} > A_c , D_{eff,wf} .$$

From these two relations, it can be easily discerned which are the important parameters and which parameters are relatively unimportant for the release of ^{239}Pu and ^{99}Tc.

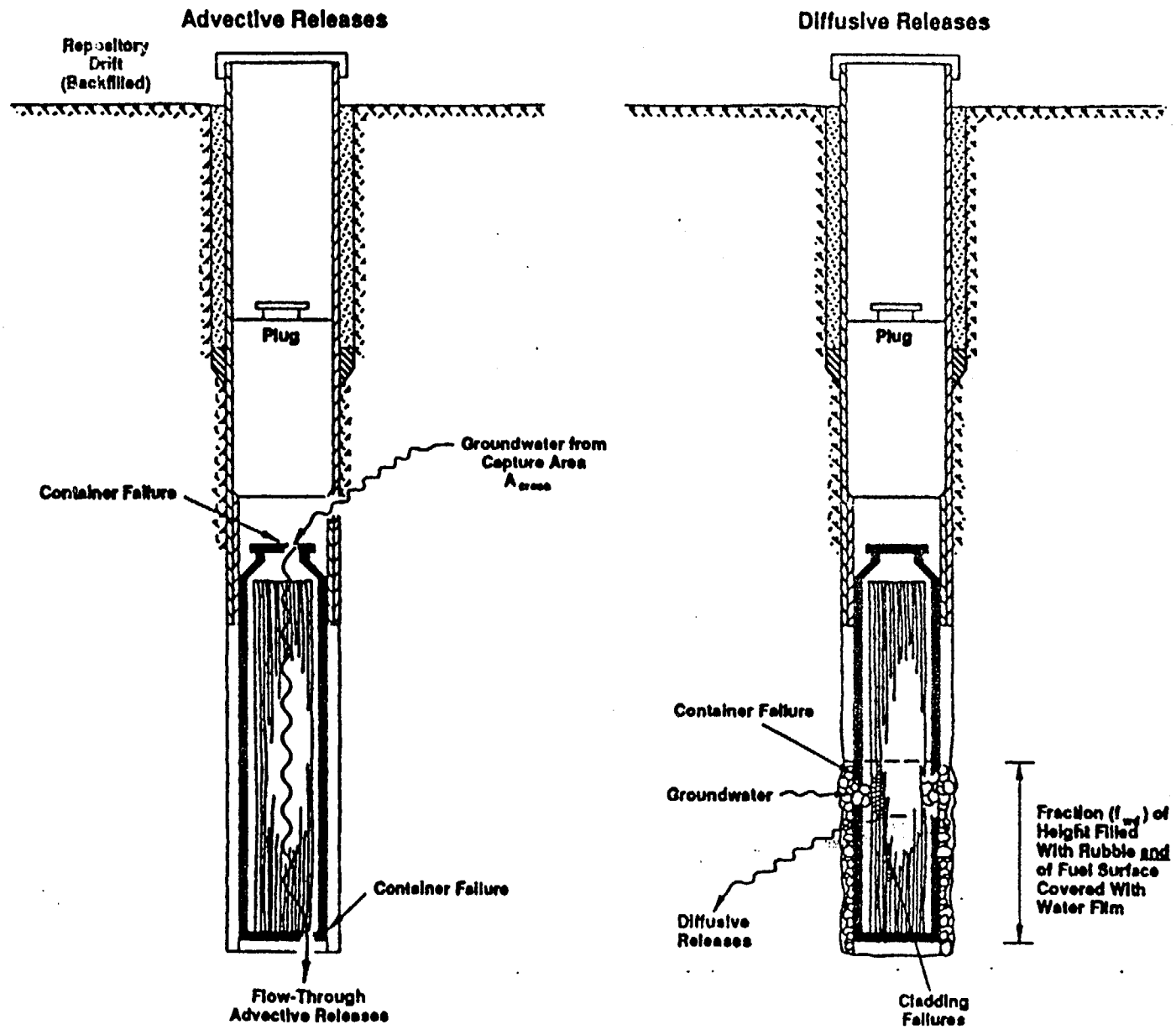

Figure 2-1. TSPA-1991 Waste Package Schematic (taken from Golder Associates, Inc., 1993)

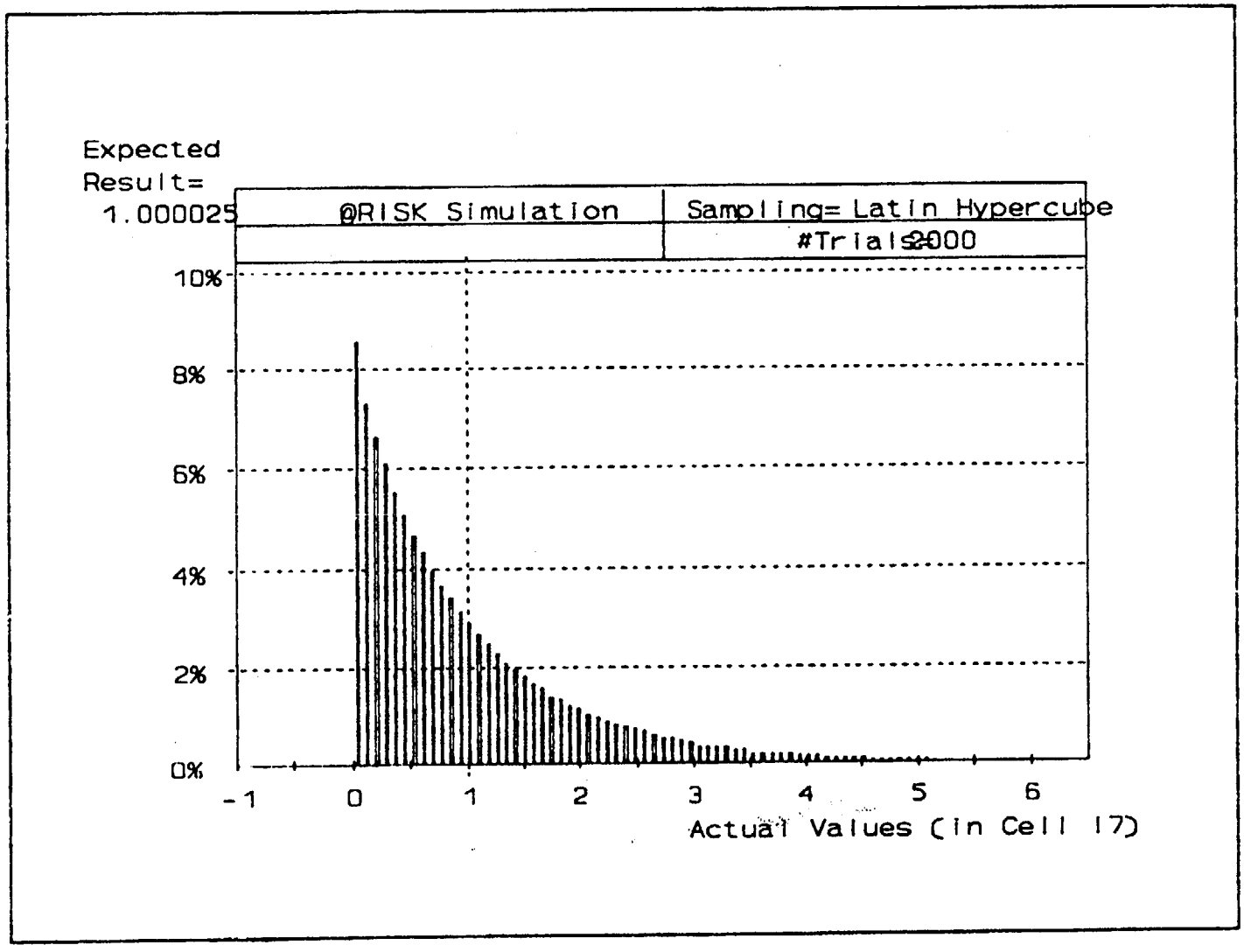

Figure 2-2. Histogram of Applied Infiltration Flux (q)

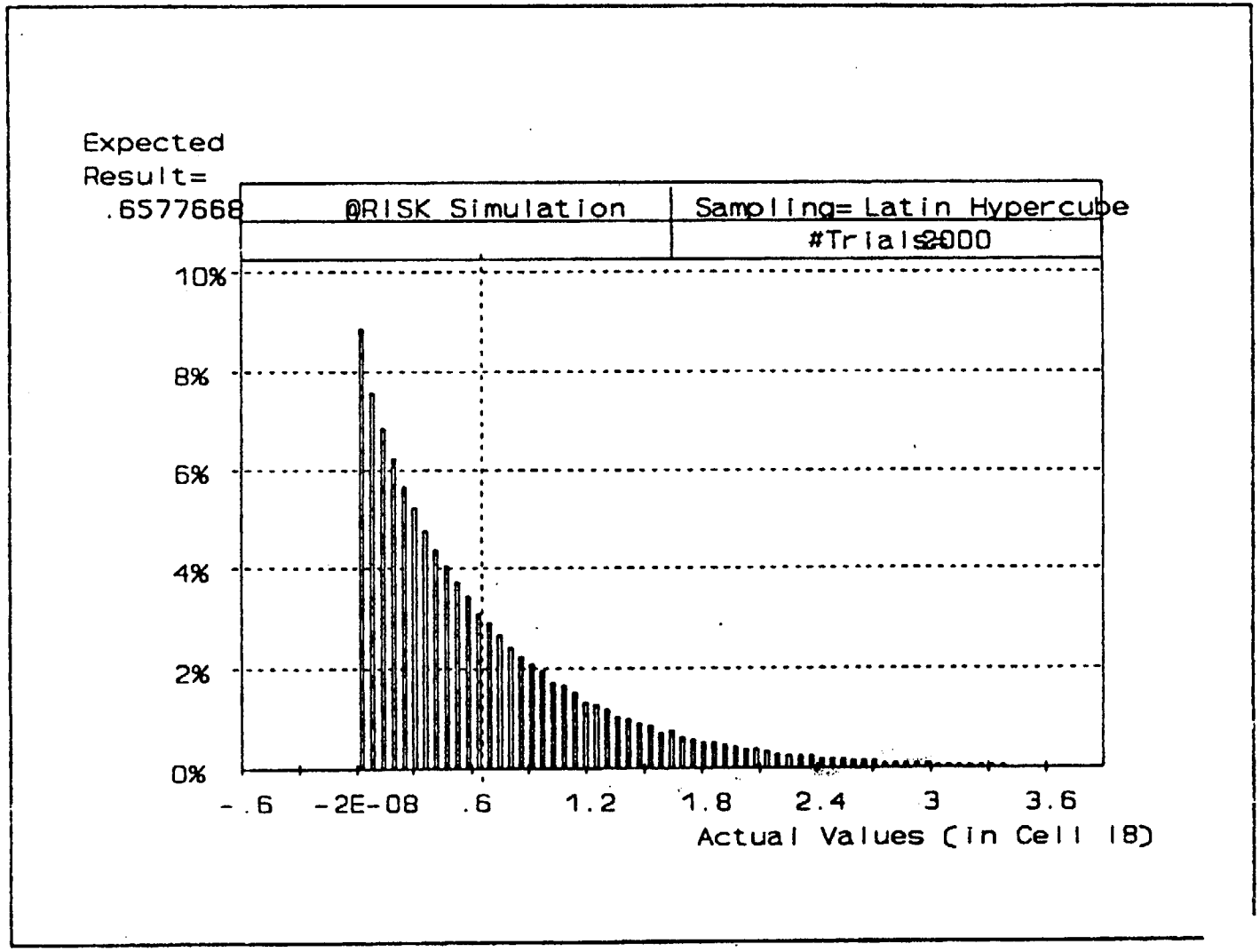

Figure 2-3. Histogram of Saturated Hydraulic Matrix Conductivity (k_0)

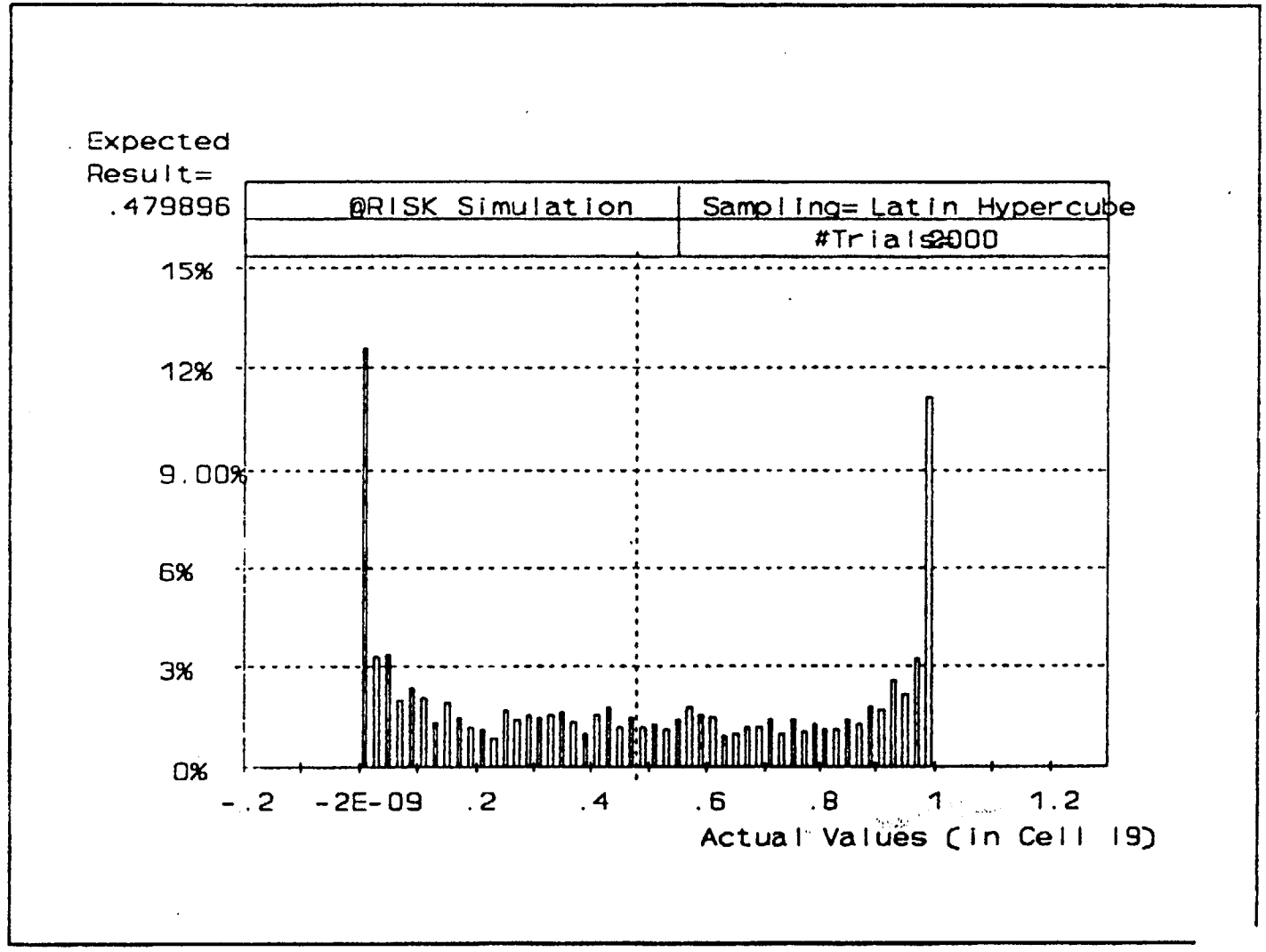

Figure 2-4. Histogram of Fraction of Containers in Seepage Areas (f_s)

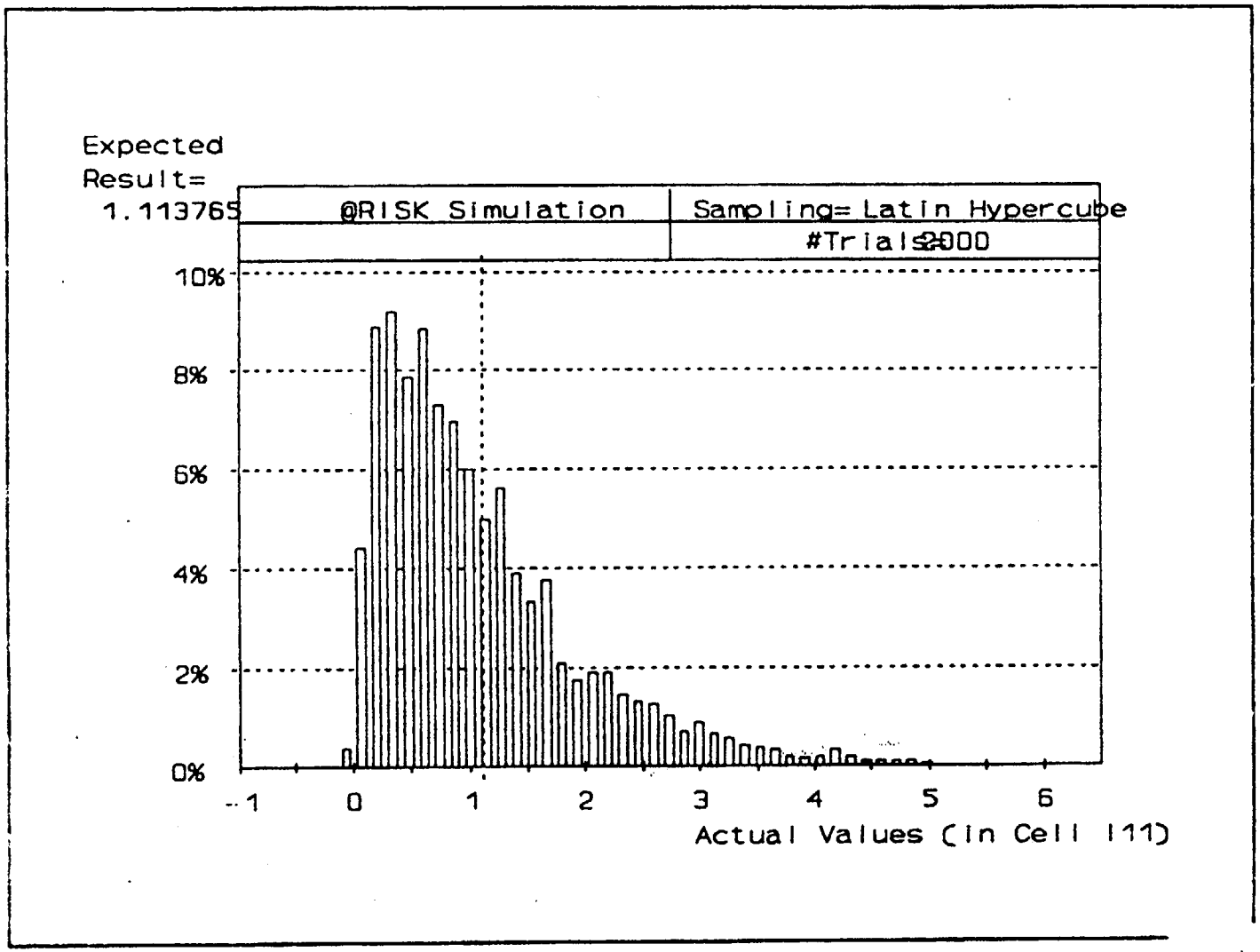

Figure 2-5. Histogram of Flux Used for Advective Release (q_s)

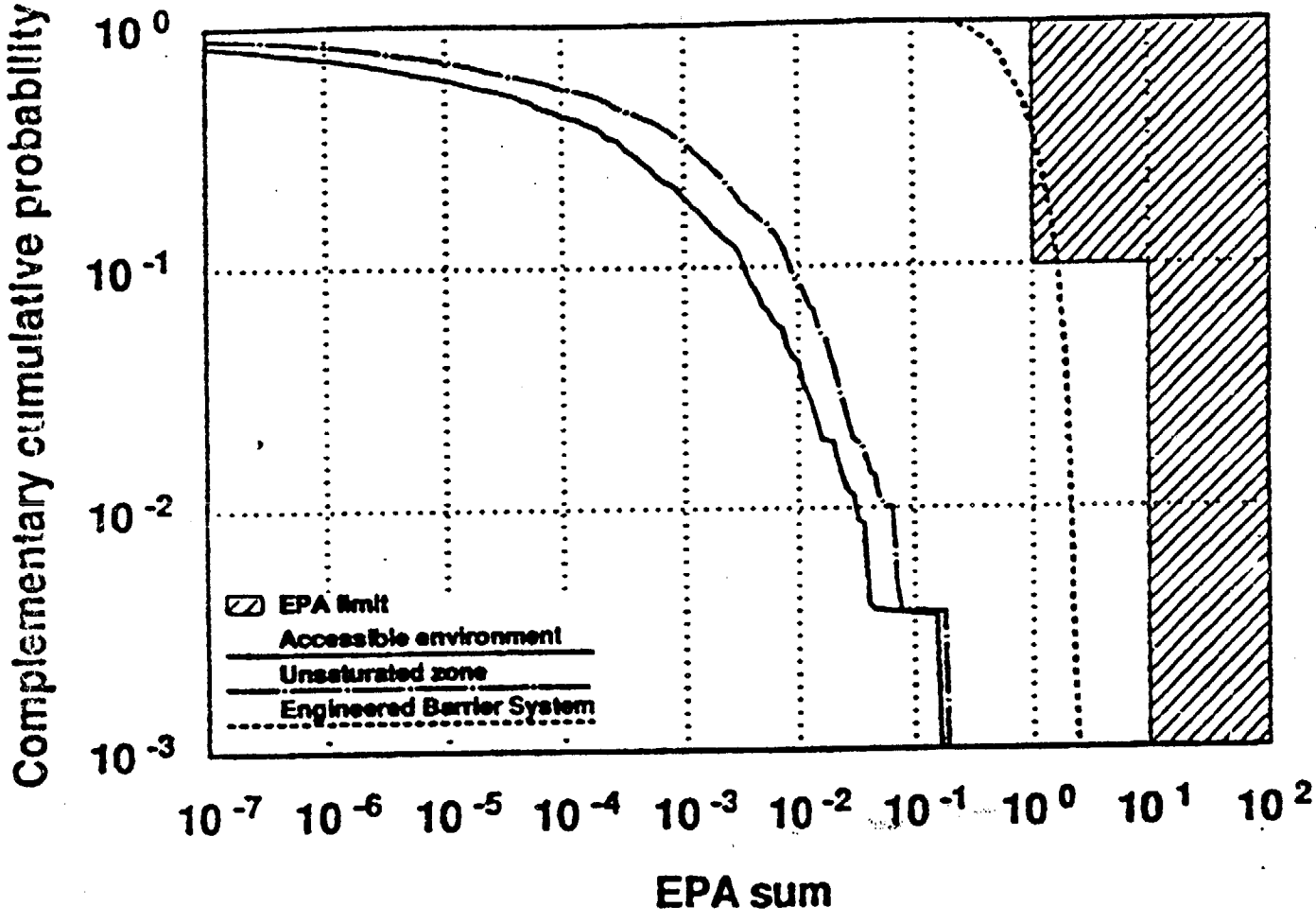

Figure 2-6. TSPA - 1991 CCDF for Waste Package/E... Release (taken from Barnard et al., 1992)

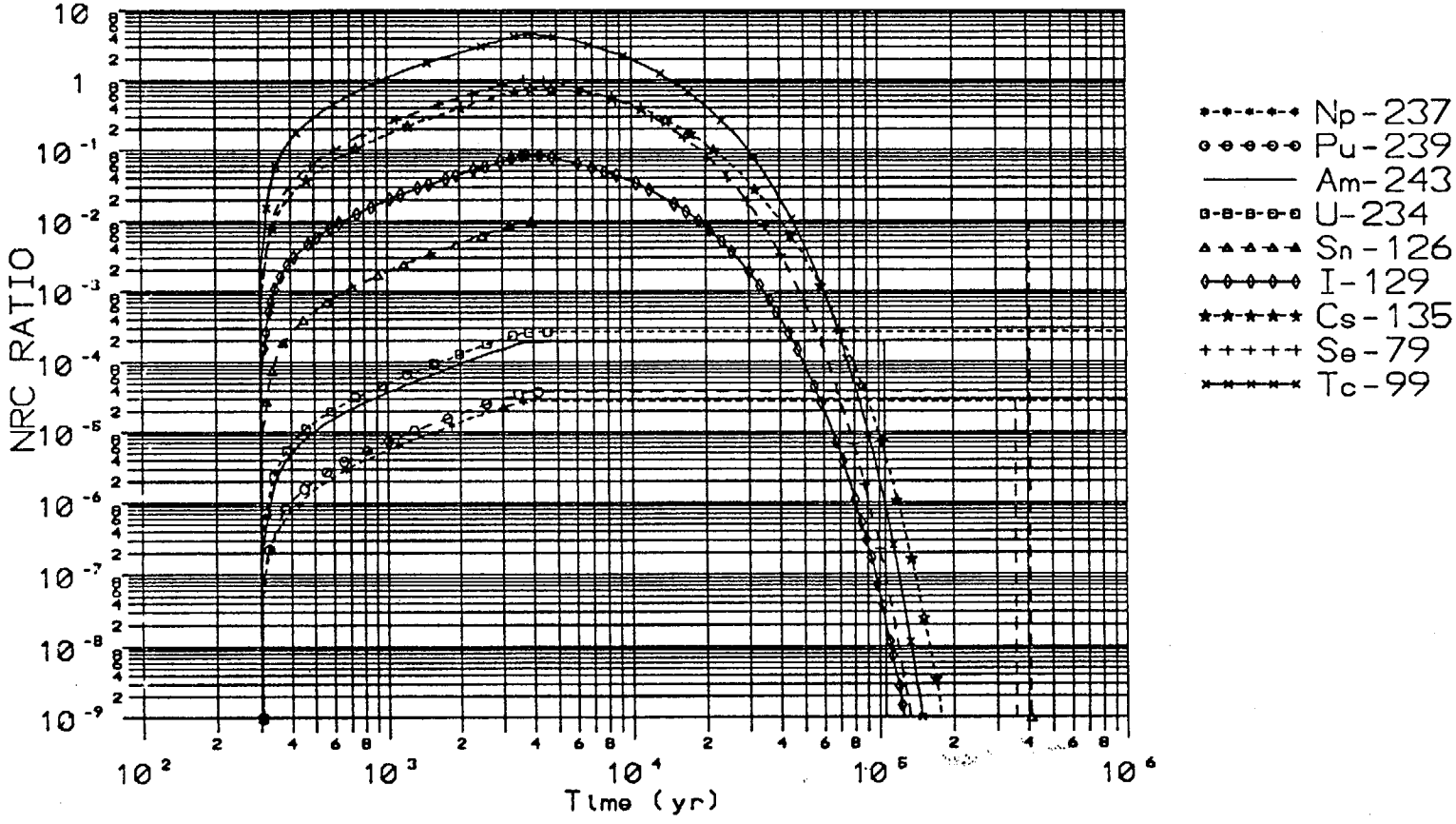

Figure 2-7. TSPA-1991 Individual Radionuclide Release Curves (normalized)

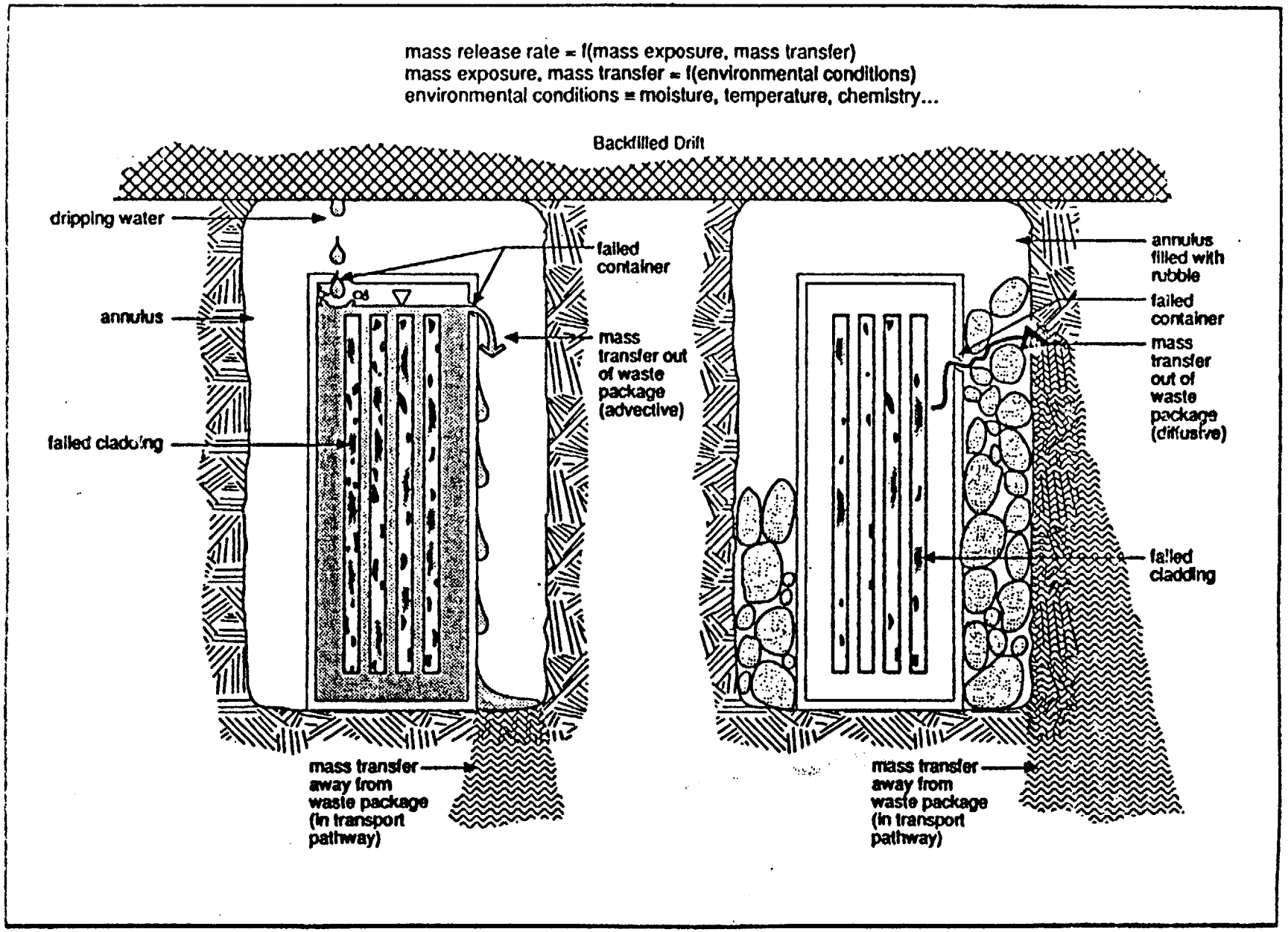

Figure 2-8. RIP Waste Package Schem (taken from Miller et al., 1993)

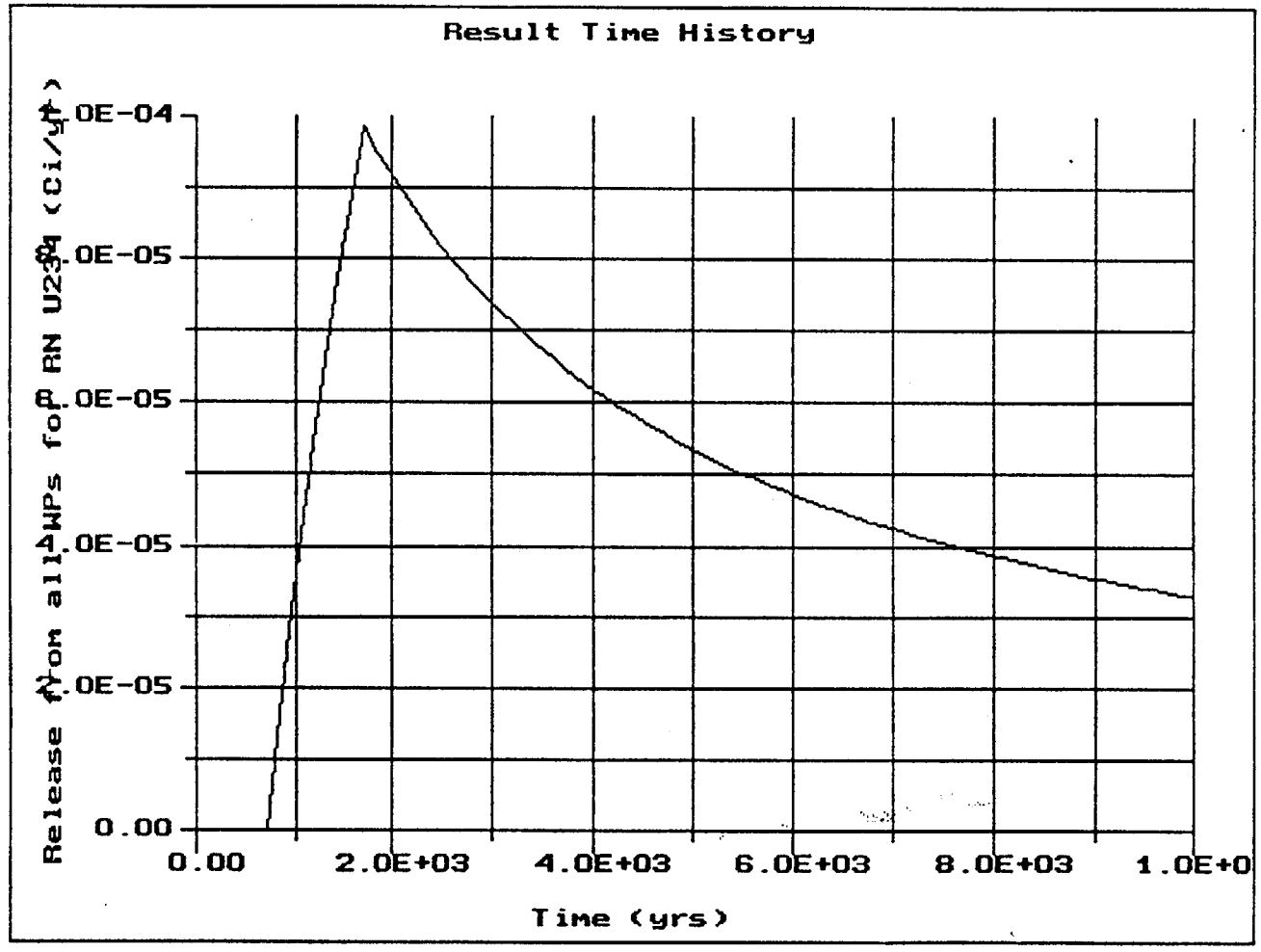

Figure 2-9. ^{234}U Release Assuming Competing Isotope Solubilities

Figure 2-10. ^{235}U Release Assuming Competing Isotope Solubilities

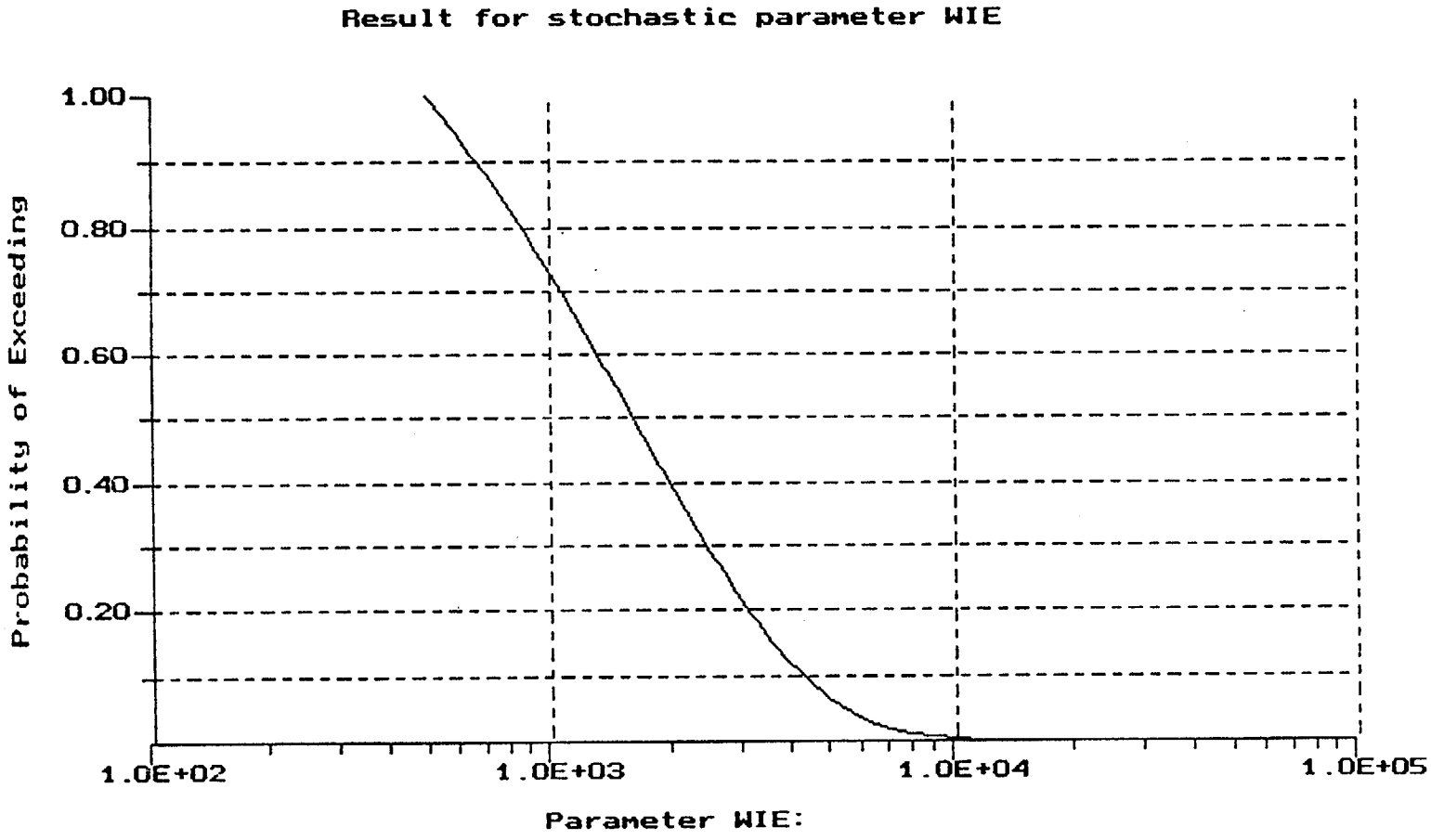

Figure 2-11. Weibull Waste Package Failure Distribution

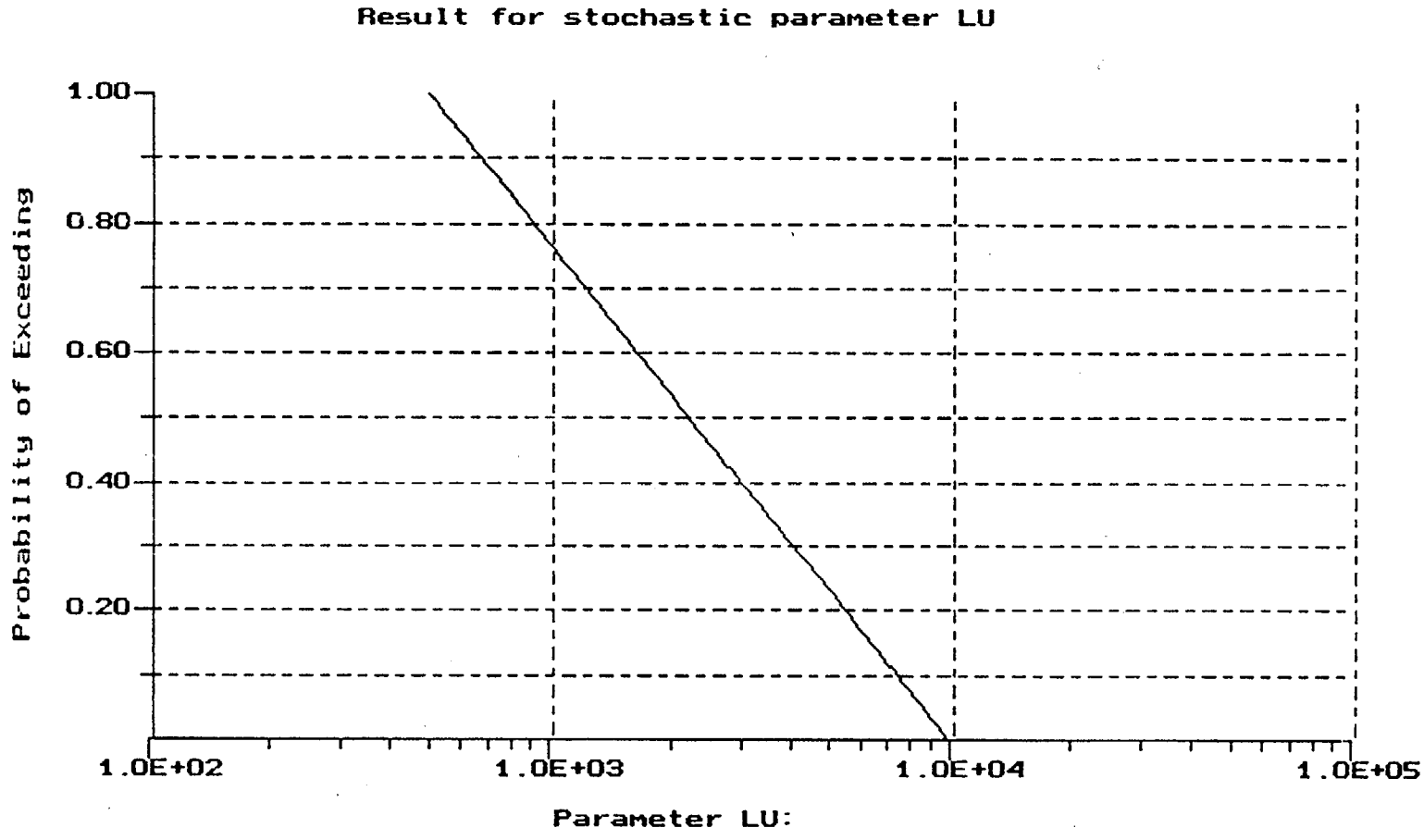

Figure 2-12. Log-Uniform Waste [illegible]age Failure Distribution

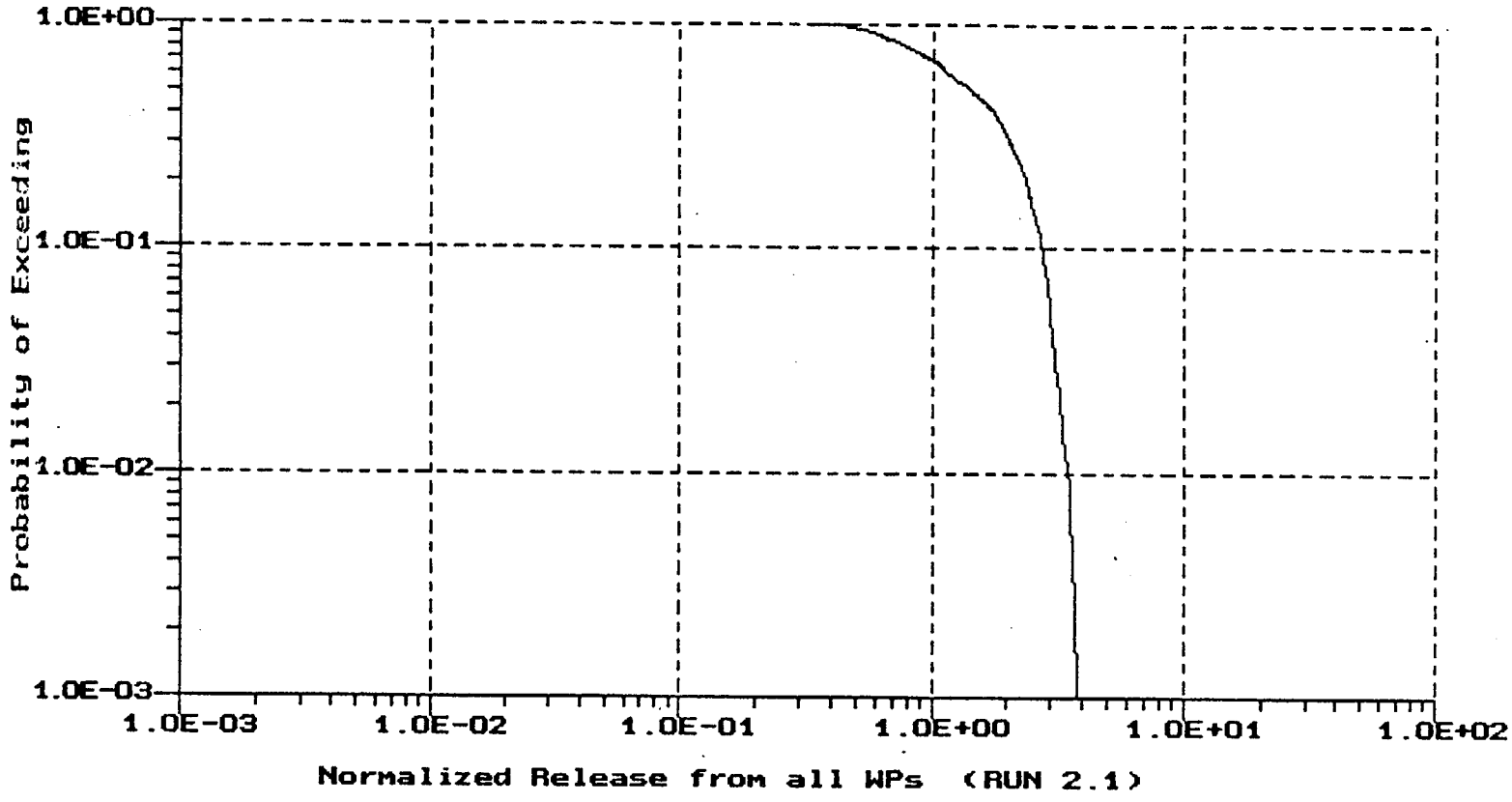

Figure 2-13. Initial Conceptualization - CCDF

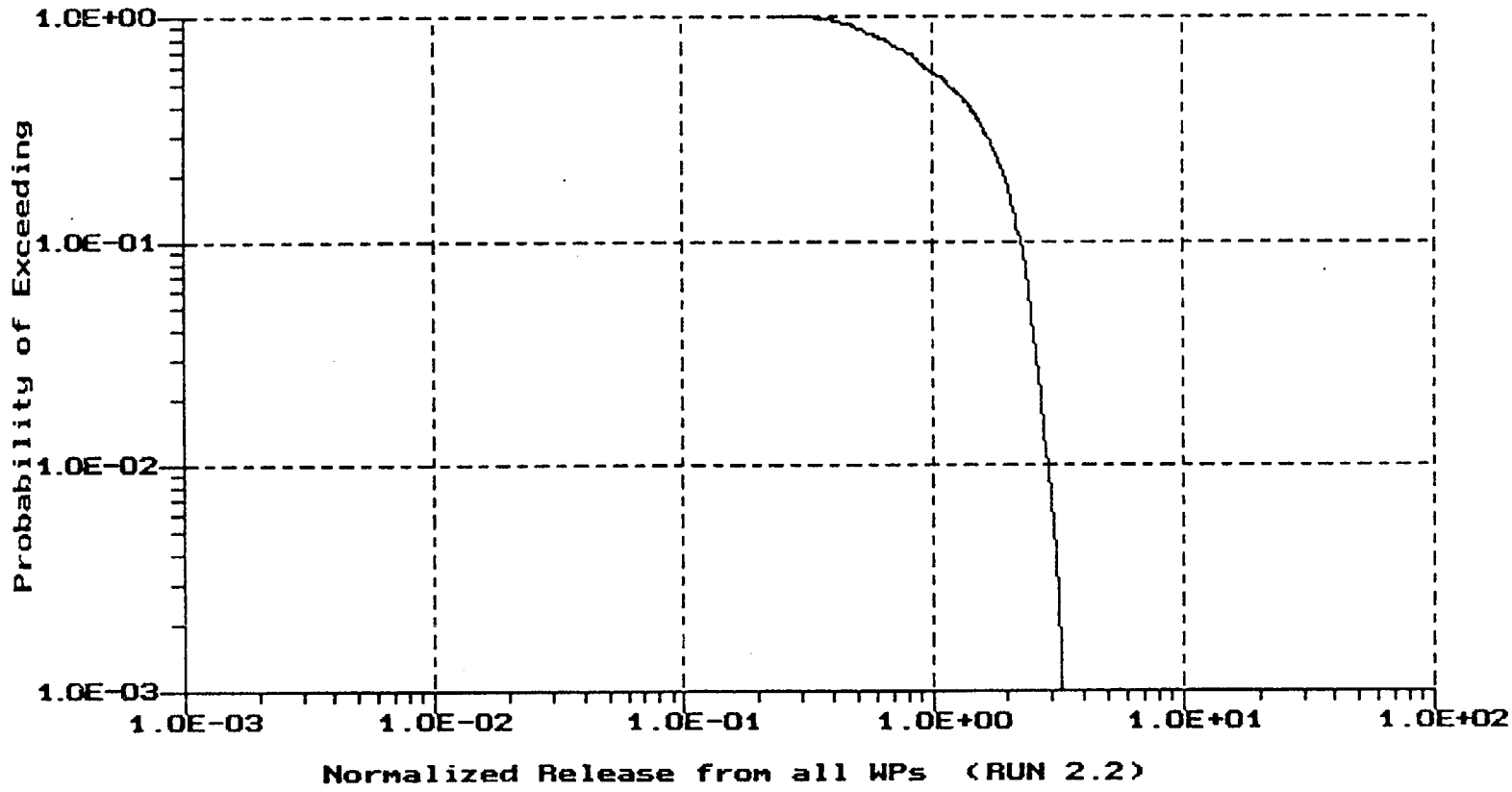

Distribution of Results

Mean= 1.287E+00

S.D.= 6.715E-01

Kurtosis= 2.282E+00

Skewness= 5.043E-01

Figure 2-14. Waste Package with Uniform Failure Distribution - CCDF

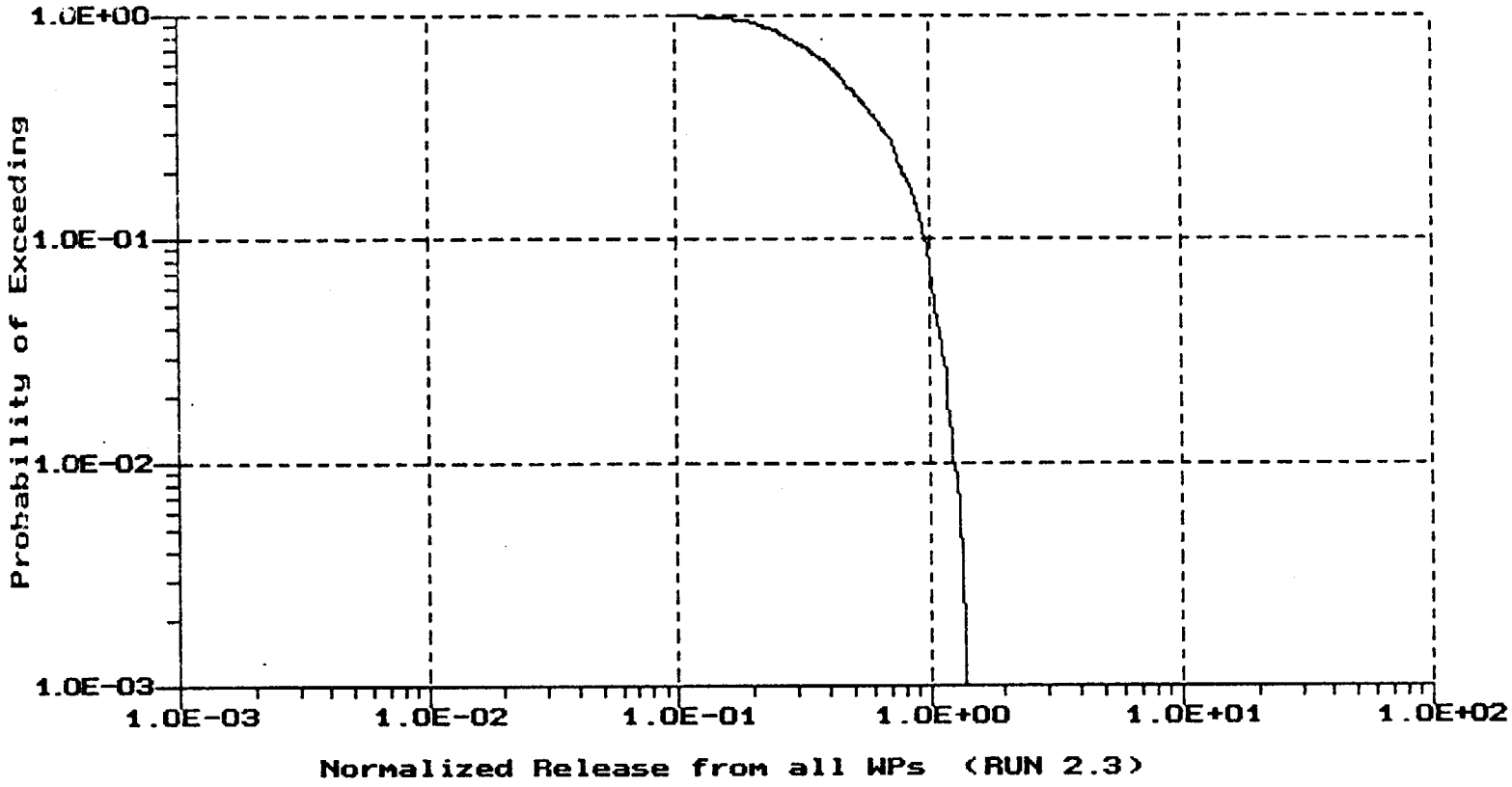

Figure 2-15. Inventory Reduced to Nine Radionuclides - CCDF

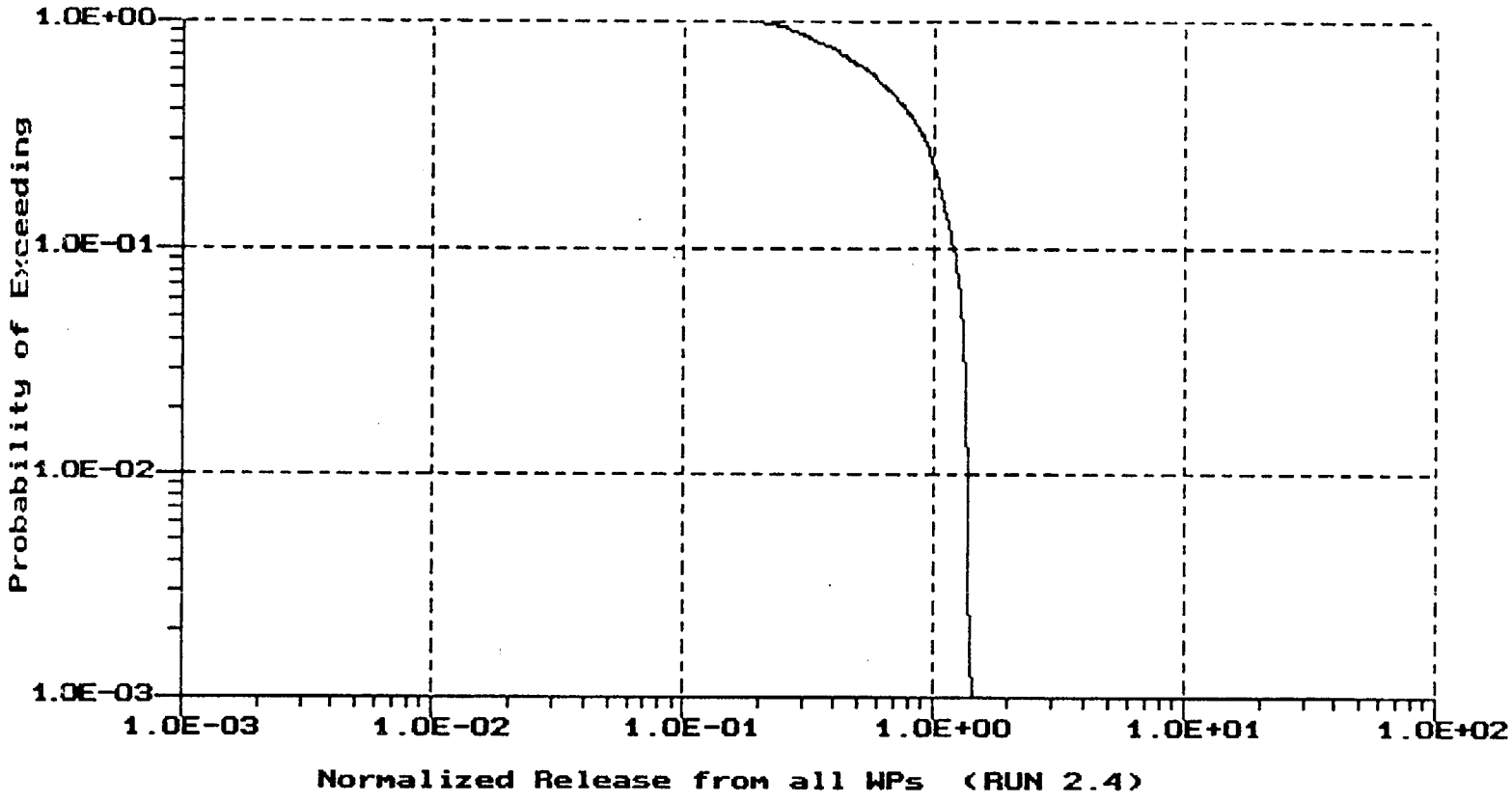

Distribution of Results

Mean= 7.027E-01

S.D.= 3.422E-01

Kurtosis= 1.910E+00

Skewness= 3.144E-01

Figure 2-16. Increase ^{99}Tc and ^{135}Cs Base Solubility - CCDF

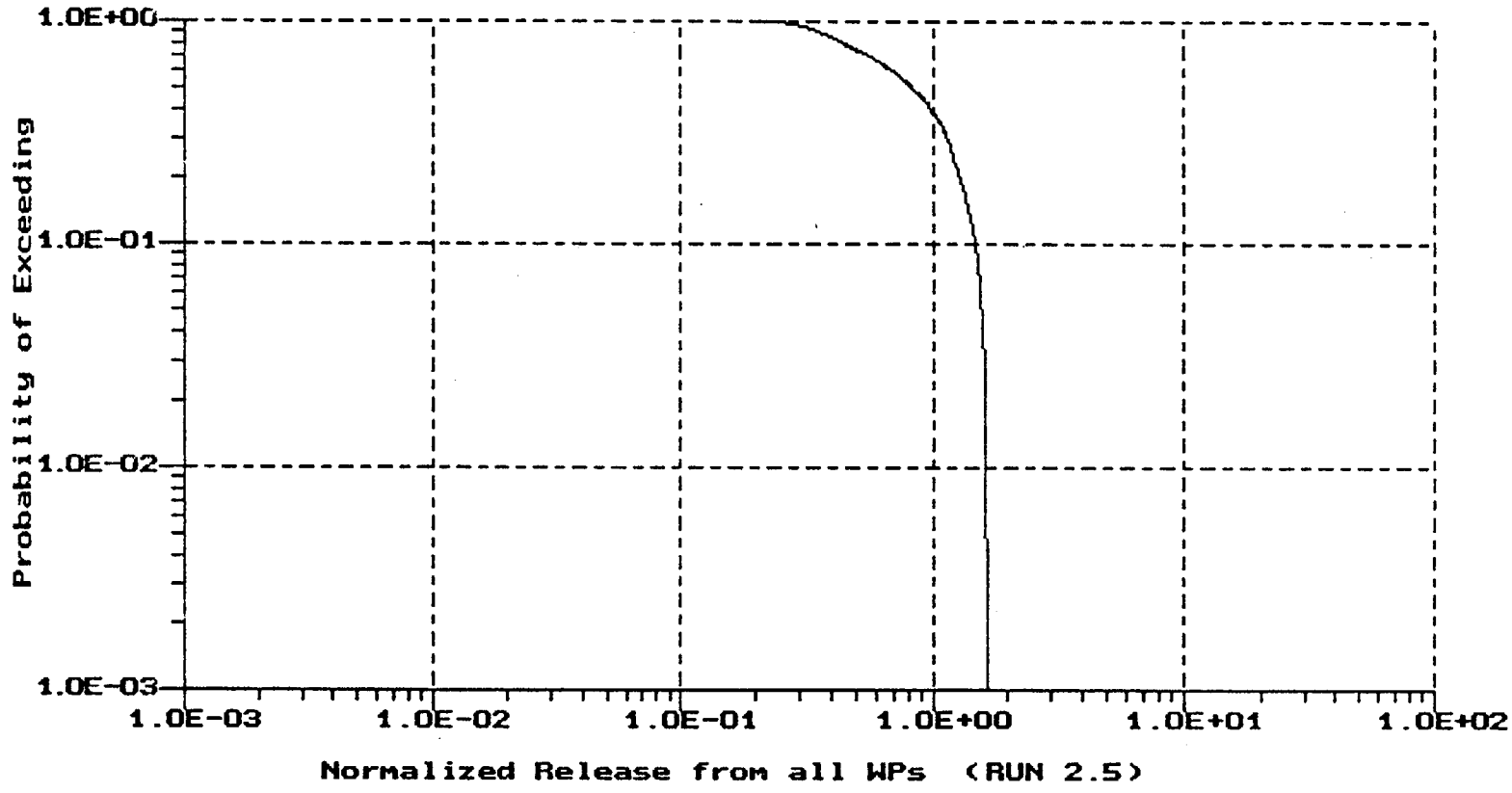

Figure 2-17. One Failure Time Per Realization - CCDF

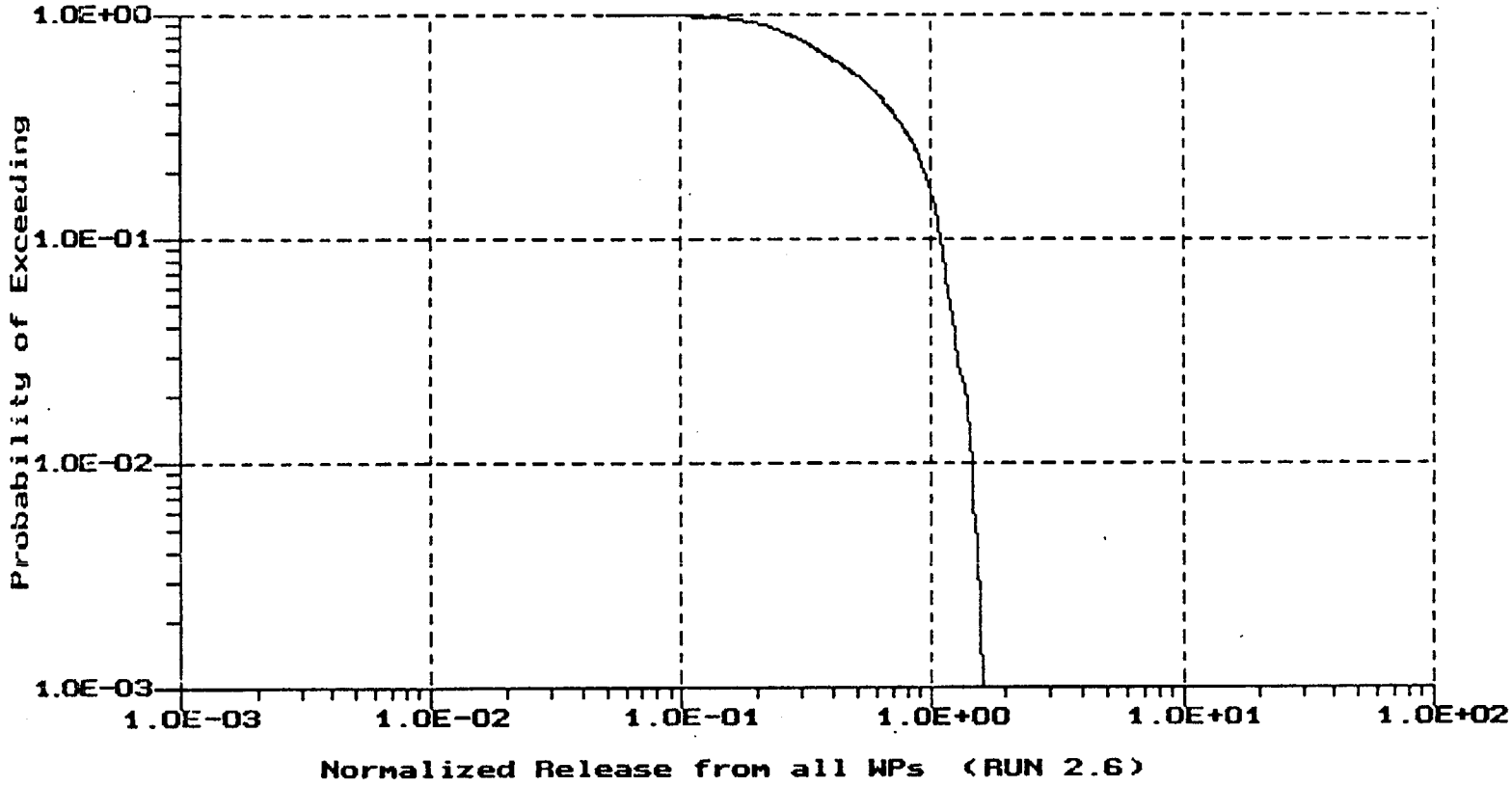

Distribution of Results

Mean= 6.064E-01

S.D.= 3.451E-01

Kurtosis= 2.388E+00

Skewness= 5.583E-01

Figure 2-18. F_s Implemented to Deter Waste Package Group Totals - CCDF

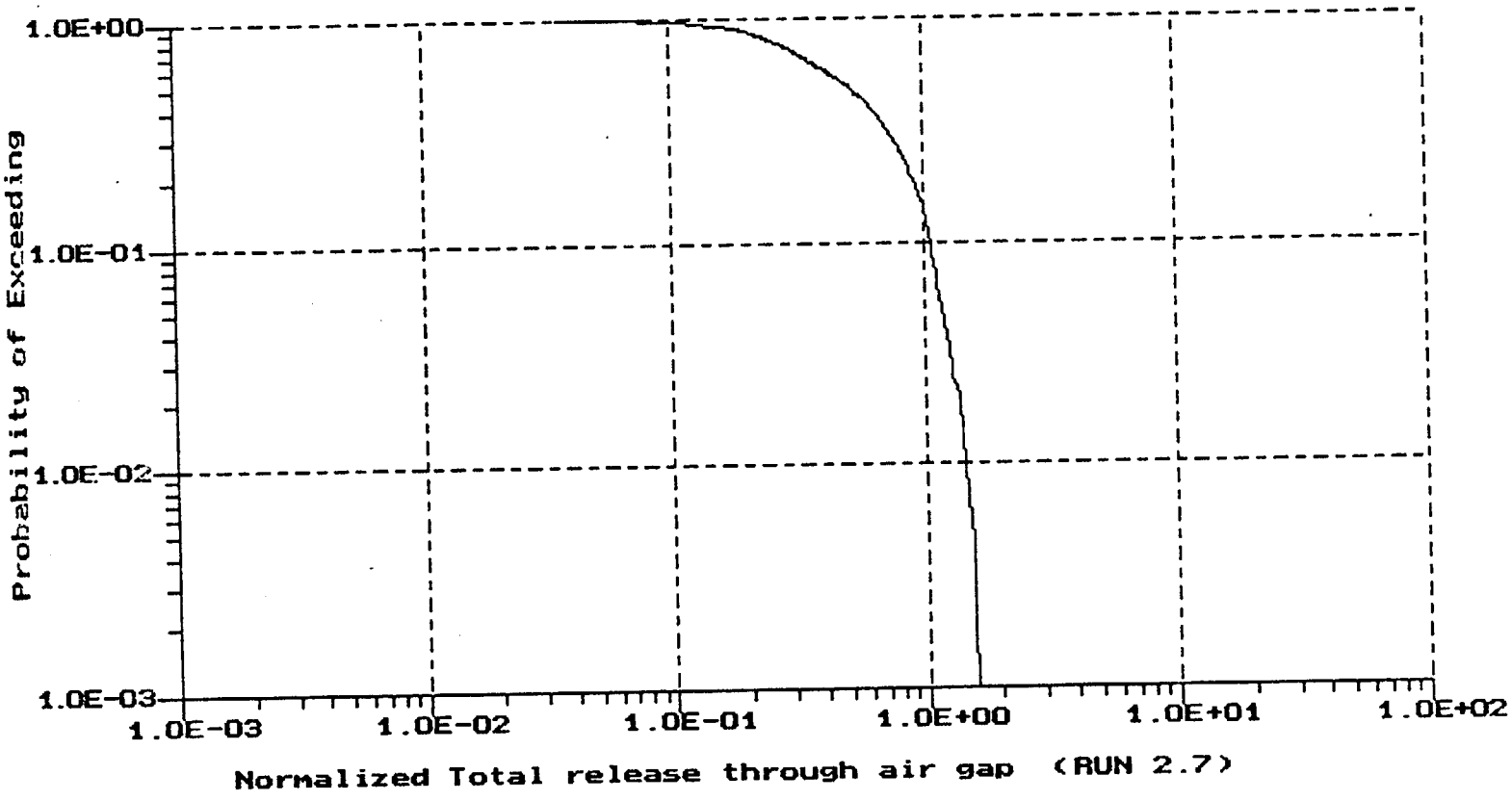

Figure 2-19. F_s Implemented to Determine Waste Package Group Totals - with Air Gap - CCDF

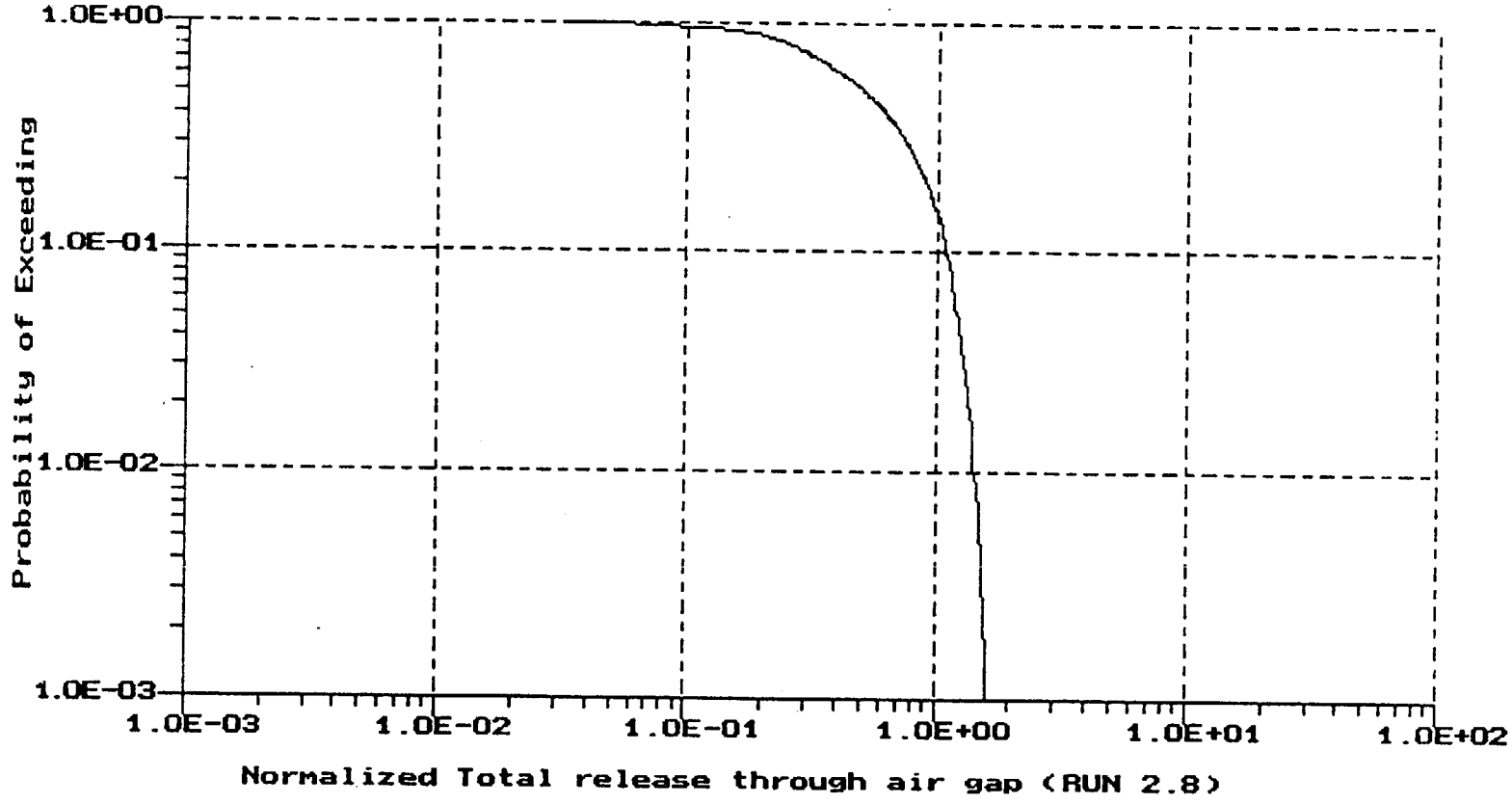

Distribution of Results

Mean= 5.819E-01

S.D.= 3.487E-01

Kurtosis= 2.505E+00

Skewness= 5.830E-01

Figure 2-20. F_s Implemente h q_s with Air Gap - CCDF

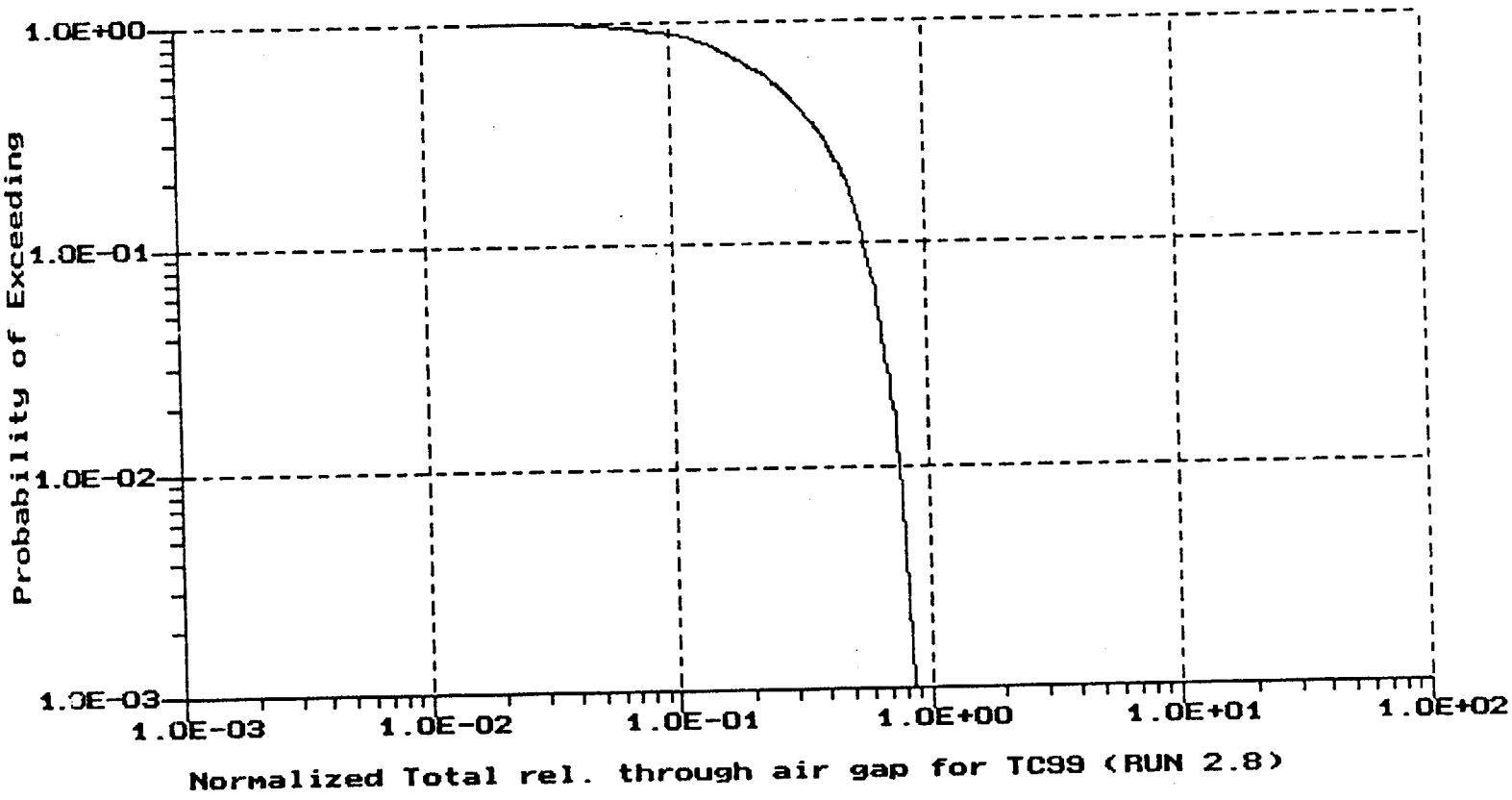

Figure 2-21. ^{99}Tc Implemented with q_s with Air Gap - CCDF

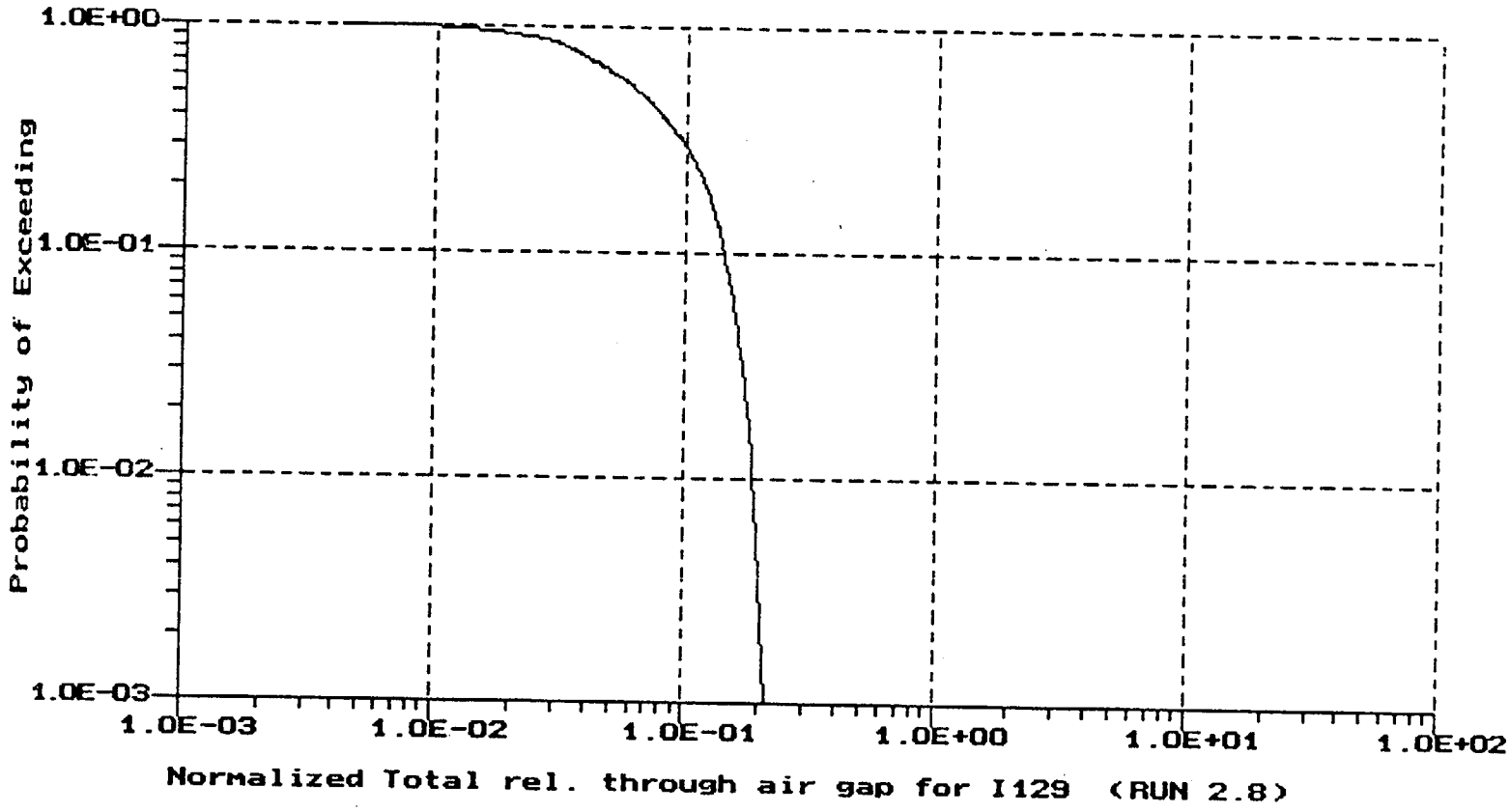

Distribution of Results

Mean= 7.553E-02

S.D.= 4.524E-02

Kurtosis= 2.520E+00

Skewness= 6.107E-01

Figure 2-22. ^{129}I Implement[illegible]ith q_s with Air Gap - CCDF

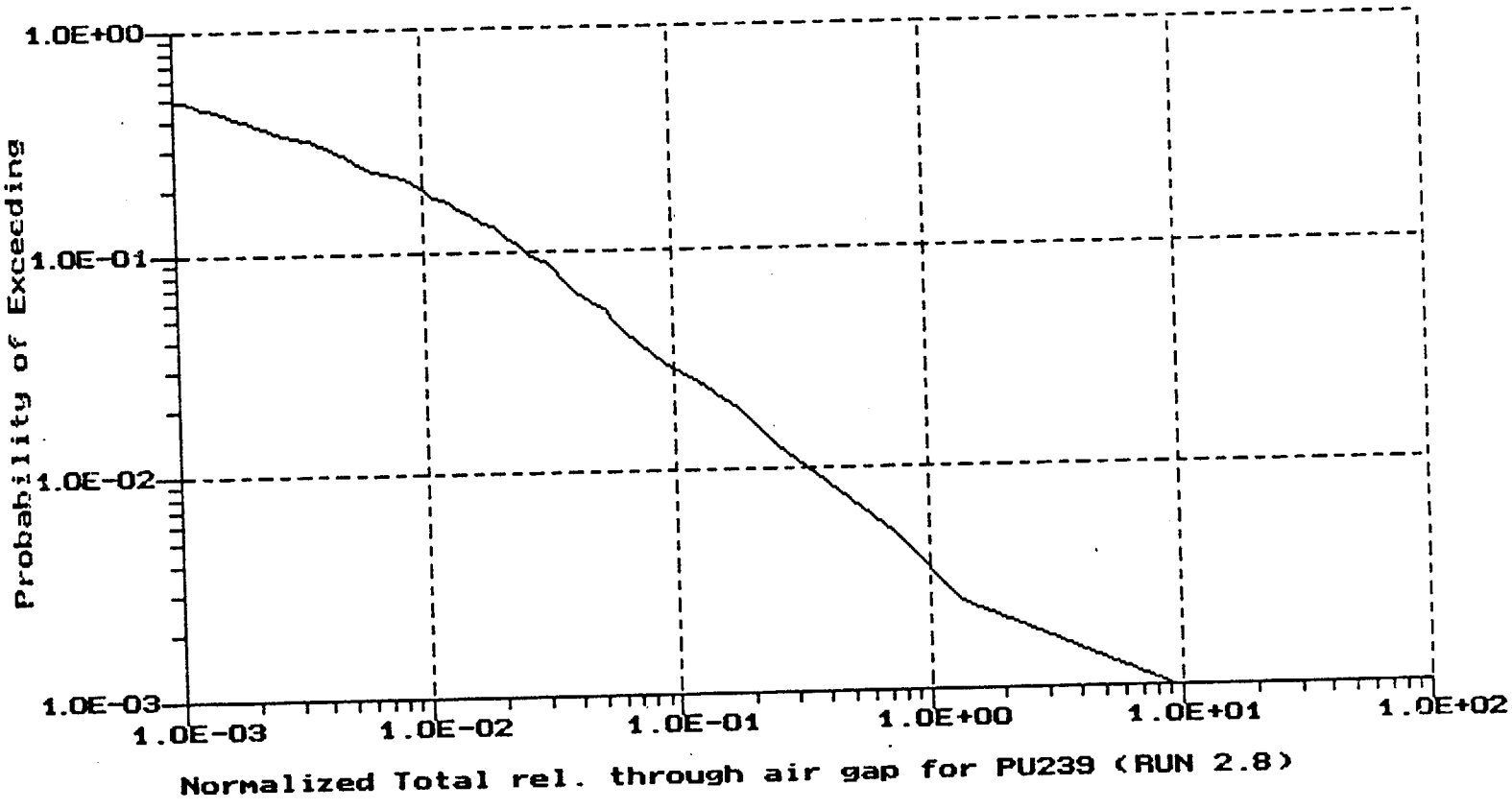

Distribution of Results

Mean= 6.970E-02

S.D.= 1.329E+00

Kurtosis= 7.592E+02

Skewness= 2.682E+01

Figure 2-23. ^{239}Pu Implemented with q_s with Air Gap - CCDF

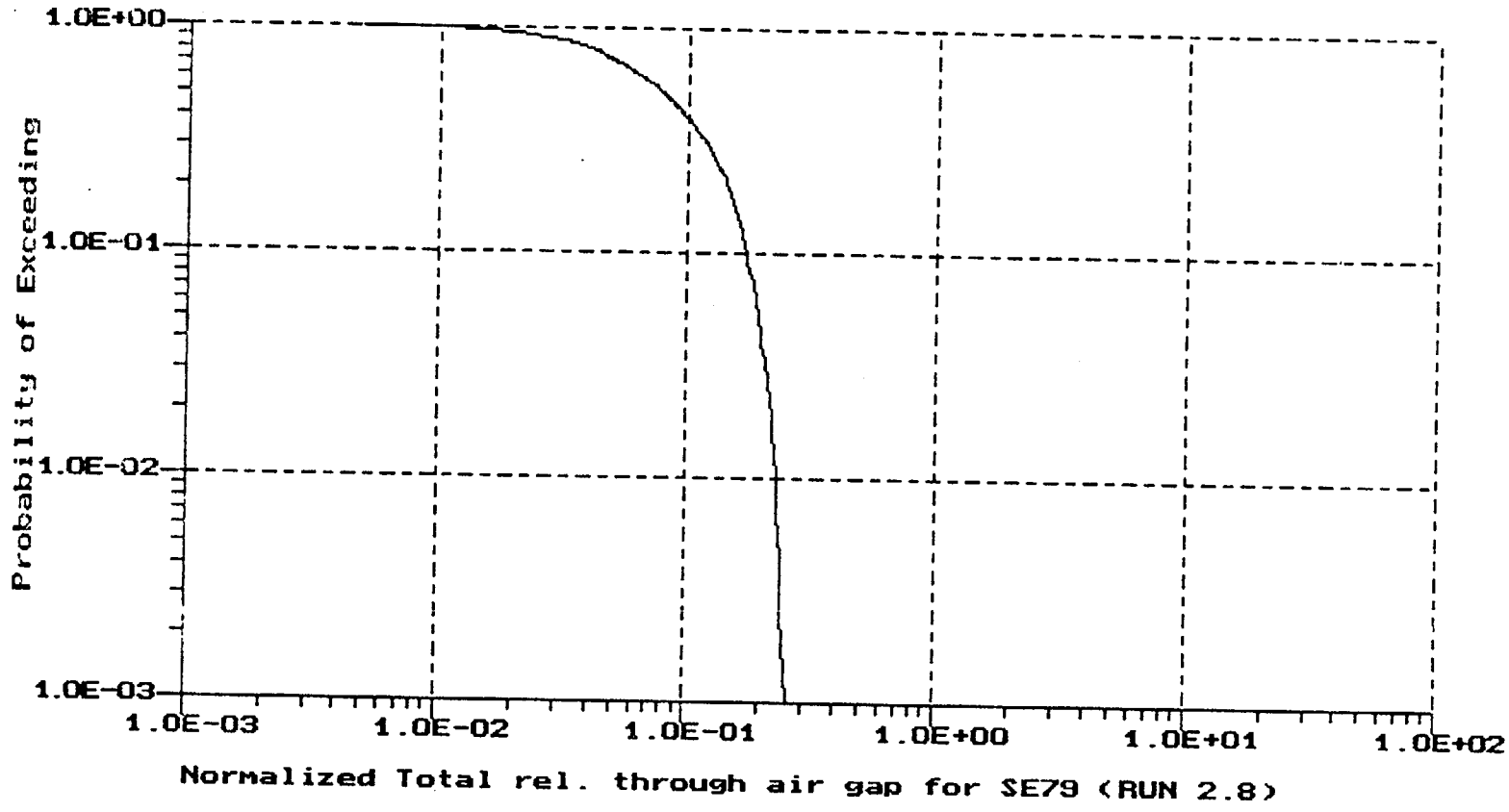

Figure 2-24. ^{79}Se Impleme with q_s with Air Gap - CCDF

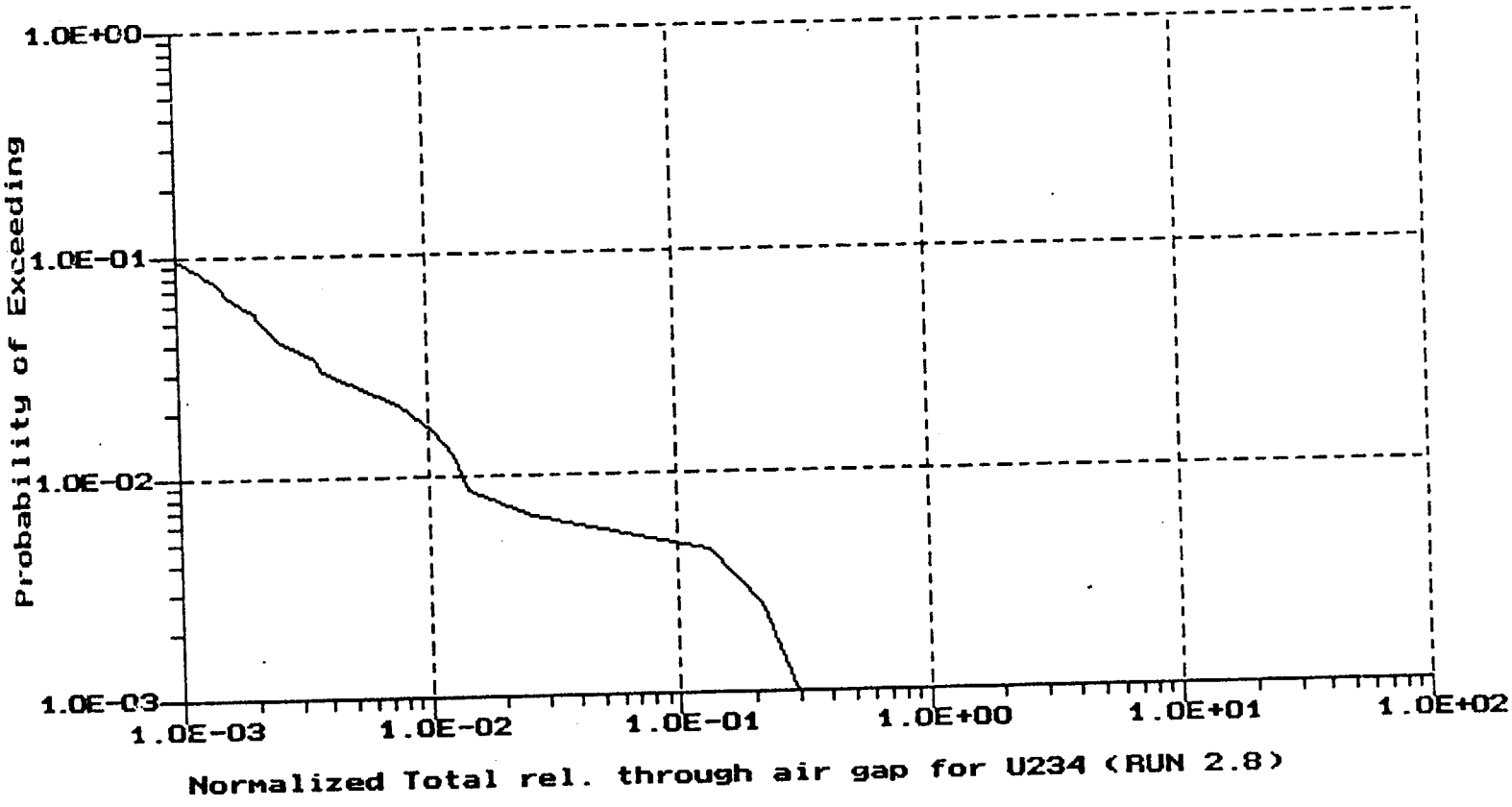

Figure 2-25. ^{234}U Implemented with q_s with Air Gap - CCDF

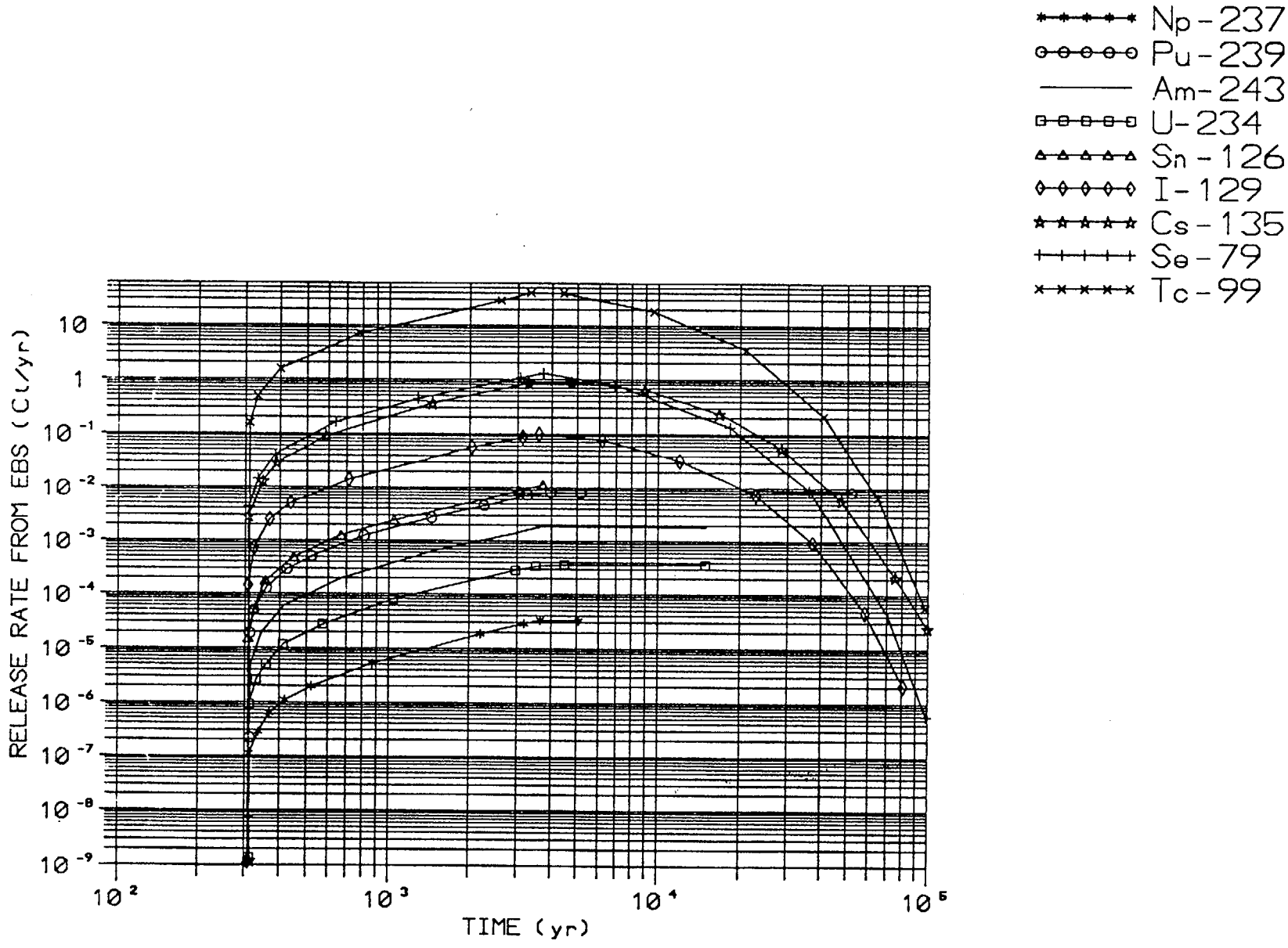

Figure 2-26. TSPA-1991 Individual Radionuclide Release Curves (non-normalized)

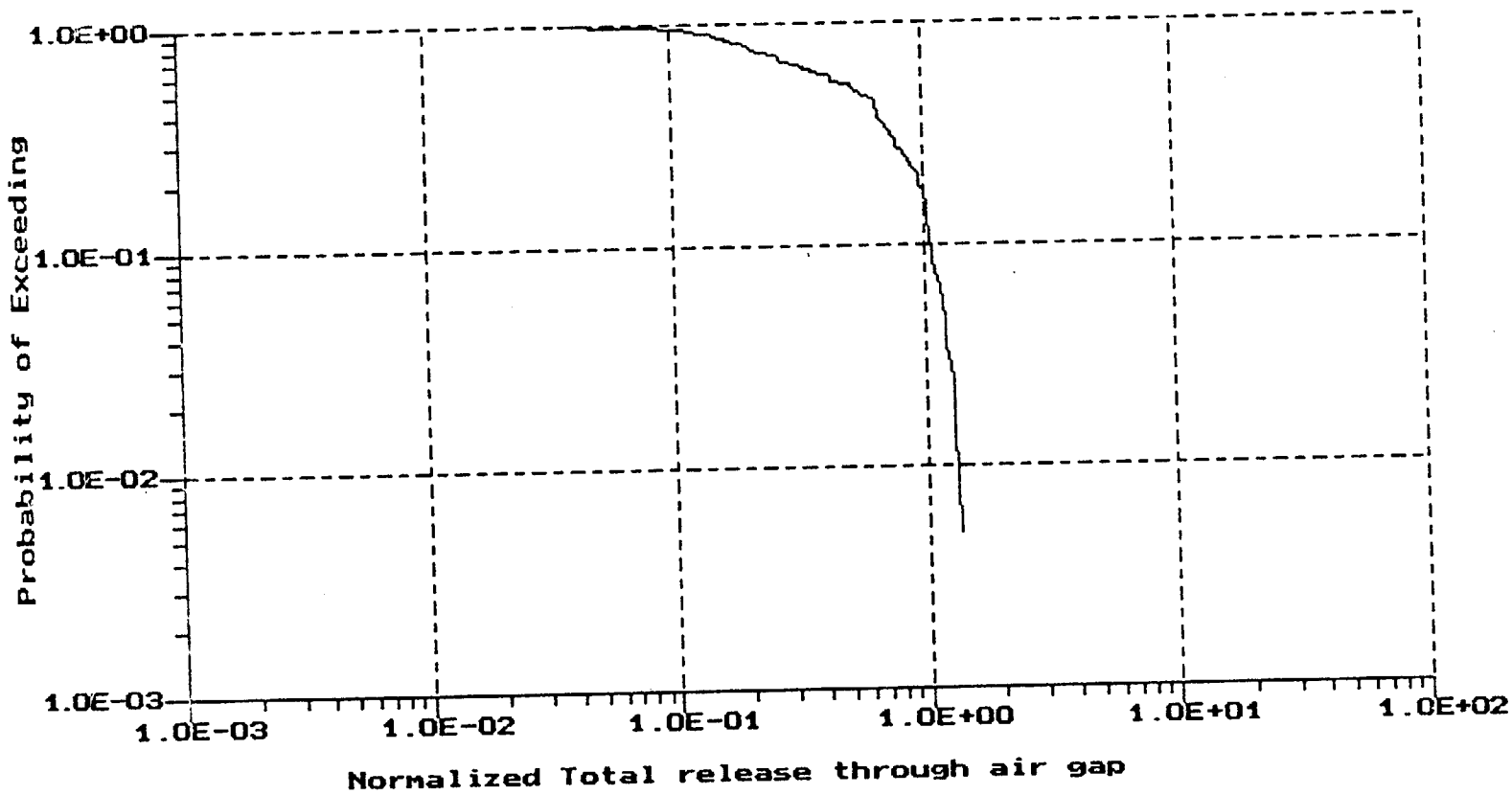

Distribution of Results

Mean= 5.701E-01

S.D.= 3.598E-01

Kurtosis= 1.906E+00

Skewness= 3.286E-01

Figure 2-27. Release Initiated at 300 Years - CCDF

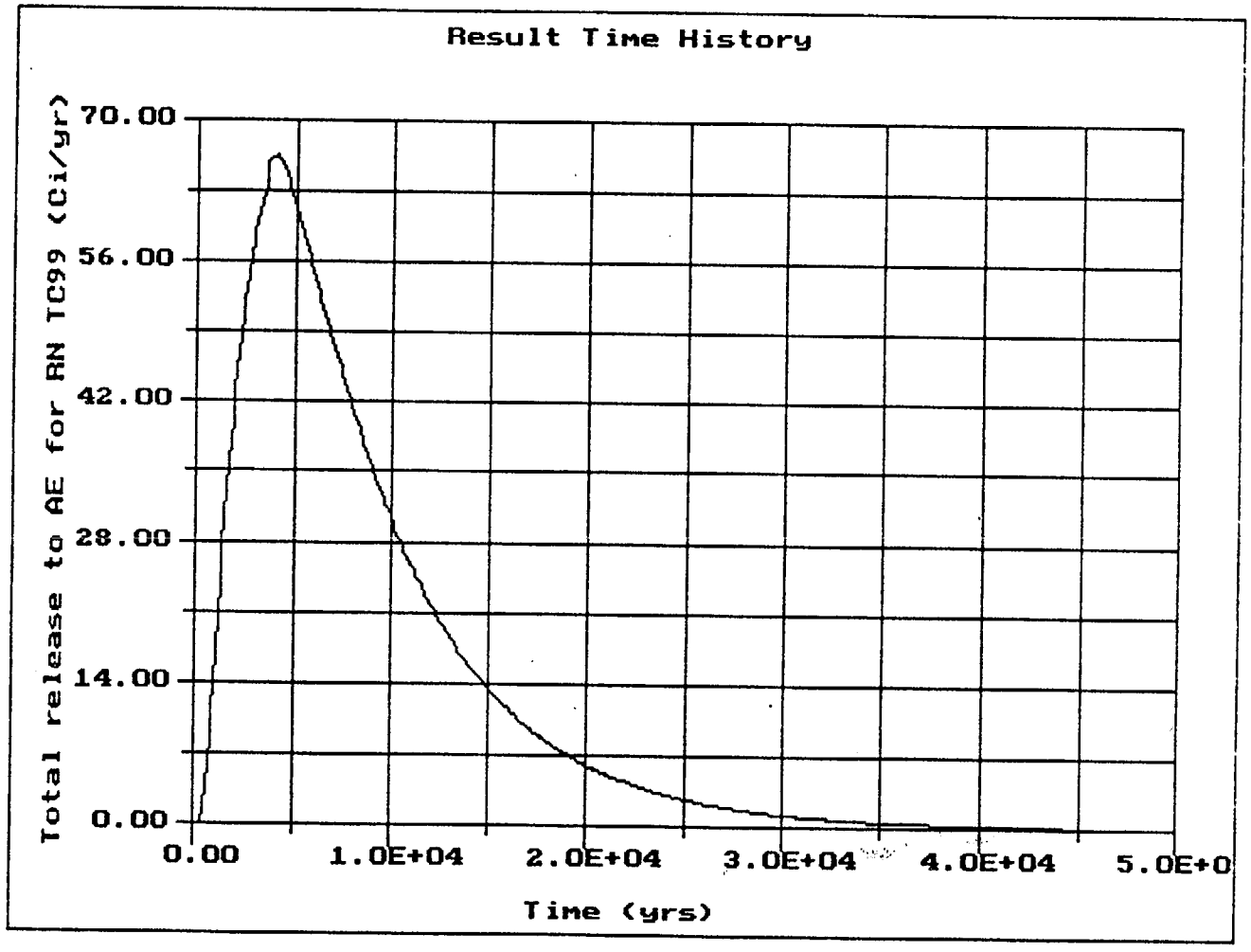

Figure 2-28. Individual F .nuclide Release Curve (^{99}Tc)

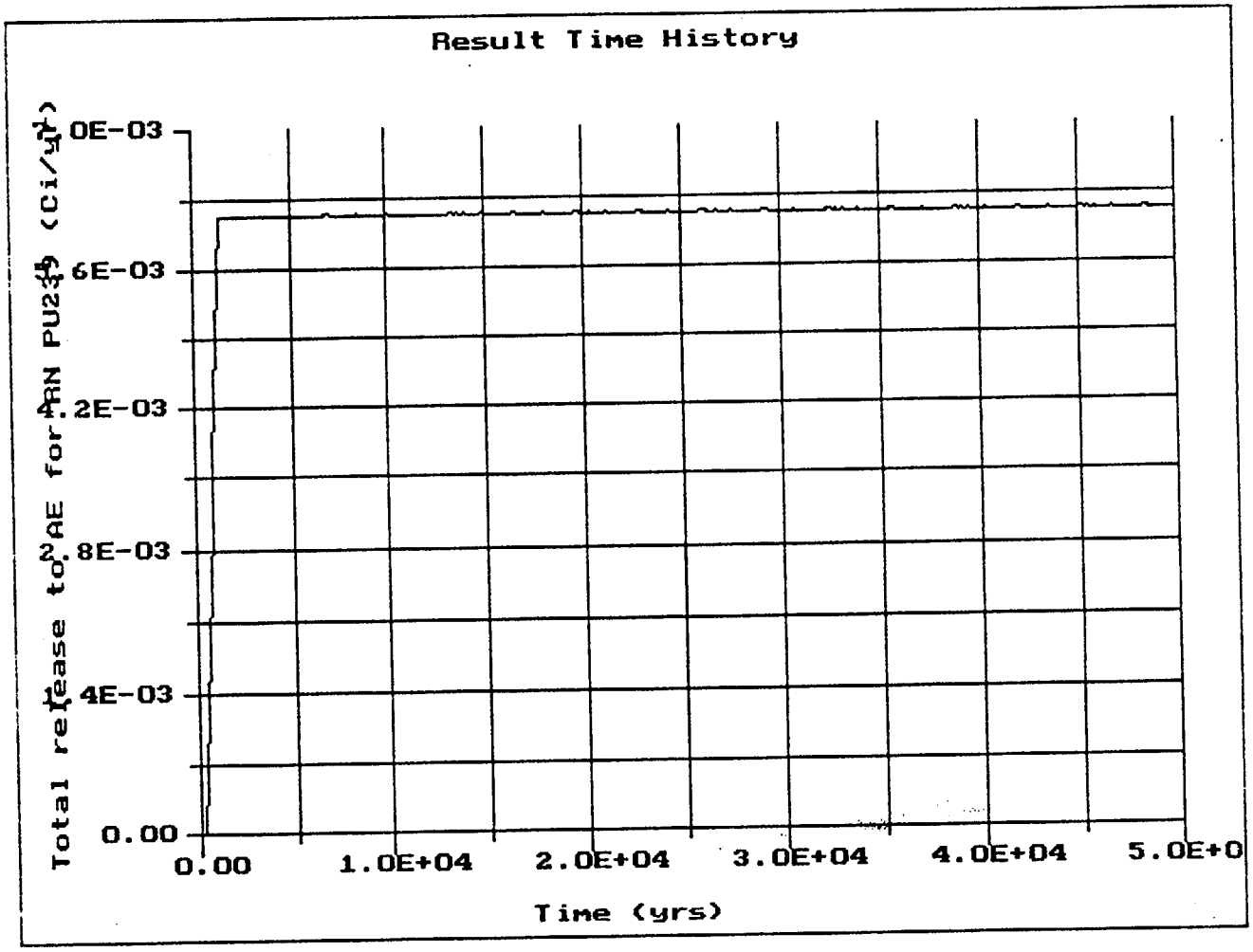

Figure 2-29. Individual Radionuclide Release Curve (^{239}Pu)

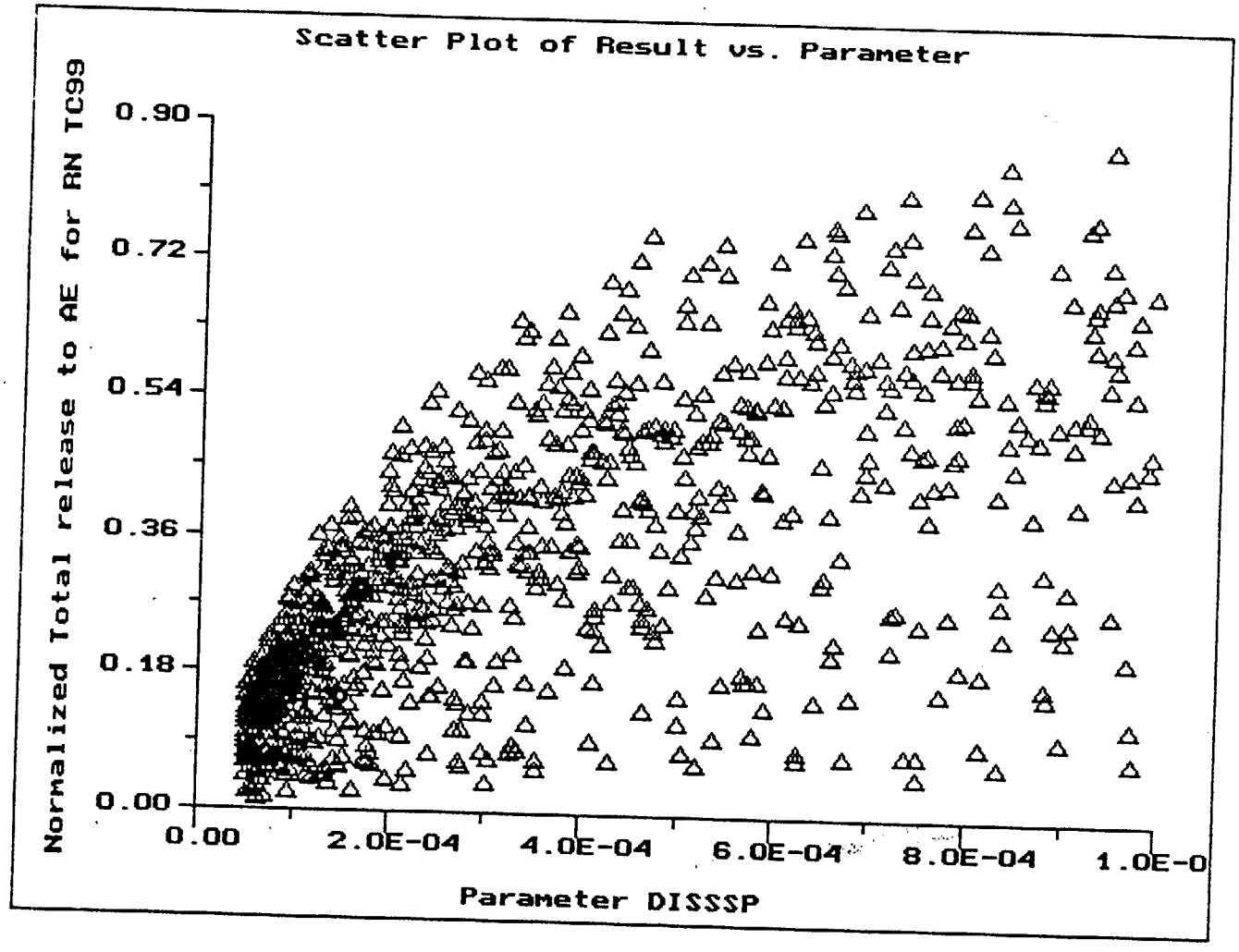

Figure 2-30. Sensitivity of ^{99}Tc Release to Matrix Dissolution Rate

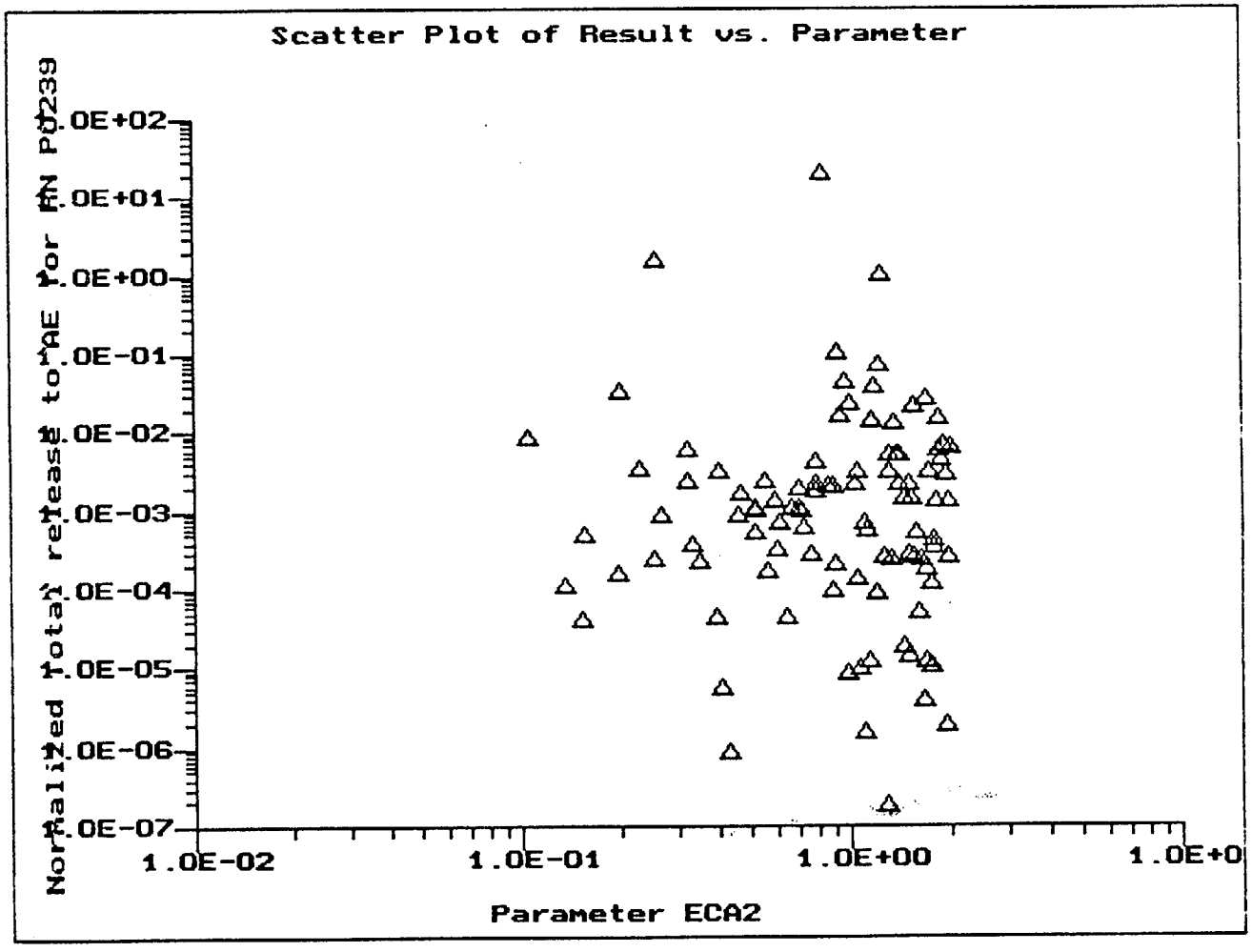

Figure 2-31. Sensitivity of ^{239}Pu Release to Effective Catchment Area

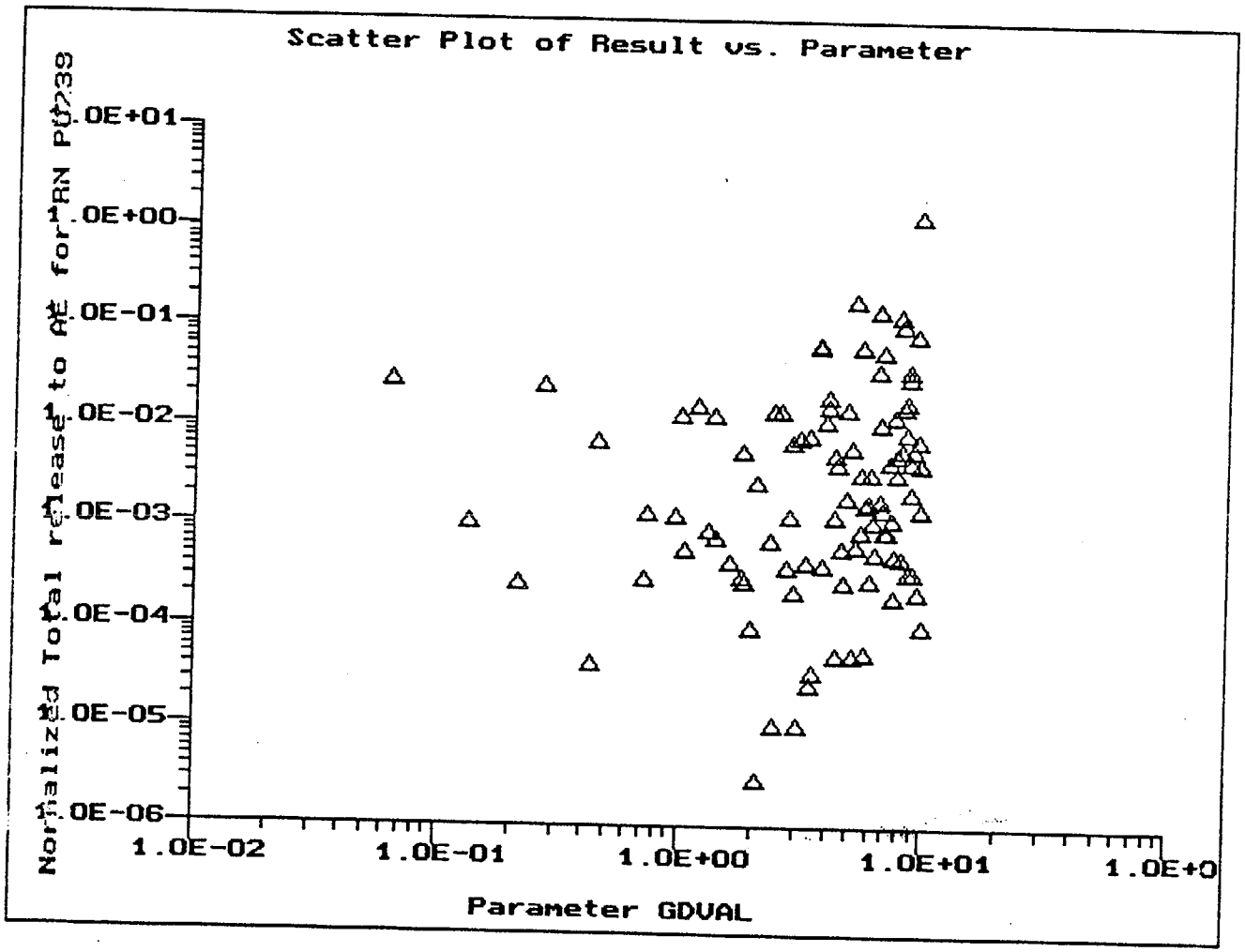

Figure 2-32. Sensitivity of ^{239}Pu release to Geometric Diffusion Factor

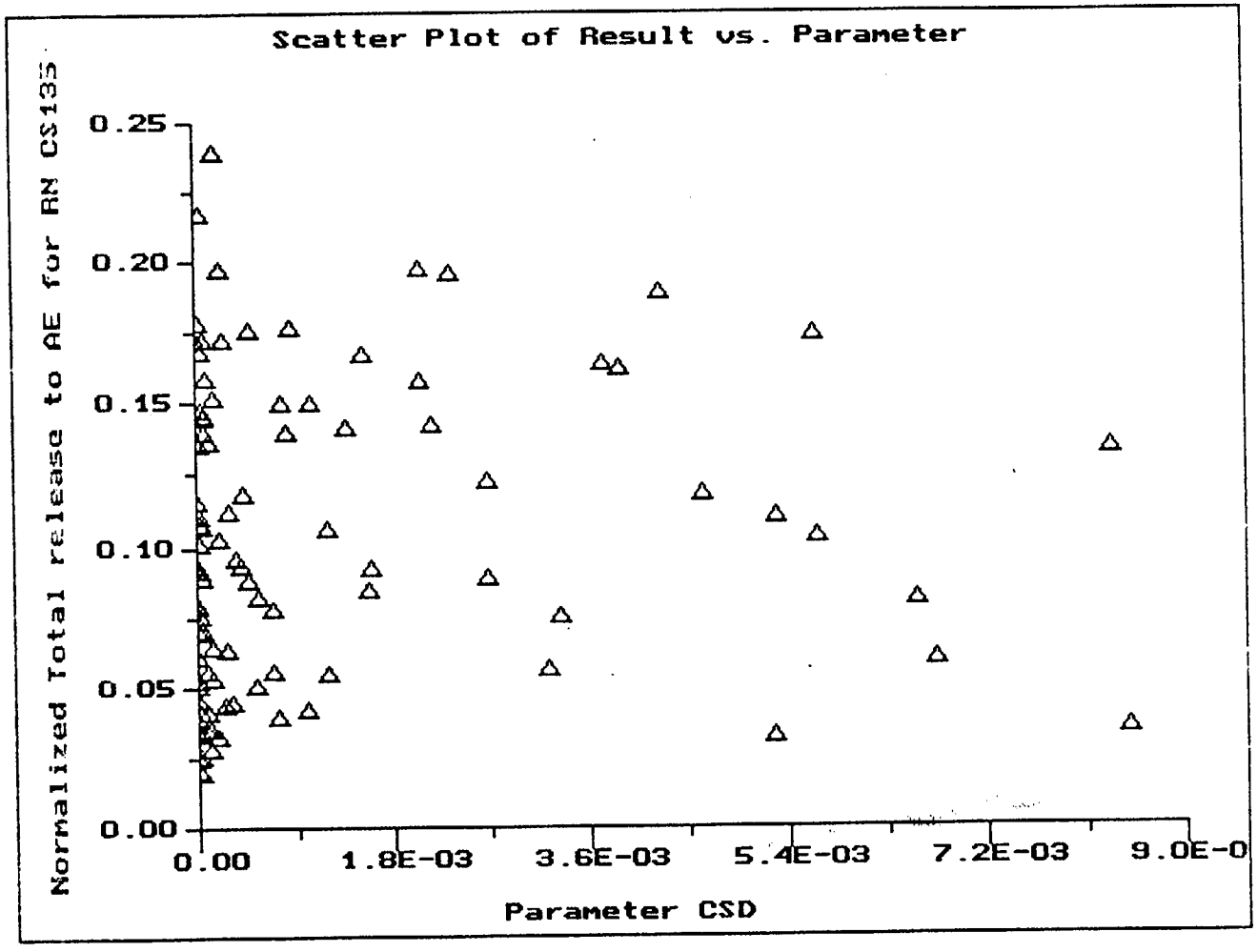

Figure 2-33. Sensitivity of ^{135}Cs to Diffusion Coefficient

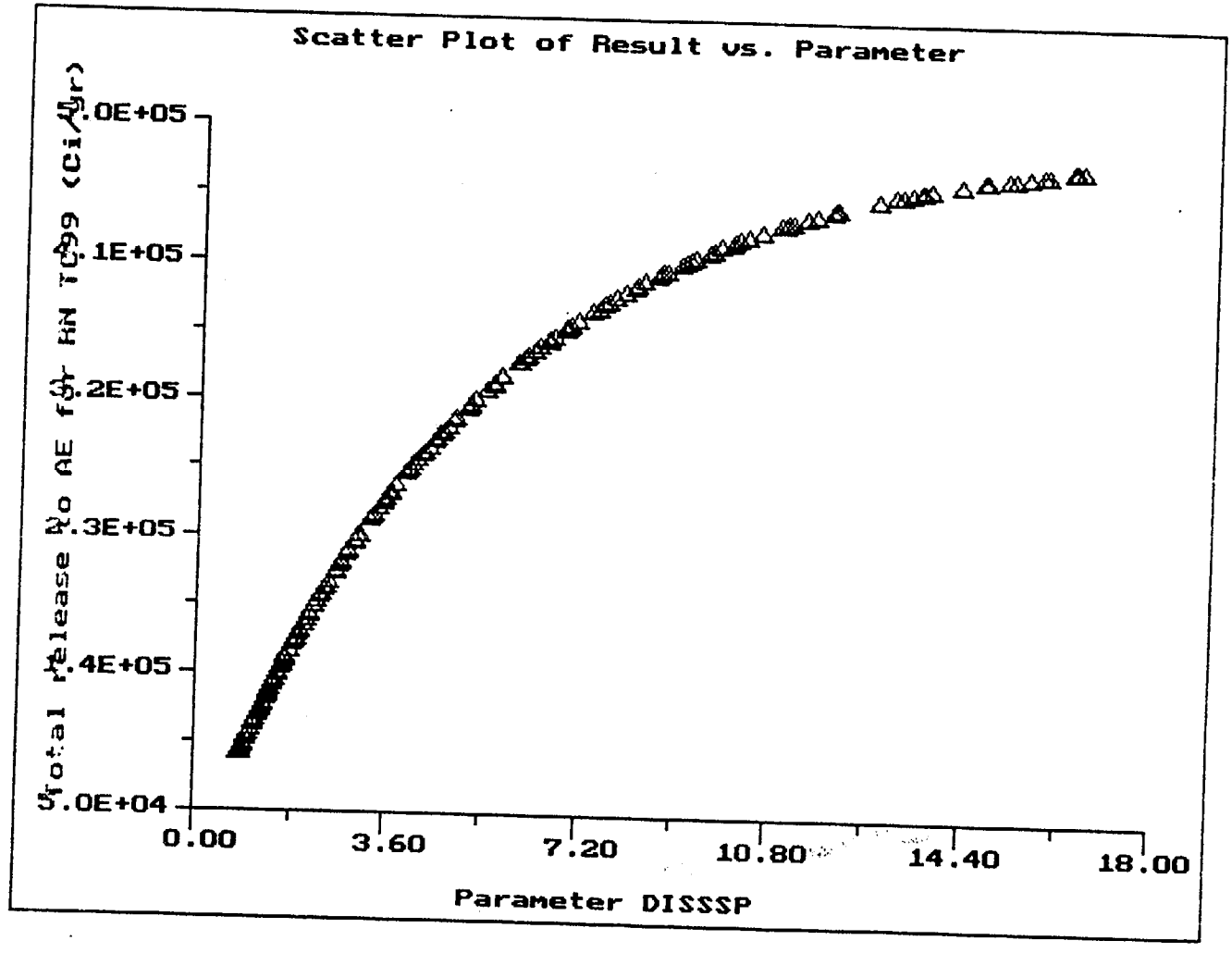

Figure 2-34. Sensitivity Curve of the Release Γc to the Accessible Environment as a Function of the Matrix Dissolution Rate

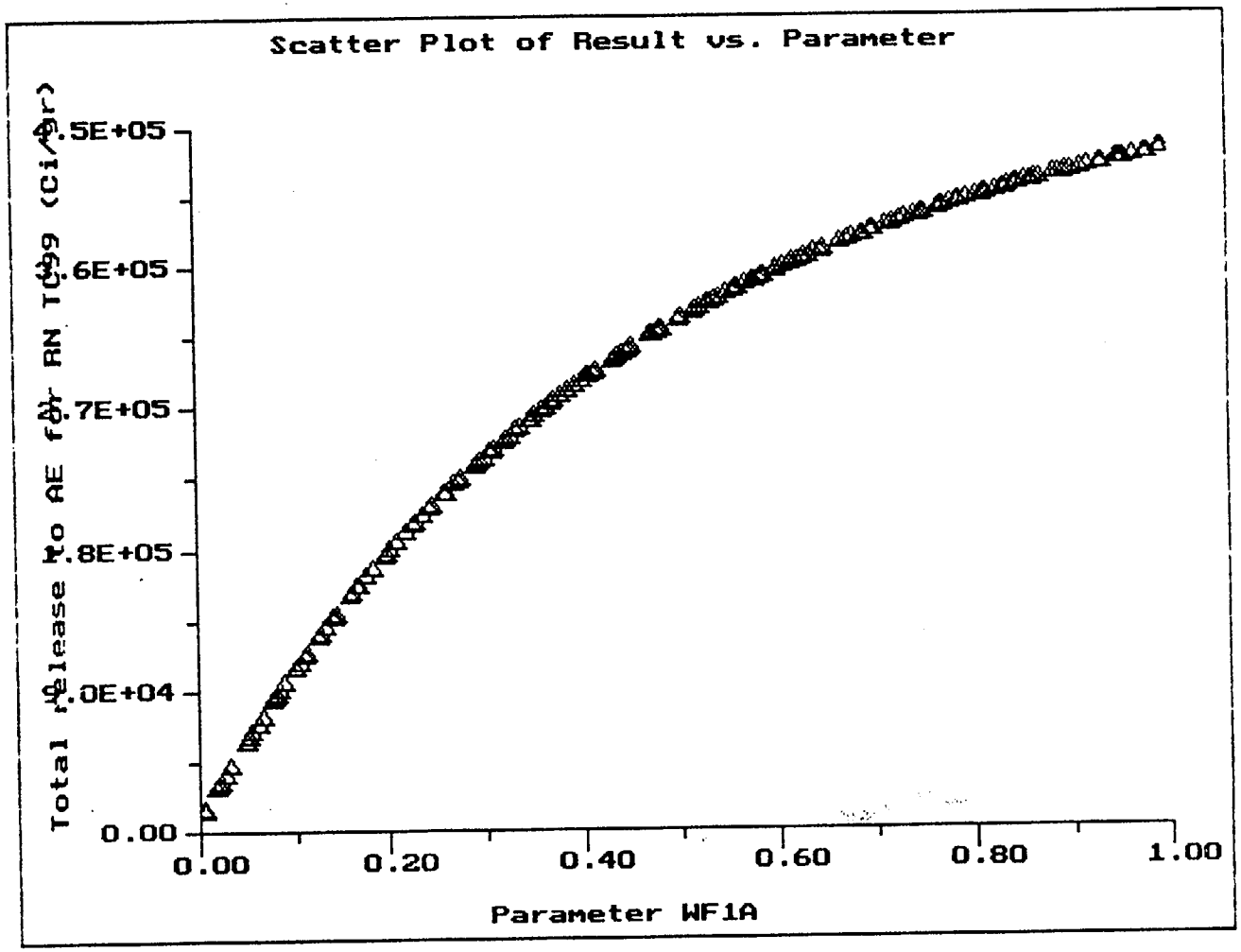

Figure 2-35. Sensitivity Curve of the Release of ^{99}Tc to the Accessible Environment as a Function of the Fraction of Waste Wetted

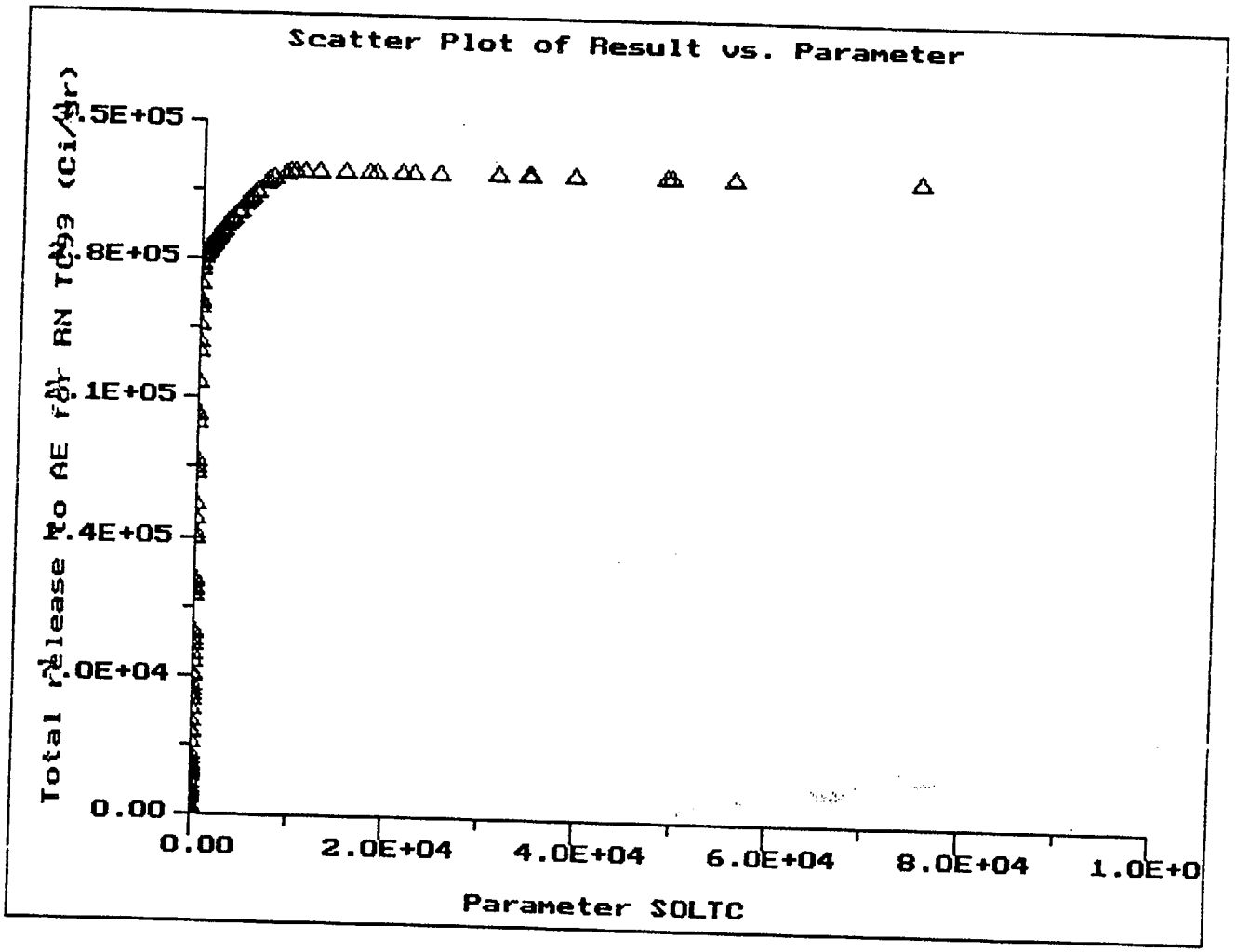

ure 2-36. Sensitivity Curve of the Release of ^{99}Tc to the ccessible Environment as a Function of Technetium Solubility

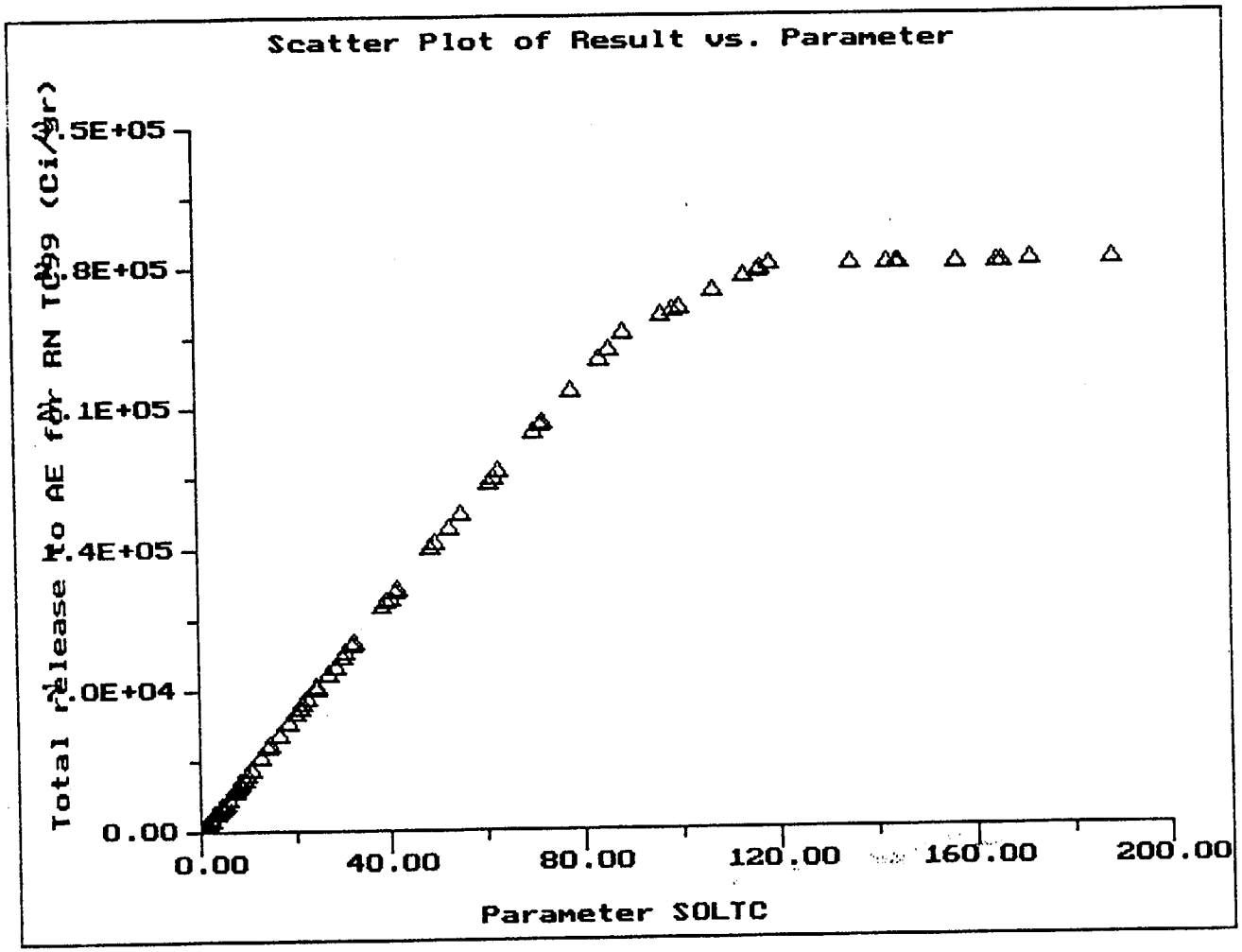

Figure 2-37. Sensitivity Curve of the Release of ^{99}Tc to the Accessible Environment as a Function of Technetium Solubility (low values of S_{Tc})

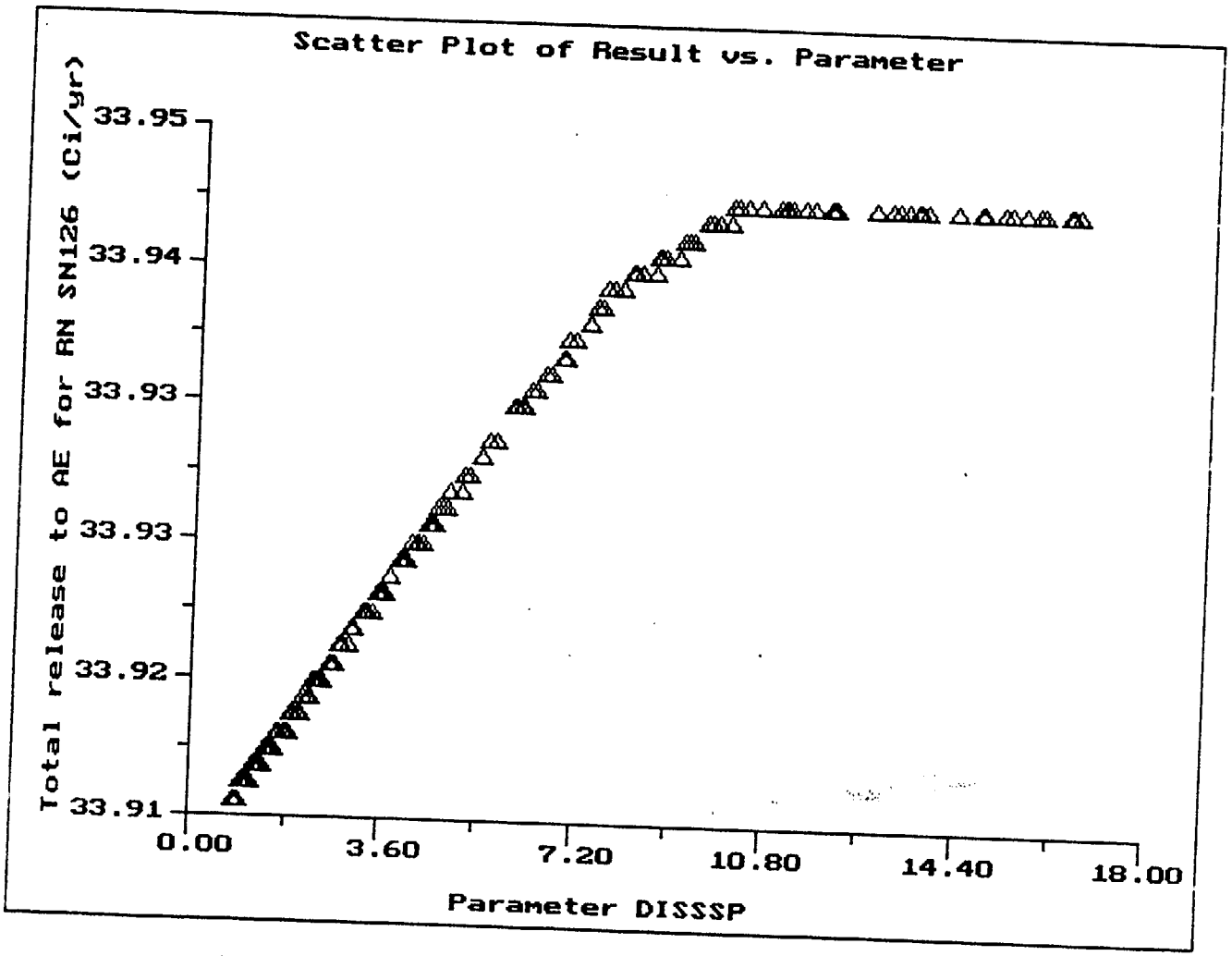

Figure 2-38. Sensitivity Curve of the Relea ^{126}Sn to the Accessible Environment as a Function of the Matrix Dissolution Rate

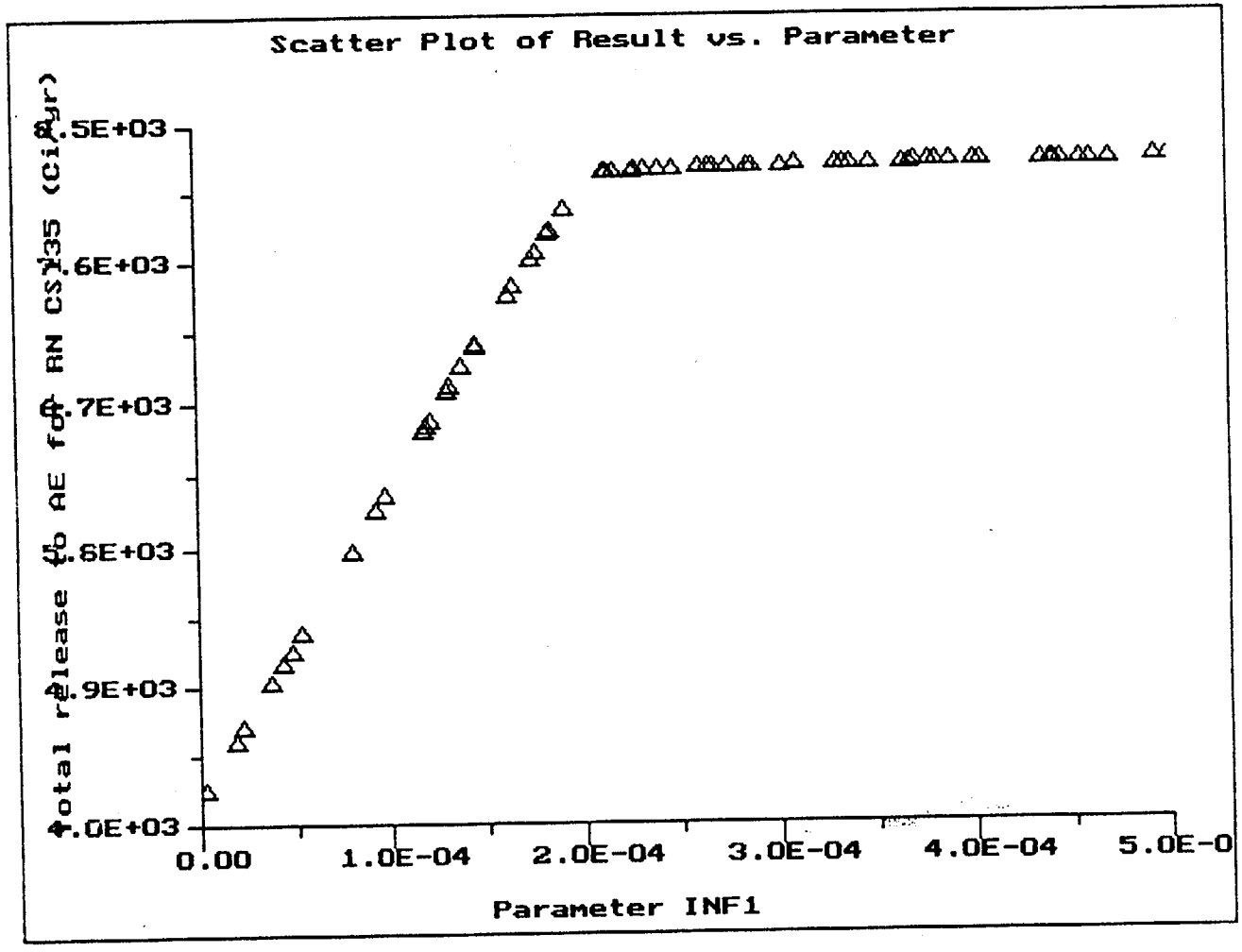

Figure 2-39. Sensitivity Curve of the Release of ^{135}Cs to the Accessible Environment as a Function of the Repository Infiltration Rate

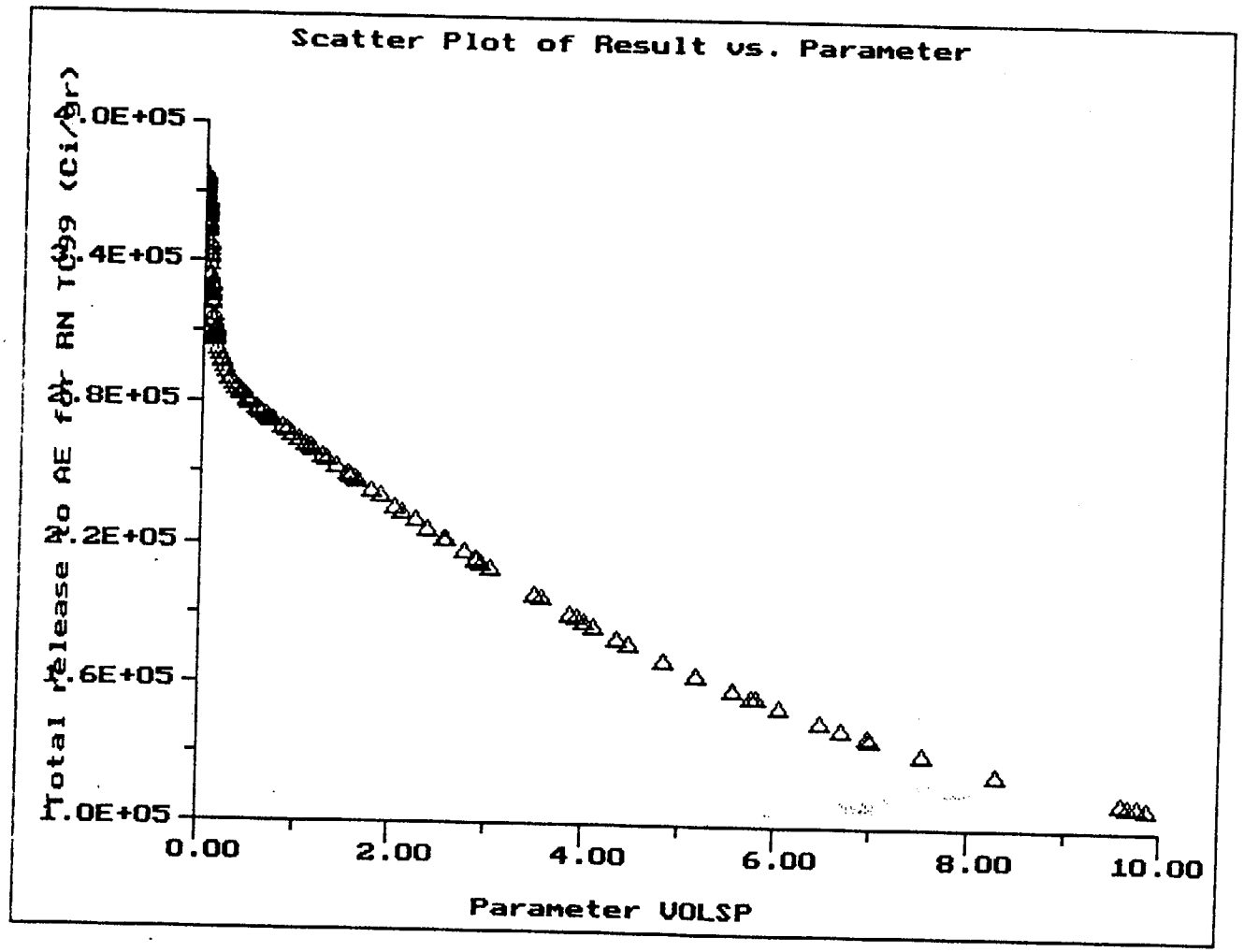

Figure 2-40. Sensitivity Curve of the Release of ^{99}Tc to the Accessible Environment as a Function of the Volume of Water Contacting the Matrix

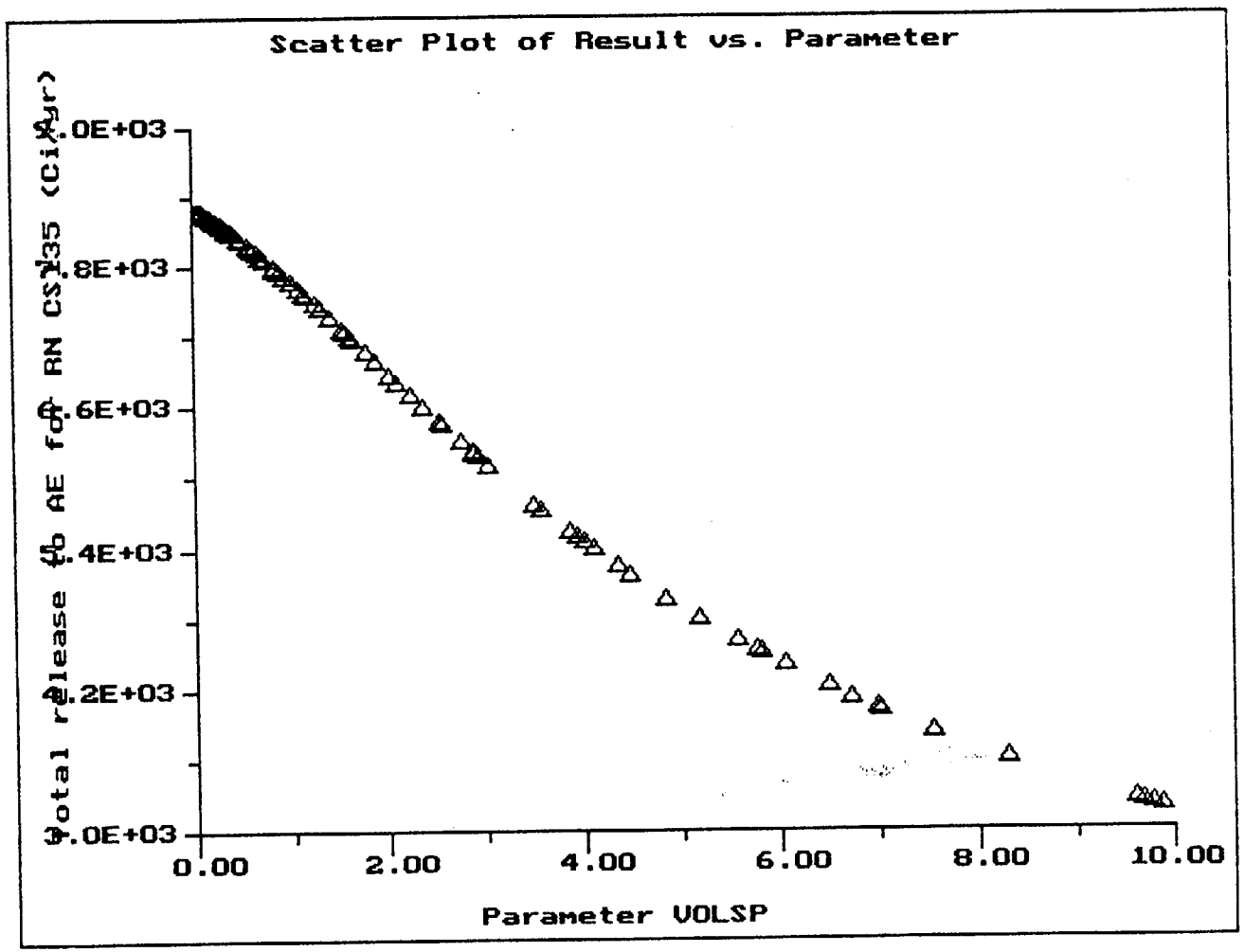

Figure 2-41. Sensitivity Curve of the Release of ^{135}Cs to the Accessible Environment as a Function of the Volume of Water Contacting the Matrix

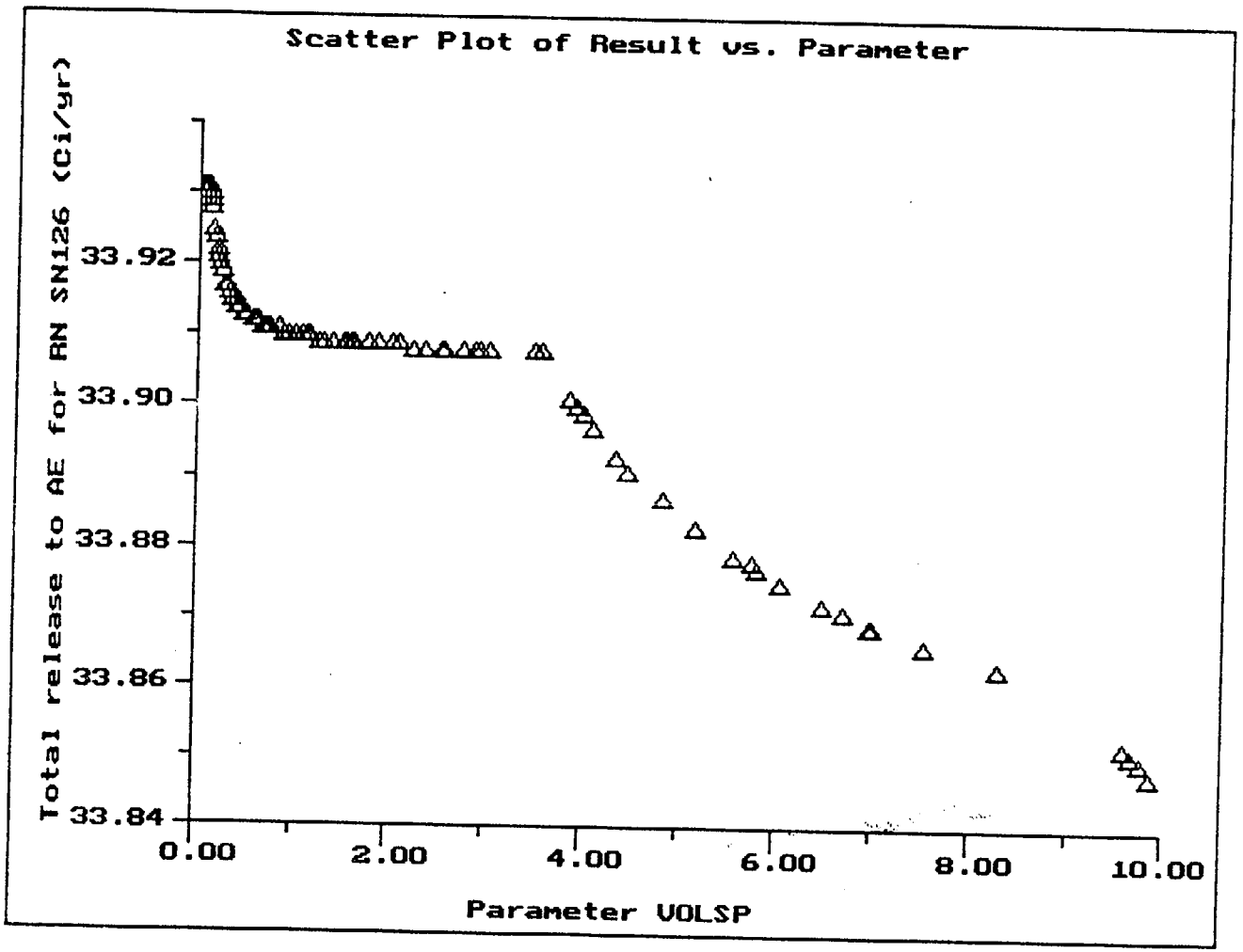

Figure 2-42. Sensitivity Curve of the Release of ^{126}Sn to the Accessible Environment as a Function of the Volume of Water Contacting the Matrix

Table 2-1. Inventory of Radionuclides for Various Analyses

Radionuclide	Aqueous Release Analyses (TSPA-1991 and RIP)	Aqueous Release Analyses Daughter Products (RIP Only)	Gaseous Release Analyses (TSPA-1991 and RIP)
^{243}Am	X		
^{135}Cs	X		
^{129}I	X		
^{237}Np	X		
^{239}Pu	X		
^{79}Se	X		
^{126}Sn	X		
^{99}Tc	X		
^{234}U	X		
^{231}Pa		X	
^{210}Pb		X	
^{226}Ra		X	
^{229}Th		X	
^{230}Th		X	
^{233}U		X	
^{235}U		X	
^{14}C			X

Table 2-2. Comparison of TSPA-1991 Container Parameters with RIP Parameters

TSPA-1991 Model Parameter	TSPA-1991 Base Case	TSPA-1991 Reference (page)	RIP Model Parameter	RIP Base Case
No. waste containers	33,300	4-29	No. packages	PWR - 19,980 BWR - 13,320
Waste burnup (MWd/MTHM)	PWR - 33,000 BWR - 27,500	4-14	Waste burnup (MWd/MTHM)	PWR - 33,000 BWR - 27,500
MTHM in repository	70,000	4-29	Mass waste/pkg = MTHM in repository/# of waste containers	2.1 MTHM/ container

Table 2-3. Comparison of TSPA-1991 Inventory Parameters with RIP Parameters

Inventory	TSPA-1991 Base Case (1) Ci/MTHM (2) Prompt release (3) Solubility (mol/l) (4) Activity (Ci/mol)	TSPA-1991 Reference (page)	RIP Base Case (1) Ci/container[1] (2) Gap fraction (3) Solubility (g/m^3) (4) Activity (Ci/g)
^{243}Am	(1) 1.54×10^{1} (2) 0 (3) LU: 1.2×10^{-11}, 3.8×10^{-9}, 6.6×10^{-10} (4) 4.84E1	4-13 4-13 4-29 4-13	(1) 32.34 (2) 0 (3) LU: 2.92×10^{-6}, 9.2×10^{-4}, 1.6×10^{-4} (4) 2×10^{-1}
^{135}Cs	(1) 3.51×10^{-1} (2) 0.02 (3) Infinite (4) 1.55×10^{-1}	4-13 4-13 Wilson, 1993 4-13	(1) 7.37×10^{-1} (2) 0.02 (3) Infinite (4) 1.15×10^{-3}
^{129}I	(1) 2.95×10^{-2} (2) 0.02 (3) Infinite (4) 2.28×10^{-2}	4-13 4-13 Wilson, 1993 4-13	(1) 6.19×10^{-2} (2) 0.02 (3) Infinite (4) 1.77×10^{-4}
^{237}Np	(1) 1.12 (2) 0 (3) LU: 5.9×10^{-11}, 1.9×10^{-8}, 3.3×10^{-9} (4) 1.67×10^{-1}	4-13 4-13 4-29 4-13	(2) 2.35 (2) 0 (3) LU: 1.4×10^{-5}, 4.5×10^{-3}, 7.82×10^{-4} (4) 7.06×10^{-4}
^{239}Pu	(1) 3.08×10^{-2} (2) 0 (3) LU: 1.6×10^{-10}, 5.1×10^{-8}, 8.8×10^{-9} (4) 1.49×10^{1}	4-13 4-13 4-29 4-13	(1) 6.47×10^{2} (2) 0 (3) LU: 3.82×10^{-5}, 1.22×10^{-2}, 2.1×10^{-3} (4) 6.22×10^{-2}
^{79}Se	(1) 3.81×10^{-1} (2) 0.02 (3) Infinite (4) 5.5	4-13 4-13 Wilson, 1993 4-13	(1) 8.0×10^{-1} (2) 0.02 (3) Infinite (4) 6.98×10^{-2}
^{126}Sn	(1) 7.15×10^{-1} (2) 0 (3) LU: 1.0×10^{09}, 3.2×10^{-7}, 5.5×10^{-8} (4) 3.58	4-13 4-13 4-29 4-13	(1) 1.50 (2) 0 (3) LU: 1.26×10^{-4}, 4.03×10^{-2}, 6.93×10^{-3} (4) 2.84E-2
^{99}Tc	(1) 1.23×10^{-1} (2) 0.02 (3) Infinite (4) 1.68	4-13 4-13 Wilson, 1993 4-13	(1) 2.58×10^{1} (2) 0.02 (3) Infinite (4) 1.7×10^{-2}
^{234}U	(1) 1.89 (2) 0 (3) LU: 7.1×10^{-11}, 2.3×10^{-8}. 4.0×10^{-9} (4) 1.46	4-13 4-13 4-29 4-13	(1) 3.97 (2) 0 (3) LU: 1.66×10^{-5}, 5.38×10^{-3}, 9.36×10^{-4} (4) 6.26E-3

LU = Log-Uniform: min, max, expected values

[1] Ci/container = Ci/MTHM · 2.1 mthm/container

Table 2-4. Comparison of TSPA-1991 WP Failure Parameters with RIP Parameters

TSPA-1991 Model Parameter	TSPA-1991 Base Case	TSPA-1991 Reference (page)	RIP Model Parameter	RIP Base Case
Beginning of resaturation period (yr)	300	4-29	Primary container failure definition: start at 800 years	Uniform: 800 - 1,800 years
Duration of resaturation period (yr)	1,000	4-29	Primary container failure definition: start at 800 years	Uniform: 800 - 1,800 years
Container lifetime when wet (yr)	LU: 500, 10,000, 3,170	4-29	Secondary container failure	1) Weibull: 1, 1650 2) LU: 500-10,000; gradual failure 3) LU: 500-10,000; all fail at once 4) LU: 500-10,000; sample maximum failure and fail gradually to that time

LU = Log-Uniform: min, max, expected value

Table 2-5. Comparison of TSPA-1991 Exposure Parameters with RIP Parameters

TSPA-1991 Model Parameter	TSPA-1991 Base Case	TSPA-1991 Reference (page)	RIP Model Parameter	RIP Base Case
Fraction of containers with rubble in air gap (f_r)	0.5	4-29	(1) Fraction of containers in water contact mode 3 - moist continuous (2) Fraction of waste wetted (3) Effective catchment area (ECA) (4) Effective diffusion coefficient (EDC)	0.25 0.5 0 SNL moist diff. coeff. (LU: 3.0×10^{-10} - 3.0×10^{-4})
Fraction of fuel wet with seepage (f_{ws})	0.5	4-29	(1) Fraction of containers in water contact mode 2 - wet drip (2) Fraction of waste wetted (3) ECA (4) EDC	0.25 0.5 1 0
Fraction of fuel wet and diffusing (f_{wd})	0.5	4-29	(1) Fraction of containers in water contact mode 1 - wet feet (2) Fraction of waste wetted (3) ECA (4) EDC	0.25 0.5 1 SNL wet diff. coeff. (LU: 9.0×10^{-4} - 9.0×10^{-3})
Nominal case - no release			(1) Fraction of containers in water contact mode 4 - nominal case	0.25
			Air alteration rate	0
Matrix alteration rate (a_m) (1/yr)	LU: 5.0×10^{-5}, 1.0×10^{-3}, 3.17×10^{-4}	4-29	Matrix dissolution rate ($g/m^2/yr$)	LU: 5.0×10^{-5}, 1.0×10^{-3}, 3.17×10^{-4}
			Surface area of matrix (m^2/g) (combined with matrix dissolution rate)	1
Prompt alteration rate (a_p) (1/yr)	0.5	4-29	N/A -- RNs put in gap fraction	
Spent fuel surface area per package (A) (m^2)	140	4-29	Included in water volume contacting matrix (m^3) (=surface area · water film thickness · fraction of fuel wet)	0.07
Water film thickness (d_{film}) (mm)	1	4-29	Included in water volume contacting matrix (m^3)	0.07

LU = Log-Uniform: min, max, expected value

Table 2-6. Comparison of TSPA-1991 Transport Parameters with RIP Parameters

TSPA-1991 Model Parameter	TSPA-1991 Base Case	TSPA-1991 Reference (page)	RIP Model Parameter	rip Base Case
Moist diffusion coefficient (m^2/yr)	LU: 3.0×10^{-6}, 3.0×10^{-4}, 6.45×10^{-5}	4-29	Effective diffusion coefficient (m^2/yr)	LU: 3.0×10^{-6}, 3.0×10^{-4}, 6.45×10^{-5}
Wet diffusion coefficient (m^2/yr)	LU: 9.0×10^{-4}, 9.0×10^{-3}, 3.52×10^{-3}	4-29	Effective diffusion coefficient (m^2/yr)	LU: 9.0×10^{-4}, 9.0×10^{-3}, 3.52×10^{-3}
Flux coefficient of variation	1.3	4-29	None	
Percolation rate (mm/yr)	Beta: 1.1, 0, 39	3-21	Repository infiltration rate (m/yr)	Beta: 1.0×10^{-3}, 9.0×10^{-4}, 0, 3.9×10^{-2} (only for contact modes 1,2)
Effective diffusion area (m^2)	0.172	4-29	Geometric factor for diffusion (m)	0.1 (only for contact modes 1,3)
Fraction of seepage through A_{cross} actually entering container	0.5	4-29	N/A (see effective catchment area)	
Water collection area (A_{cross}) (m^2)	2	4-29	Effective catchment area (m^2) = water collection area · fraction of seepage entering container	Contact 1 = 1 Contact 2 = 1 Contact 3 = 0 Contact 4 = 0
Rubble thickness (cm)	3	4-29	Delay pathway (only in moist continuous)	3 cm

LU = Log-Uniform: min, max, expected value

Table 2-7. Major Parameter Differences between RIP Simulations

Run	Log-Uniform WP Failure Distribution	Nine RNs	Hi-Solubility for ^{99}Tc, ^{135}Cs	Revised Failure Distri-bution	Implement f_s, f_r WP Distribution Calculations	Air Gap	Figure No.
2.1	N	N	N	N	N	N	2-13
2.2	Y	N	N	N	N	N	2-14
2.3	Y	Y	N	N	N	N	2-15
2.4	Y	Y	Y	N	N	N	2-16
2.5	Y*	Y	Y	Y	N	N	2-17
2.6	Y*	Y	Y	Y	Y	N	2-18
2.7	Y*	Y	Y	Y	Y	Y	2-19
2.8	Y*	Y	Y	Y	Y	Y	2-20

* Log-uniform distribution is implemented in the start time of the secondary container failure distribution.

Table 2-8. Comparison of Peak Values for Individual Radionuclide Release (Ci/yr)

Radionuclide	TSPA-1991	Run 2.8	Run 2.5	Run 2.4
SOLUBILITY-LIMITED				
^{237}Np	3.2×10^{-5}	2.6×10^{-5}	2.6×10^{-5}	2.6×10^{-5}
^{239}Pu	8.0×10^{-3}	6.1×10^{-3}	6.1×10^{-3}	6.1×10^{-3}
^{243}Am	1.9×10^{-3}	1.5×10^{-3}	1.5×10^{-3}	1.5×10^{-3}
^{234}U	3.4×10^{-4}	2.7×10^{-4}	2.7×10^{-4}	2.7×10^{-4}
^{126}Sn	1.2×10^{-2}	9.3×10^{-3}	9.3×10^{-3}	9.3×10^{-3}
ALTERATION-LIMITED				
^{129}I	0.10	0.17	0.18	0.11
^{135}Cs	0.88	2.0	2.1	1.3
^{79}Se	1.2	2.1	2.2	1.4
^{99}Tc	40	70	73	46

Table 2-9. High-Solubility Radionuclides (^{99}Tc) Waste Alteration Sensitivity Analyses

Parameter	Range	Expected Value	Sensitivity	Sensitivity Due To Modes
Matrix dissolution rate ($g/m^2/yr$)	0.84 - 16.8	5.33	Log-like: 440% increase	WF, WD, MC
Fraction of waste wetted	0.0 - 1.0	0.5	Log-like: 2900% increase	WF, WD, MD
Solubility (g/m^3)	0.035 - 990,000	12,540	Linear:(1) 0-90: $m_1 = 2,700$ 120 - 9,000: $m_2 = 5.2$ 9,000 - 9.9×10^{-5}: $m_3 = 0$	WF, WD, MC

(1) The sensitivity curve is a series of three line segments, decreasingly steep as the solubility increases. The transition from one line segment to the next is smooth, and it does not appear that there are discontinuities in slope.

Table 2-10. Low-Solubility Radionuclides (^{239}Pu) Waste Alteration Sensitivity Analyses

Parameter	Range	Expected Value	Sensitivity	Sensitivity Due To Modes
Matrix dissolution rate ($g/m^2/yr$)	0.84 - 16.8	5.33	None(1)	N/A(1)
Fraction of waste wetted	0.0 - 1.0	0.5	None(2)	N/A(2)
Solubility (g/m^3)	3.8×10^{-5} - 0.012	0.0021	Linear: m = 10,627	WF, WD, MC

(1) Of the low-solubility radionuclides, only ^{126}Sn exhibits any sensitivity to changes in the matrix dissolution rate. The release increases linearly (m=0.004) until it becomes constant at R_{dis}=10. Tin has a higher solubility than the other low-solubility radionuclides, and this accounts for its sensitivity. The *wet-feet* and *wet-drip* modes are the important mechanisms for this release.

(2) ^{239}Pu and ^{237}Np are not dependent on f_w, but the release of ^{234}U and ^{126}Sn increase and then becomes constant as f_w increases. However, the overall increases are relatively small (0.1% and 0.7%, respectively). The release is dependent on the WF, WD, and MC modes.

Table 2-11. High-Solubility Radionuclides (^{99}Tc) Release Parameter Sensitivity Analyses

Parameter	Range	Expected Value	Sensitivity	Sensitivity Due to Modes
Repository infiltration rate (m/yr)	0.0 - 0.039	0.001	0 - 0.00008: linear $m = 1.2 \times 10^9$ 0.0004 - 0.039: constant	WF, WD
Water volume contacting matrix	0.001 - 10	0.07	Monotonically decreasing: 244%	WF, SD, MC
MC diffusion coefficient (m^2/yr)	3×10^{-6} - 3×10^{-4}	6.45×10^{-5}	0 - 0.0006:(1) linear: $m = 1.5 \times 10^9$ 0.00006 - 0.0003: constant	MC
WF diffusion coefficient (m^2/yr)	9×10^{-4} - 9×10^{-3}	3.52×10^{-3}	None	N/A
Geometric factor for diffusion (m)	0.1 - 10.0	1.0	Left-most point(2)	MC
Effective catchment area (m^2)	0.1 - 10.0	1.0	None(3)	N/A(3)

(1) The sensitivity depends on the radionuclide and the range of values of the parameter of interest. The release of ^{135}Cs increases linearly over the entire range of interest. ^{99}Tc and ^{79}Se increase linearly before they become constant, and ^{129}I is constant.

(2) The sensitivity depends on the radionuclide. ^{135}Cs increases linearly from 0.1 to 3.2, with a slope m = 1270, then becomes constant at w = 3.2. ^{99}Tc seems to have a similar dependence, only it is shifted left so that almost all the linear rise is outside the range of interest. The sensitivity curves for ^{129}I and ^{79}Se are shifted over even more, so that the 0.1 - 10 window covers the constant region only; there is no dependence.

(3) As for the two comments above, the sensitivity to A_c depends on the radionuclide. ^{135}Cs release increases linearly, then becomes constant. The sensitivity arises from the *wet-drip* waste packages. ^{79}Se, ^{99}Tc, and ^{129}I are constant over the range of interest.

Table 2-12. Low-Solubility Radionuclides (^{239}Pu) Release Parameter Sensitivity Analyses

Parameter	Range	Expected Value	Sensitivity	Sensitivity Due to Modes
Repository infiltration rate (m/yr)	0.0 - 0.039	0.001	Linear: m = 19,000	WF, WD
Water volume contacting matrix	0.001 - 10	0.07	None(1)	N/A(1)
MC diffusion coefficient (m^2/yr)	3×10^{-6} - 3×10^{-4}	6.45×10^{-5}	Linear: m = 950	MC
WF diffusion coefficient (m^2/yr)	9×10^{-4} - 9×10^{-3}	3.52×10^{-3}	Linear: m = 953	WF
Geometric factor for diffusion (m)	0.1 - 10.0	1.0	Linear: m = 33.9	WF, MC
Effective catchment area (m^2)	0.1 - 10.0	1.0	Linear: m = 19.0	WF, WD

(1) The releases of ^{239}Pu and ^{237}Np are constant. For sufficiently large volumes, the releases of ^{234}U, ^{243}Am, and ^{126}Sn decrease as the volume increases. The dependence is due to the WF, WD, and MC water contact modes.

Table 2-13. Correlation Coefficients for RUN 2.9

RN	$D_{eff,mc}$	R_{dis}	f_w	S_{Tc}
^{243}Am	0.901	0.045	0.031	-0.00
^{237}Np	1.005	0.054	0.045	-0.00
^{239}Pu	1.013	0.055	0.046	-0.00
^{126}Sn	0.104	0.034	0.063	0.008
^{234}U	0.909	0.044	0.027	-0.00
^{135}Cs	0.120	0.710	0.618	-0.00
^{129}I	0.077	0.711	0.618	-0.00
^{79}Se	0.077	0.714	0.609	-0.00
^{99}Tc	0.115	0.378	0.336	0.226

Table 2-14. Correlation Coefficients for RUN 2.10

RN	$D_{eff,wf}$	$D_{eff,mc}$	A_c	w	q_{int}	S_{Pu}
^{234}Am	0.362	0.008	0.335	0.640	0.290	-0.03
^{237}Np	0.362	0.008	0.335	0.640	0.290	-0.03
^{239}Pu	0.149	-0.00	0.143	0.296	0.113	0.562
^{126}Sn	0.361	0.008	0.336	0.640	0.290	-0.03
^{234}U	0.362	0.008	0.335	0.640	0.290	-0.03
^{135}Cs	-0.00	0.504	0.176	0.501	0.297	0.014
^{129}I	-0.00	-0.00	-0.00	-0.00	-0.00	-0.00
^{79}Se	0.001	0.001	-0.00	0.000	0.000	0.000
^{99}Tc	-0.04	0.397	-0.02	0.394	0.058	0.029

3. AQUEOUS FLOW AND TRANSPORT TO THE ACCESSIBLE ENVIRONMENT

This section presents the analyses related to aqueous transport of radionuclides from the potential repository to the accessible environment, through the unsaturated and saturated flow zones. The approach adopted by Sandia National Laboratories for TSPA-1991 (Barnard et al., 1992) is described briefly, along with their choice of the different hydrogeological and geochemical parameters. The present approach to these analyses with RIP uses different models which involve different conceptualizations of the flow and transport regimes. These conceptualizations are also described here, together with the parameters used for these analyses.

The present analyses use the same definitions of the problem domain and stratigraphy used in TSPA-1991. Most of the hydrogeologic and geochemical parameters are common to the previous analysis of Barnard et al. (1992). The RIP analysis seeks to use the same values for such parameters. However, RIP imposes restrictions on the parameter distributions which are different from those in TSPA-1991 (Barnard et al., 1992). The present analyses incorporate such required modifications in the distributions of those parameters.

This section also presents the results of the RIP simulations and compares them with those of the TSPA-1991 (Barnard et al., 1992) analyses.

3.1 PROBLEM DOMAIN

The details related to the definition of the problem domain and the stratigraphy are presented here. These are taken directly from TSPA-1991 (Barnard et al., 1992).

The flow and transport problem domain sampled the volume directly beneath the potential repository to the water table and, in the saturated zone, out to the accessible environment. Figure 3.1 shows the boundary of the potential repository. A 2-D cross-section across the potential repository block was chosen in TSPA-1991 to represent unsaturated-zone hydrologic conditions throughout the potential repository block (Figures 3-1 and 3-2). The potential repository was divided into six equal subregions. Each subregion is represented by a vertical column for simulating unsaturated flow. The subregions and the location of the columns are shown in Figure 3-1.

The saturated zone parameters used in TSPA-1991 were based on flow models by Czarnecki and Waddell (1984) and Czarnecki (1985).

A five-layer model was used in TSPA-1991 to define the unsaturated zone (Figure 3-3). The layers represent different types of ash-flow tuff observed at Yucca Mountain. From the top of the domain to the bottom, the layers are given in Table 3-1. The elevations of each layer are summarized in Table 3-2.

The percolation rate was modeled in TSPA-1991 by a beta distribution with a total range from 0.0 to 39 mm/year with a mean of 1.0 mm/yr.

3.2 CONCEPTUALIZATION AND MATHEMATICAL MODEL (TSPA-1991)

Two different conceptual models of flow in the unsaturated zone are studied in TSPA-1991: (1) the composite-porosity model that combines matrix and fractures into a single composite porosity medium for analysis; this model permits unrestricted water movement between fractures and matrix; and (2) the weeps model, a model that depicts essentially all of the percolating water traveling down fractures. The potential repository thermal effects are ignored. Radionuclide retardation during transport is modeled by a simple distribution coefficient (K_d).

In the TSPA-1991 analyses using the composite porosity model, the characteristic curves, i.e., the relative permeability versus the capillary pressure and saturation curves used to describe the hydrologic properties of the matrix and fractures, determine the distribution of flow between matrix and fractures. These curves for the matrix and fractures are dissimilar, and as a result flow tends to reside primarily in the matrix until the flux exceeds the saturated conductivity of the matrix, at which point the excess flow would be diverted into the fractures.

Models that allow the matrix and fractures to be completely decoupled (e.g., the weeps model) result in markedly different steady-state flow solutions. The results of such models are not comparable to the analyses presented herein, which assume a composite-porosity formulation. The details of such models, pursued in TSPA-1991, are not presented here.

Figure 3-3 shows the six columns used for the composite-porosity model in TSPA-1991 and this study. The top of each column is 10 m above the repository horizon. Elevations for each of the units within each column, and at each drill hole, are presented in Table 3-3.

For the TSPA-1991 calculations, the saturated zone was simplified to a one-dimensional flow tube 5000 m in length. For every calculation, radionuclides released from the repository were provided as a point-source to the flow tube underlying the potential repository.

The transport model in the TRANS module of TOSPAC is a one-dimensional dual-porosity model of solute transport, containing two generalized advection-dispersion differential equations. The equation models retardation and the transfer between matrix and fracture due to advection and diffusion mechanisms. The model is used for transport both in saturated and unsaturated zones.

The parameter distributions used by the TSPA-1991 analyses are given in Tables 3-4 through 3-9. Most of the distributions are taken to be described by beta distributions. In addition, these tables also provide the distributions as used in the present analyses using the RIP code.

The Yucca Mountain tuffs were represented by three rock types for purposes of defining the sorption-coefficient distributions: devitrified, zeolitic, and vitric. The relationship between those rock types and the stratigraphy defined earlier is shown in Table 3-9. The distributions of K_d values for the different nuclides in the different rock types are shown in Table 3-10.

3.3 RIP MODEL: FLOW AND TRANSPORT SIMULATION CAPABILITY

In the RIP model, the physical domain of flow and transport is represented as a network of one-dimensional legs, designated as *pathways*. Each leg may have flow in one mode or in several modes. When there are multiple modes in a leg, each mode relates to one flow velocity. A leg with one mode may represent a homogeneous medium. In a leg with two modes, for example, mode 1 can correspond to flow in a fracture, while mode 2 can correspond to flow in the matrix. For purposes of the present application, a maximum of two modes is used. In each mode (fracture and matrix), the flow velocity is considered uniform (constant) for a given leg. The degree of interaction between the modes is governed by the choice of a Poisson transition rate parameter.

In reality, the RIP model cannot simulate flow conditions. It demands an input of flow velocity (interstitial), either directly or indirectly. It requires input of flow parameters such as flow rate (Q), the cross-sectional area of the leg (A), and porosity (ϕ), and computes the interstitial velocity (v), by:

$$v = \frac{Q}{A \cdot \phi} \tag{3-1}$$

The user may input interstitial velocity for each mode directly, which then overrides the above computed value. When there are two modes, the user also needs to input the flow fraction for the fracture mode. The input parameters may be given as numerical values, or as algebraic or logical functions of other input parameters. The model does not distinguish between saturated and unsaturated flow conditions.

The transport simulation within RIP consists of two stages. The principle behind the actual algorithm may be explained as follows:

- Computing a breakthrough curve and deducing an impulse source response function
- Convolution of the source rate with the impulse source response to give the nuclide release rate.

For legs with a single flow mode, the analytical solution for the one-dimensional advection-dispersion transport equation is used to generate the breakthrough curve. For this purpose, the dispersivity of the medium needs to be input.

For legs with multiple modes, a Markov process algorithm is used to generate the breakthrough curve. In RIP, a simplified version of the Markov process is implemented. In the Markov process, a particle is released into the flow system and may enter mode 1 or mode 2. The probability of the particle entering any mode is proportional to the flow fraction for that mode. The particle travels a random length in that mode, and then tranfers into the other mode (in a system with only two modes, as in the present application). In a true Markov process, the process of traveling a random length in a given mode and transitioning to the next mode may occur a number of times before the particle exits the leg. In the simplified version implemented in RIP, the particle travels only one random length in the given medium, with the remaining

length of the leg traveled at the temporal mean velocity of the two modes. An analytical expression for the cumulative distribution function of the travel times for this simplified Markov process is available and is used to represent the breakthrough curve. (For a true Markov process, random simulation of travel times is required to obtain the CDF, which constitutes the breakthrough curve.) Breakthrough curves are derived separately for each radionuclide, considering their retardation factors. The impulse source response can be constructed by a procedure of numerical differentiation.

For numerical implementation of the above scheme, discretization in the time domain is done as follows. Discrete time points are defined by:

$$0,\ \Delta t,\ f\Delta t,\ f^2\Delta t,\ f^3\Delta t,\ f^4\Delta t,\ \text{etc.}$$

where Δt is a user-specified time step and f is a time-stepping factor, set at f = 2 in the current version of RIP. For example, if Δt = 100 years, the time points would be:

$$0,\ 100,\ 200,\ 400,\ 800,\ 1600,\ \text{etc.}$$

Consider, for example, the time window from 800 years to 1600 years. The mass of nuclides released during this time window is the difference between the ordinates of the breakthrough curve at 1600 years and 800 years. This mass is released at the end of the leg, at a uniform rate, starting from 800 years to 1600 years. (This corresponds to a piece-wise linear approximation of the breakthrough curve.) Further, nuclide decay will also be accounted for during this time period. This numerical algorithm produces an earlier breakthrough than the true case (see Appendix B). The error of the earlier breakthrough time reduces if f is chosen closer to one, but this dramatically increases the run time.

The parameters governing the nuclide release rates, which are essential inputs, are:

- Length of the leg
- Flow proportions of each mode
- Flow velocity in each mode (v)
- Retardation factors (R)
- Poisson transition rate (λ).

The *Poisson Transition Rate* parameter, λ, is a parameter defining the exponential distribution, which is assumed for random travel length in a mode. The reciprocal of λ gives the particle's mean length of travel in the mode. The standard deviation for this distribution equals the mean value.

3.4 CONCEPTUALIZATION OF FLOW AND TRANSPORT IN RIP

The problem domain, stratigraphy, and the six one-dimensional vertical columns used for unsaturated flow in the composite-porosity model of TSPA-1991 have been used with our RIP analyses without modifications. Also, the horizontal leg for the saturated flow is used in exactly the same way as in the TSPA-1991 analysis. The differences that arise due to the code features are described below.

The six vertical columns shown in Figure 3-3 and defined in Table 3-3 are used for simulating the unsaturated flow. Each stratigraphic unit is treated as one leg (or pathway) per column. Thus, columns 1 through 4 have five legs each, while columns 5 and 6 have four legs each, giving a total of 28 legs for unsaturated flow.

As mentioned earlier, the RIP code does not distinguish between saturated and unsaturated flow. However, the special input capabilities of the code have been exploited to mimic the physics of unsaturated flow. In this analysis, the legs simulating unsaturated flow have been assigned two modes, corresponding to the fracture and the matrix. The logic presented below describes the apportionment of the infiltration rate between the matrix and the fracture. This logic is designed to mimic the physics of the composite-porosity model of TSPA-1991.

It is known that the matrix can carry the infiltration at a maximum rate equal to the saturated hydraulic conductivity of the matrix (under a unit hydraulic gradient). Thus, if the infiltration rate is less than the saturated hydraulic conductivity of the matrix, the entire infiltration would pass through the matrix, with no flow in the fractures. If, however, the infiltration rate is higher, the matrix carries the flow rate equal to its saturated hydraulic conductivity, and the balance will be carried by the fractures. This conceptualization is illustrated in Figure 3-4. The composite-porosity flow model, which can simulate the physics of unsaturated flow, with complete interaction between fractures and the matrix, results in a similar apportionment of flow between matrix and fractures. It may be noted that the RIP model does not use soil characteristic parameters that define the water-retention properties of the matrix and fractures. (These are used by the composite-porosity model of TSPA-1991.) For the determination of the interstitial pore velocity, the matrix is assumed to be fully saturated. The degree of saturation in fractures is assumed to be 10% (see Appendix C).

The geometry of the one-dimensional leg used for the simulation of saturated flow is the same as in the TSPA-1991 analysis. All the input parameters used (velocity, porosity, retardation parameters) are also the same as in the TSPA-1991 analysis. In RIP, this leg is used with one mode which corresponds to a homogeneous porous medium.

The transport parameters used in the RIP analysis, such as retardation parameters for the unsaturated and saturated zones, and dispersivity for saturated zones, remain the same as those used in TSPA-1991. A new transport parameter, the Poisson transition rate, λ, is required as input to RIP. Although this parameter has limited physical significance, it is an important model input for the two-mode (fracture and matrix) transport in the unsaturated zone. The sensitivity of the results (e.g., EPA sum at the accessible environment) are investigated for a range of values of λ (10^{-8}, 10^{-3}, 10^{-2}, 10^{-1}, 10^{0}, 10^{1}, 10^{8} m^{-1}) by repeating the stochastic simulations of 1,000 realizations for each value of λ chosen.

The parameters used for the RIP model, and their distributions, are essentially the same as used in the TSPA-1991 analysis. It has already been noted that the RIP model does not use the soil characteristic parameters characterizing the water-retention properties of the matrix and fractures. For this analysis, the Poisson transition rate λ value has been kept as constant and is not defined by a distribution. Most of the probability density functions are defined by beta distributions. The RIP model imposes some restrictions on the beta distributions. For example, the coefficient of variation (C_v) should be less than one for RIP, while many of the beta distributions in

TSPA-1991 have a C_v of unity. Similarly, the range between the maximum and minimum should be less than 40 times the standard deviation in the RIP model. Thus, the beta distributions input to the RIP model are different from those in TSPA-1991. However, those differences are insignificant and are not considered to have any effect on the results.

Tables 3-4 through 3-9, which show the distributions for the different parameters used in TSPA-1991, also show the corresponding values used for the RIP model.

3.5 RESULTS OF RIP SIMULATIONS

Several simulations have been performed for the flow and transport through the unsaturated and saturated zones. The results from the RIP model are compared with those from the TSPA-1991 analysis. For purposes of presentation, these results are separated into three categories:

- Verification tests for RIP (see Appendixes B and C)
- CCDFs for nuclide release
- Sensitivity analyses.

3.5.1 Distribution of Nuclide Releases

Using the RIP model, 1,000 realizations of the stochastic input parameters are generated and the nuclide releases at the end of a 10,000-year period for each realization are computed. The 10,000-year release has been computed -

- At the edge of the EBS
- At the end of the unsaturated flow zone, i.e., at the water table
- At the accessible environment.

Figure 3-5 presents conditional CCDFs for aqueous releases from the EBS, from the unsaturated zone, and to the accessible environment, as calculated by RIP for the particular case of $\lambda = 0.1$ m^{-1} (RUN 3.1). The plot shows the probability of exceeding a given release in terms of the EPA sum.

The cross-hatched area in Figure 3-5 indicates regions where the EPA limit is exceeded; however, it applies only to releases to the accessible environment (the normalized releases from the EBS and from the unsaturated zone are not actually EPA sums because they do not represent releases to the accessible environment). Also, note that the EPA sums shown in Figure 3-5 are really *partial* EPA sums because they include only aqueous releases and not releases by other mechanisms, such as gaseous releases or other scenarios.

The figure indicates that the calculated aqueous releases to the accessible environment are approximately two orders of magnitude below the EPA limit. The releases to the water table are well below those from the EBS, indicating that the unsaturated zone provides an important barrier to the release of radionuclides. As indicated on the plot, however, the saturated zone adds little additional impediment to the radionuclides. Although matrix diffusion and radionuclide retardation are just as operable in the saturated zone, the ground-water travel time for the present

saturated-zone model is only about 1200 years and the unretarded radionuclides are transported relatively quickly through the saturated zone to the accessible environment.

Figure 3-6 shows the releases to the accessible environment, normalizing the EPA limits as contributed by ^{99}Tc and ^{129}I and the total release for the case $\lambda = 0.1$ m^{-1}. It may be noted that these nuclides are unretarded through the saturated and unsaturated zones and provide the bulk of the cumulative release over the 10,000-year time period of interest.

It may be recalled that, in the present application of RIP, the important transport parameter, the Poisson transition rate, λ, has been kept constant across all the 1000 realizations generated for deriving the CCDF. The CCDF result presented earlier corresponds to the case of $\lambda = 0.1$ m^{-1}, which happens to be the closest to the TSPA-1991 analysis. To determine the sensitivity of the results to this parameter, CCDF computations have been repeated for several other values of λ: 10^{-8}, 10^{-3}, 10^{-2}, 10^{-1}, 1, 10 m^{-1}. Figure 3-7 shows the results for two values of λ, 0.01 and 0.1 m^{-1}, which bound the CCDF from the TSPA-1991 analysis. It can be seen that the $\lambda = 0.1$ m^{-1} case is closer to the CCDF derived by the TSPA-1991 analysis. Figure 3-8 presents CCDFs for the EPA sum for all the λ values cited above and the CCDF for the TSPA-1991 analysis. The releases increase with decreasing λ, as expected and in agreement with the definition of λ. It may be recalled that λ is a measure of the interaction between the matrix and the fracture, with smaller λs denoting less interaction. Thus, smaller λs generate more fracture transport leading to higher releases. It is interesting to note that, for all λ less than 10^{-3} m^{-1}, the CCDFs are insensitive to the λ chosen.

Although the above results indicate that it is possible to reproduce the TSPA-1991 results with a properly chosen matrix-fracture transition rate (λ) in RIP, there is little physical basis for how one should choose an appropriate value of λ. In order to test the importance of λ in comparison to the simulated numerical results generated with TOSPAC, we conducted a number of single column "tests." These results (presented in Appendix C) indicate that using the two-mode approximation of fracture-matrix flow and transport in RIP overpredicts the mass breakthrough in comparison to TOSPAC (or TRACR3D). While fracture-matrix flow is important in layers 1, 2, and 4, layers 3 and 5 are predominantly matrix flow for virtually all realizations. As a result, we conducted additional "tests" treating these matrix-dominated flow layers as one-mode flow and transport media in RIP. This produced much better breakthrough curves (in comparison to the dispersion-dominated breakthrough predicted in the numerical models; see Appendix C). In order to test the significance of this on the CCDF, we conducted a simulation with layers 3 and 5 treated as equivalent porous media for all six unsaturated zone columns. (Note: layer 5 does not exist in columns 5 and 6.) The results of this simulation are presented in Figure 3-9. These results match the TSPA-1991 results very well.

While it is possible to compare CCDFs to determine qualitatively how well RIP is able to reproduce the results presented in TSPA-1991 (Barnard et al., 1992), it is also useful to compare other measures of performance. Figures 3-10a through 3-10e display time history plots of radionuclide releases to the accessible environment for ^{99}Tc, ^{120}I, ^{237}Np, ^{234}U, and ^{79}Se, respectively. For the case $\lambda = 0.1$ m^{-1}, these plots can be compared with Figure 4-45 of Barnard et al. (1992), reproduced here as Figure 3-11. While our plots are linear-linear rather than the log-log plots presented in TSPA-1991, it is apparent that, in general, the RIP peaks occur a little

earlier than those in TSPA-1991, and are either slightly higher or slightly lower than the maximum release rate determined in TSPA-1991.

3.5.2 Sensitivity Studies

The RIP model has been used to perform sensitivity studies. For this purpose, all the parameters are kept at their expected values, except for the parameter whose sensitivity is studied. For that parameter, the stochastic description using its probability density function is retained. Two hundred realizations of the sensitivity parameter are generated and simulated. Since only one parameter varies across the realizations, a scatter-plot of the 10,000-year EPA sum and the chosen parameter provides an understanding of the sensitivity.

The chosen parameters of sensitivity are:

- Infiltration rate
- Matrix hydraulic conductivity in layer 3
- Poisson transition rate (λ).

Figure 3-12 shows the scatter plot of infiltration flux versus cumulative release. The EPA sum is directly related to the infiltration rate. The EPA sum would increase continuously with infiltration. For comparison, Figure 3-13 illustrates the sensitivity of cumulative release to the infiltration flux when all parameters are sampled. There is clearly a very high correlation between infiltration and release in both cases.

Figure 3.14 shows the sensitivity of the release to the matrix hydraulic conductivity in layer 3. If the matrix hydraulic conductivity is greater than the infiltration rate, no flow occurs in the fractures. Since the expected infiltration rate is 1 mm/year, matrix hydraulic conductivities equal to or greater than 1 mm/year cause the fractures to be dry. In these cases, the total release depends on the travel time through the matrix and does not change for values of hydraulic conductivity greater than 1 mm/year (all other parameters constant). This aspect becomes evident in the scatter plot, shown in Figure 3-14. Furthermore, when the matrix conductivity is lower than 1 mm/year, the infiltration goes partly through fractures, and thus greater releases are seen at the accessible environment. A greater proportion of the infiltrating water goes into fractures as the matrix conductivity is reduced progressively below 1 mm/year, resulting in larger releases at the accessible environment.

Figure 3-15 presents the scatter plot of the EPA sum versus the Poisson transition rate. The range of λ is from 0.01 to 0.1, the limits between which the CCDF of the TSPA-1991 analysis remains bounded. As expected, the EPA sum decreases for increasing λ. If λ was chosen over a wider range, it would have shown that, for values of λ smaller than a particular value, λ_{min}, the EPA sum would remain constant. Similarly, when λ is increased beyond a particular value λ_{max}, the nuclide releases would reach a small value and would then remain invariant with a further increase in λ.

3.5.3 Additional Sensitivity to Infiltration Flux

The net flux at the potential repository is one of many uncertain parameters. A range of values has been developed, generally with 1 mm/yr as the expected value. Additional simulations were conducted to determine the effect of using different infiltration distributions. The four distributions used in these additional simulations are listed in Table 3.11.

The infiltration distributions are presented graphically in Figures 3-16a to 3-16e. Figure 3-16d shows the distribution when sampled 1000 times, rather than the theoretical results. These distributions were applied to the case $\lambda = 0.1\ m^{-1}$.

When evaluated at the edge of the waste package domain, the different infiltration distributions had no discernible effect on release. This reflects the fact that the high solubility, alteration-limited radionuclides, ^{99}Tc and ^{129}I, control the release from the EBS. However, at the accessible environment, the differences are quite pronounced. The results for the four simulations using different infiltration distributions are presented in Figures 3-17a to 3-17d. Note that the results for the beta distribution (RUN 3.1) are presented in Figure 3-5.

When compared with the CCDF for the release (Figure 3-5) corresponding to the beta distribution for infiltration (RUN 3.1), run 3.2 produces greater release; RUN 3.3 produces even greater release; RUN 3.4 produces greater release than RUN 3.1 but less than RUN 3.2; and RUN 3.5 produces the greatest release. These differences can be explained by reviewing the infiltration distributions. The uniform infiltration distribution has a higher probability for exceeding higher infiltration values than does the log-uniform distribution. The log normal infiltration distribution has a greater probability for low infiltration values and a lower probability for high infiltration values than the beta distribution and the log-uniform distribution. The distribution for RUN 3.5 is higher than the other distributions, with 64 percent probability that the values will be greater than or equal to 5.0 mm/yr. The sensitivity to the infiltration flux distribution shape and range is as expected, given the high correlation between flux and release exhibited in the sensitivity analyses (Figures 3-12 and 3-13).

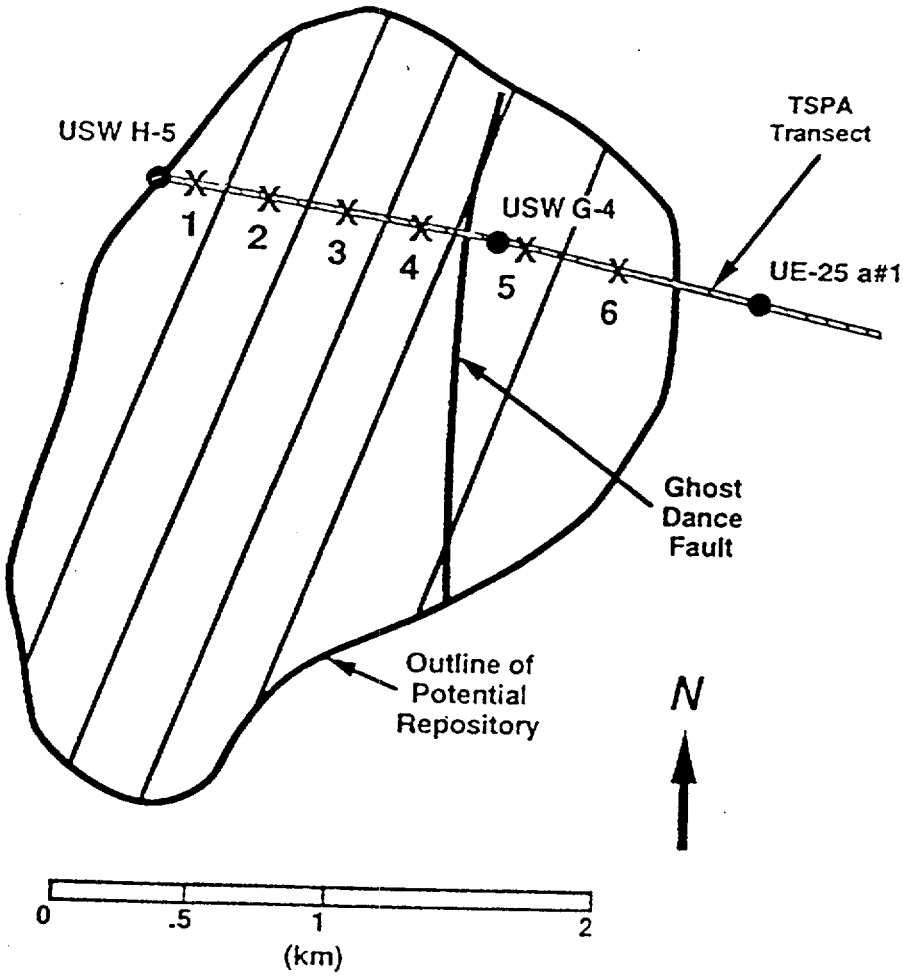

Figure 3-1. Map of the Boundary of Potential Repository at Yucca Mountain (taken from Barnard et al., 1992)

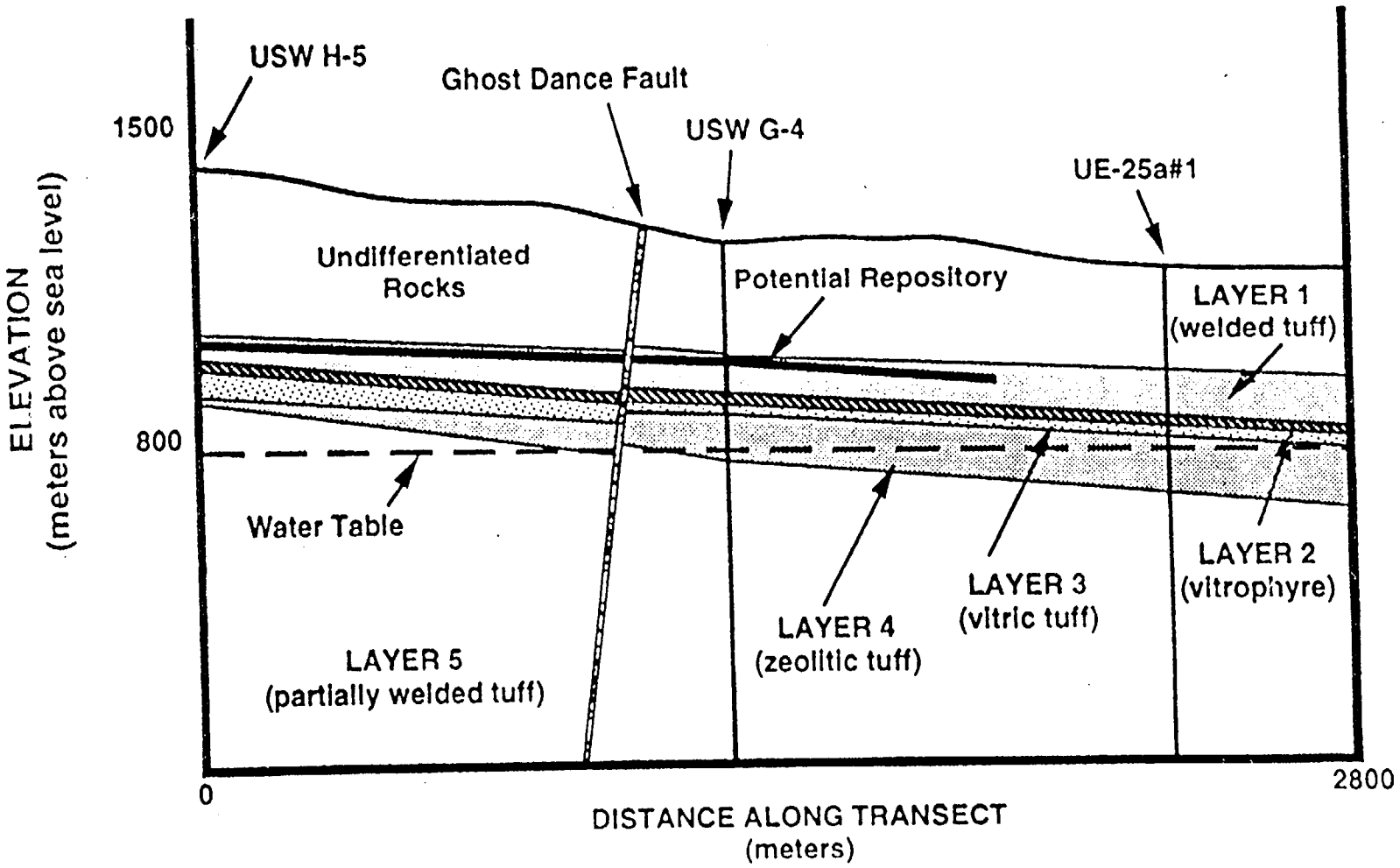

Figure 3-2. Schematic Cross-Section of Unsaturated-Zone Stratigraphy (taken from Barnard et al., 1992)

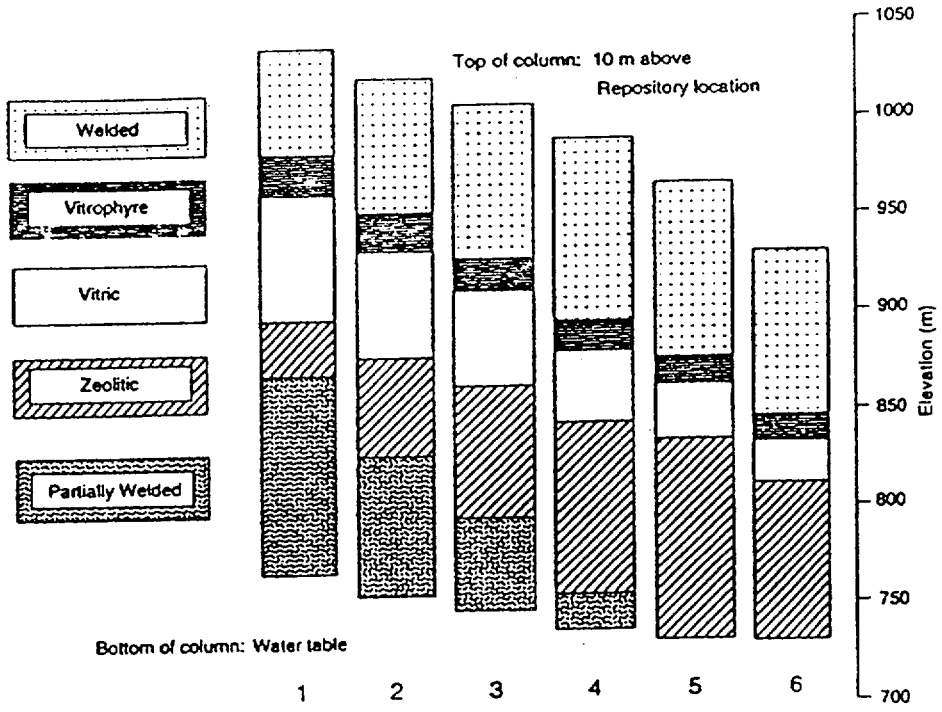

Figure 3-3. Stratigraphies of the Six Vertical Columns Used for the Simulation of Unsaturated Flow (taken from Barnard et al., 1992)

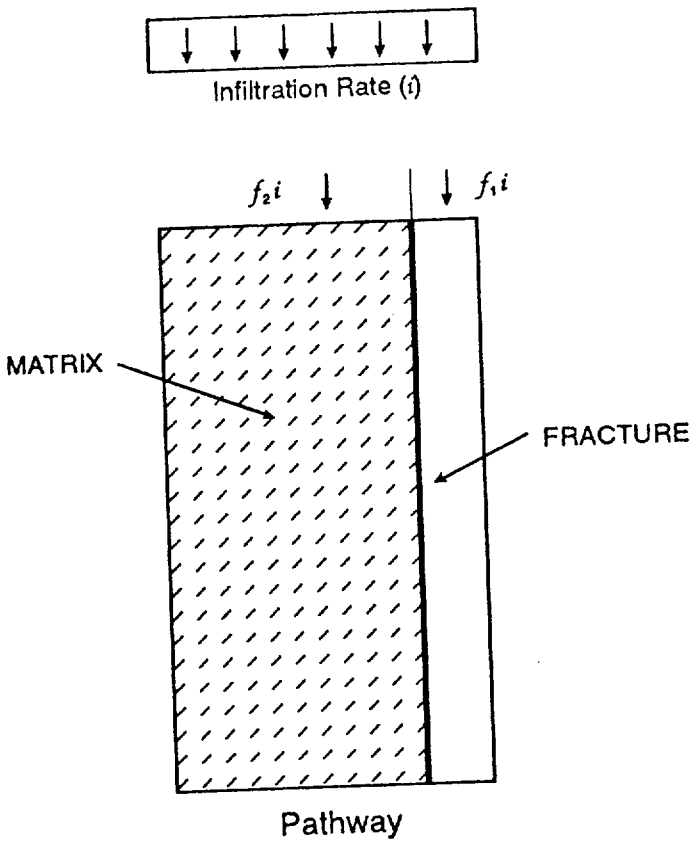

$$f_1 = \text{Max}\left(0, \frac{i - K_m}{i}\right)$$

$$f_2 = 1 - f_1$$

K_m = Saturated Hydraulic Conductivity of Matrix

Figure 3-4. Apportionment of a Flow Rate to Matrix and Fractures: A Conceptualization

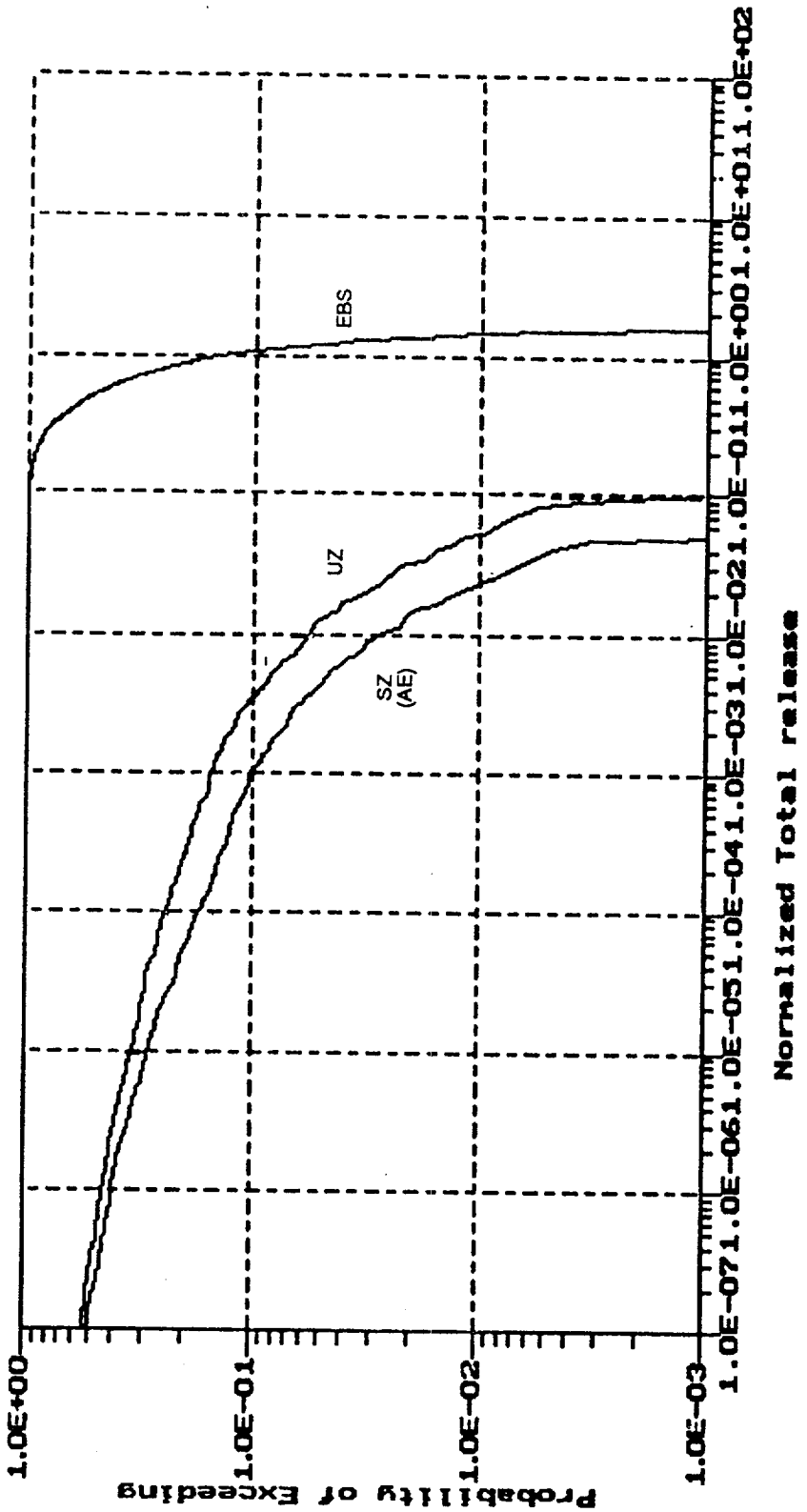

Figure 3-5. CCDFs for Nuclide Releases (EPA Sum) for the Case $\lambda = 0.1 m^{-1}$

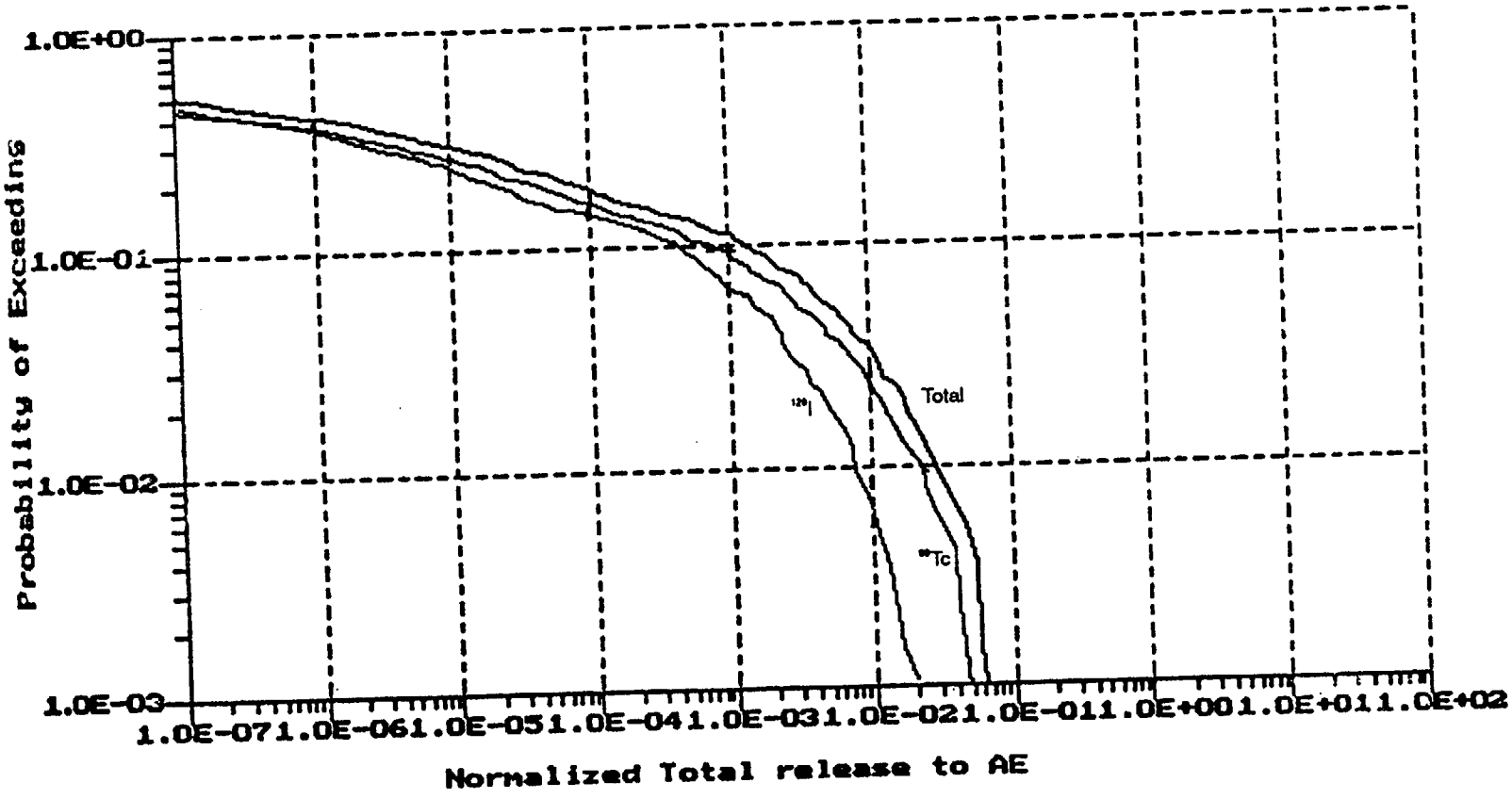

Figure 3-6. CCDFs for EPA Sum and Ratios for ^{99}Tc and ^{129}I for the Case $\lambda = 0.1\ m^{-1}$

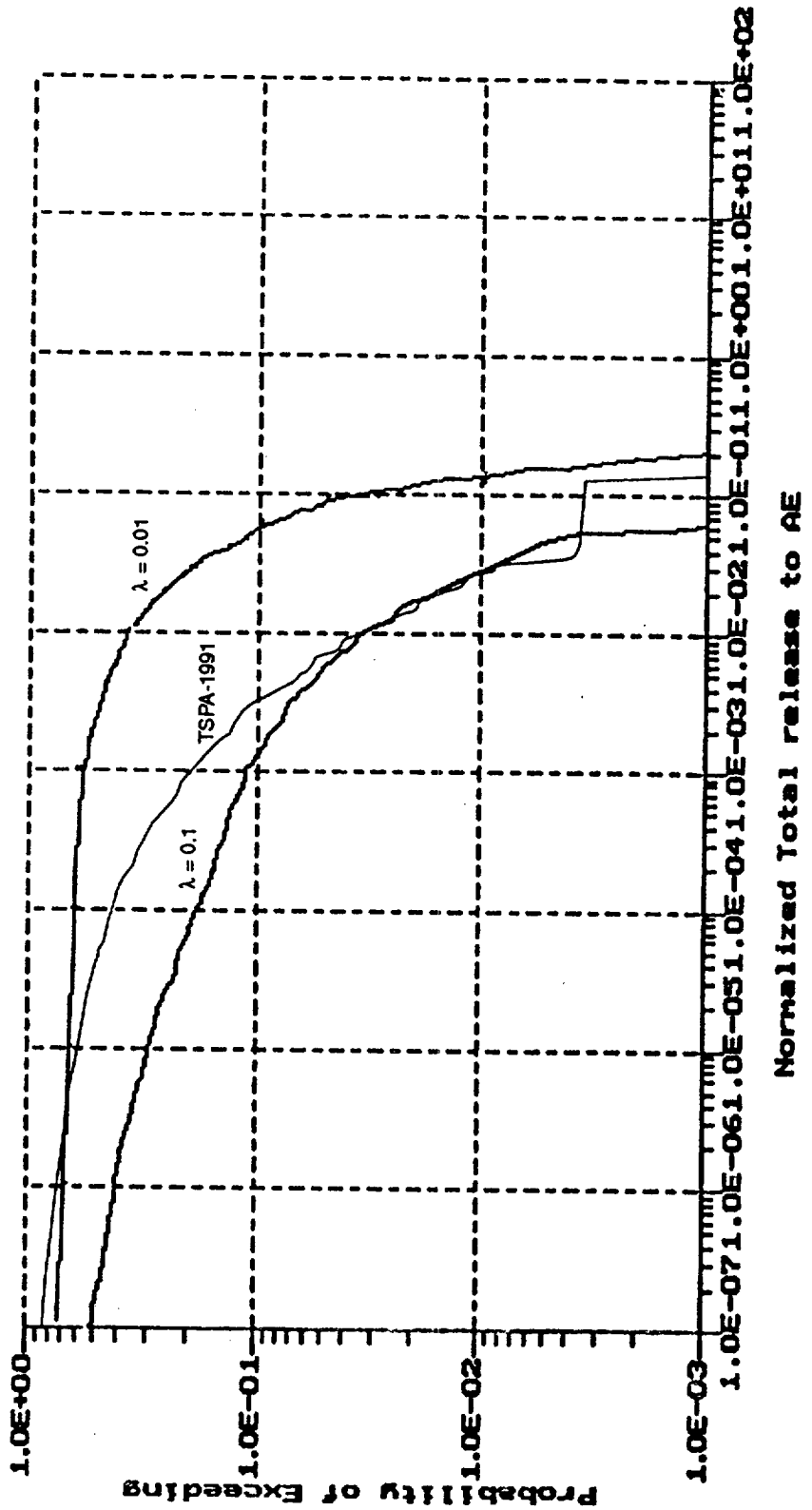

Figure 3-7. CCDFs for EPA Sum λ = 0.1, 0.01 m^{-1}, and from TSPA-1991

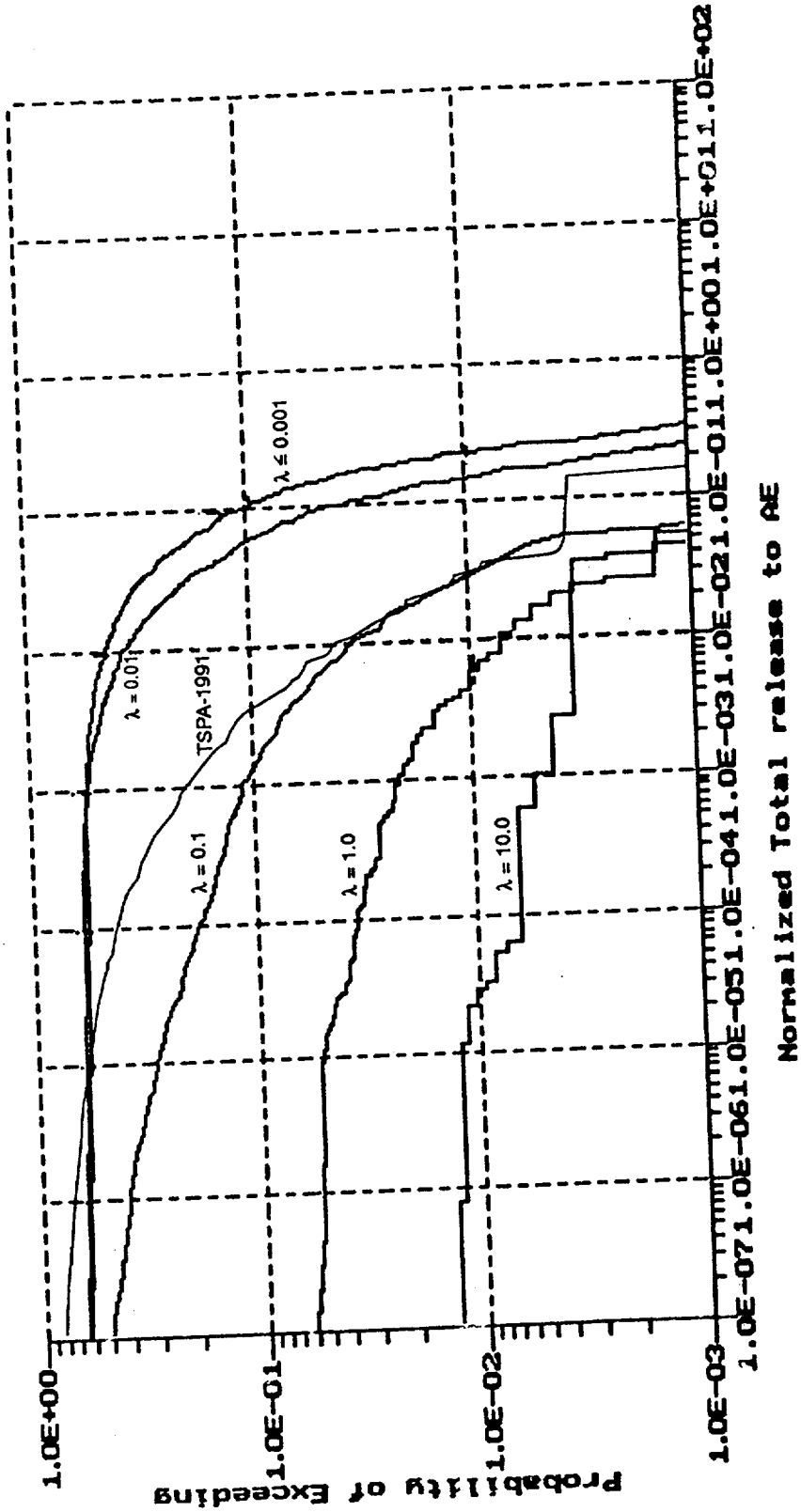

Figure 3-8. Sensitivity of CCDFs for EPA Sum to Poisson Transition Rate

Figure 3-9. CCDFs for the EPA Sum: Layers 3 and 5 Th[illegible]d as Single Mode Media in RIP (λ = 0.1 m^{-1} for other la[illegible]

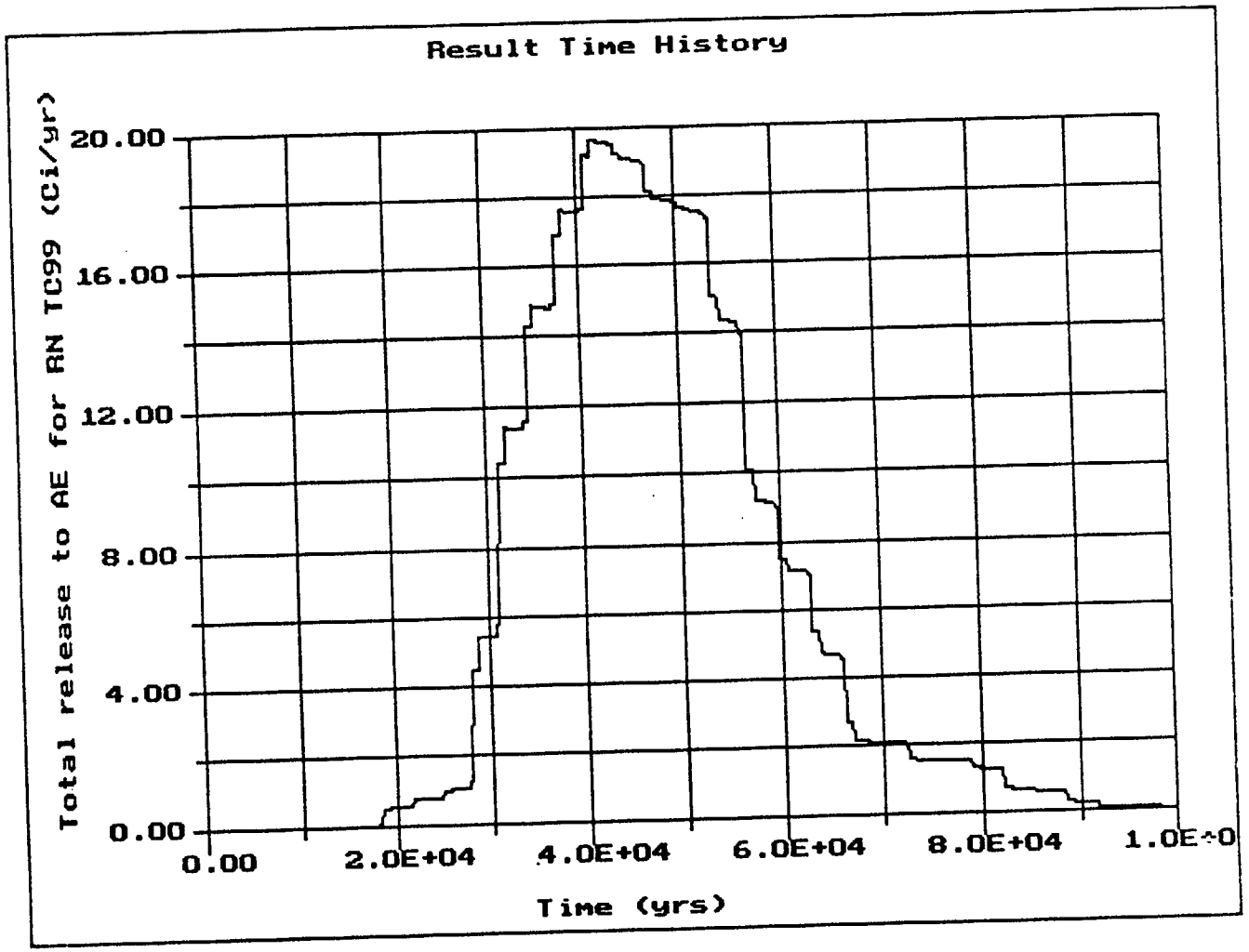

Figure 3-10a. Time History of Release Rate to Accessible Environment for ^{99}Tc

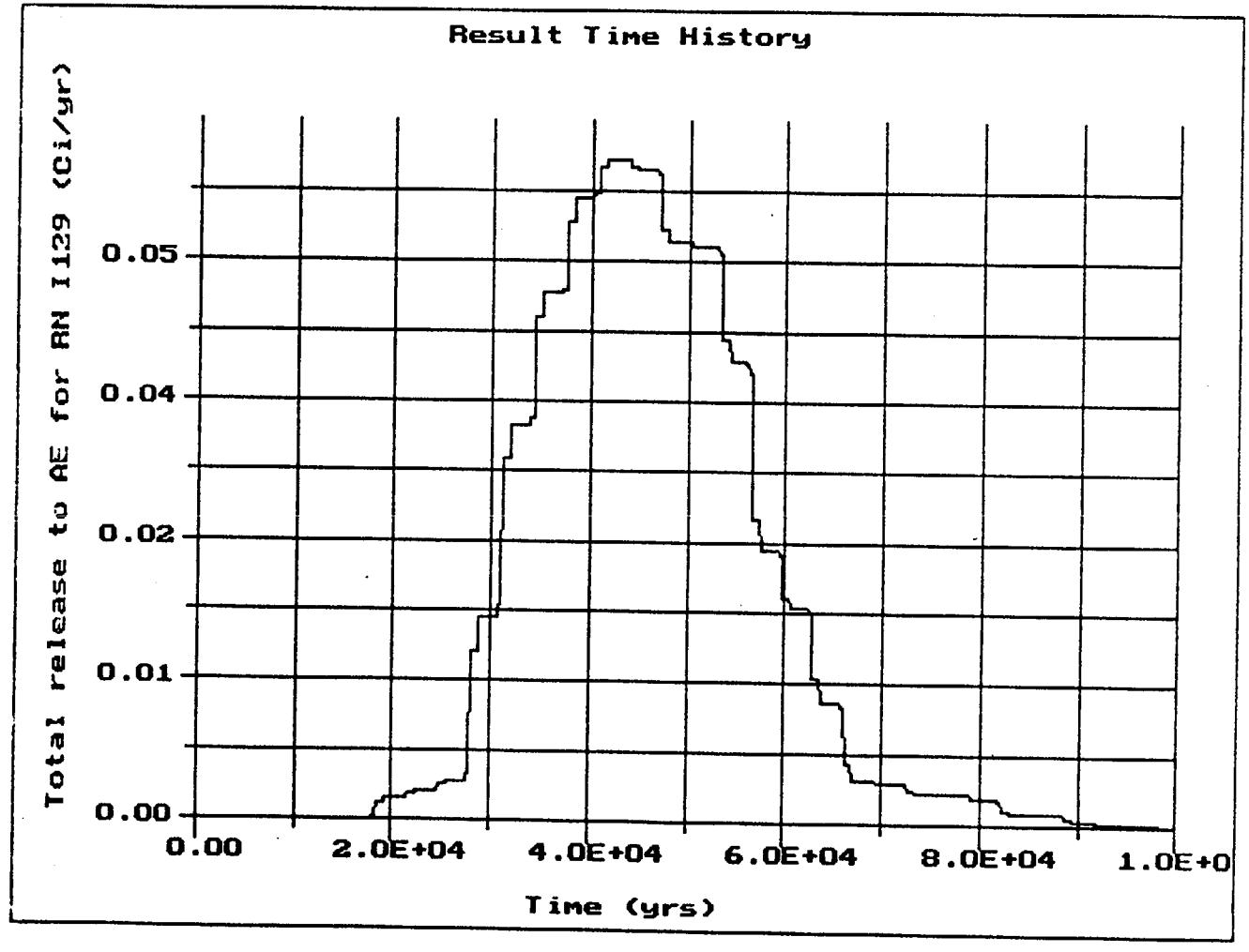

Figure 3-10b. Time History of Rele... Rate to Accessible Environment for ^{129}I

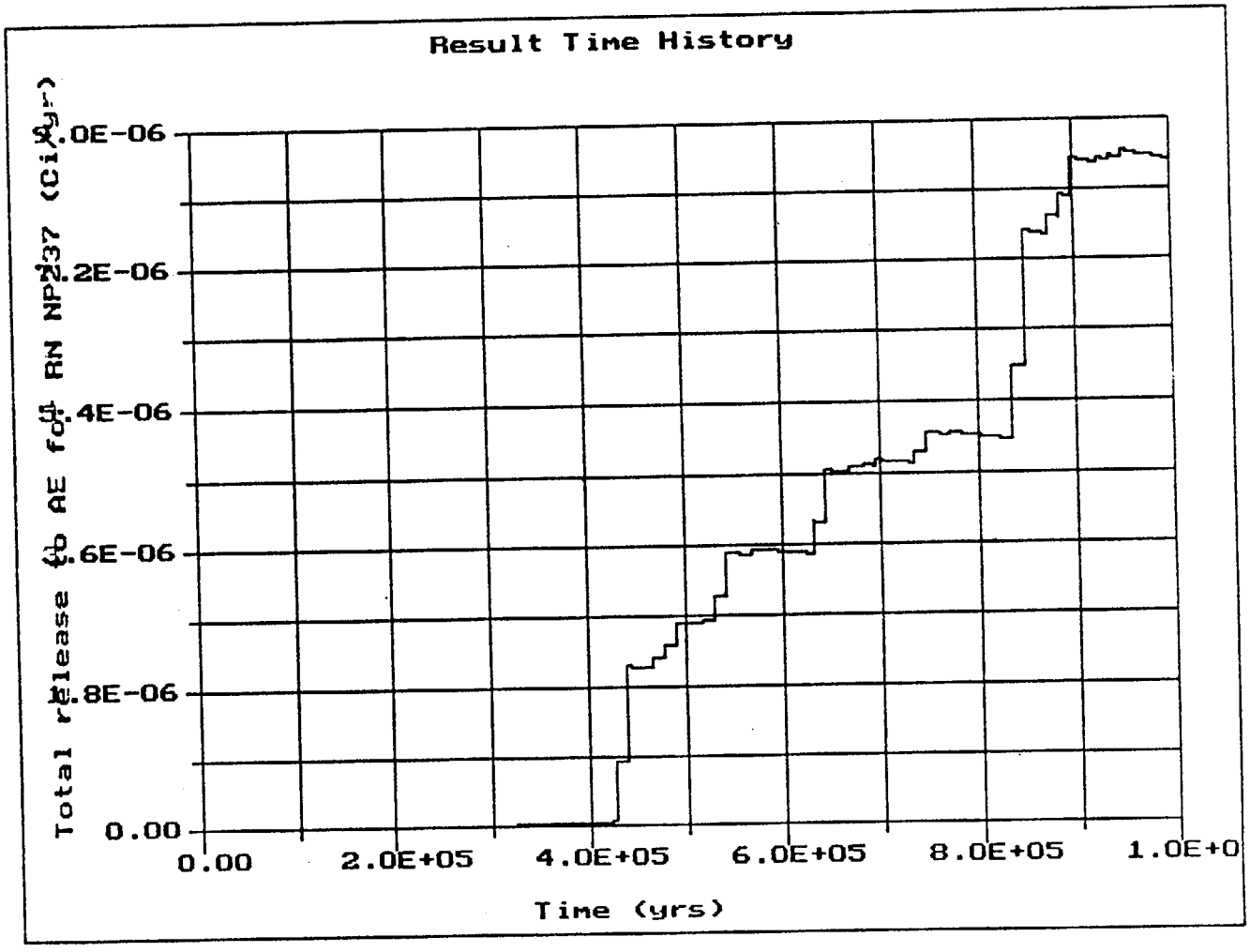

Figure 3-10c. Time History of Release Rate to Accessible Environment for ^{237}Np

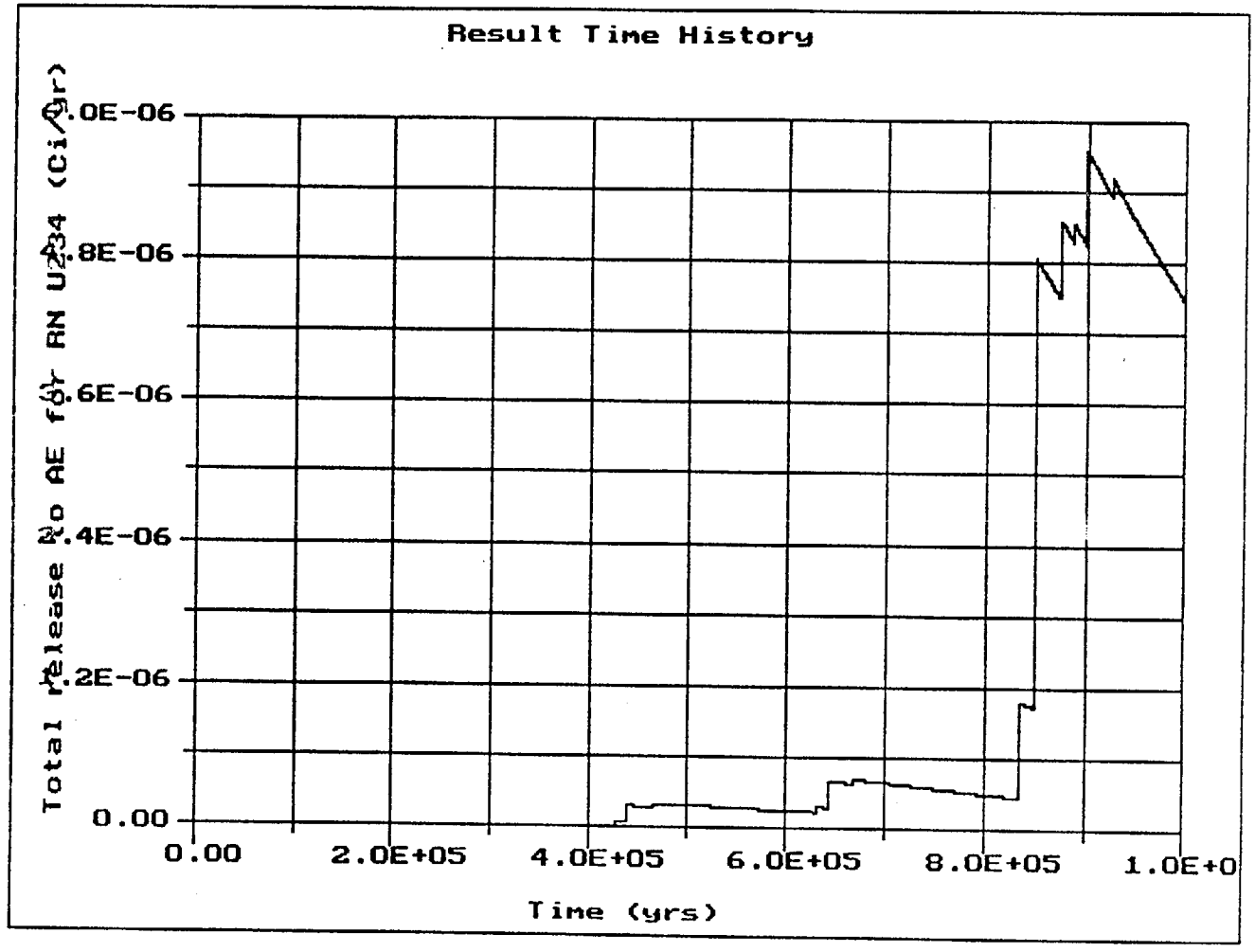

Figure 3-10d. Time History of Release Rate to Accessible Environment for ^{234}U

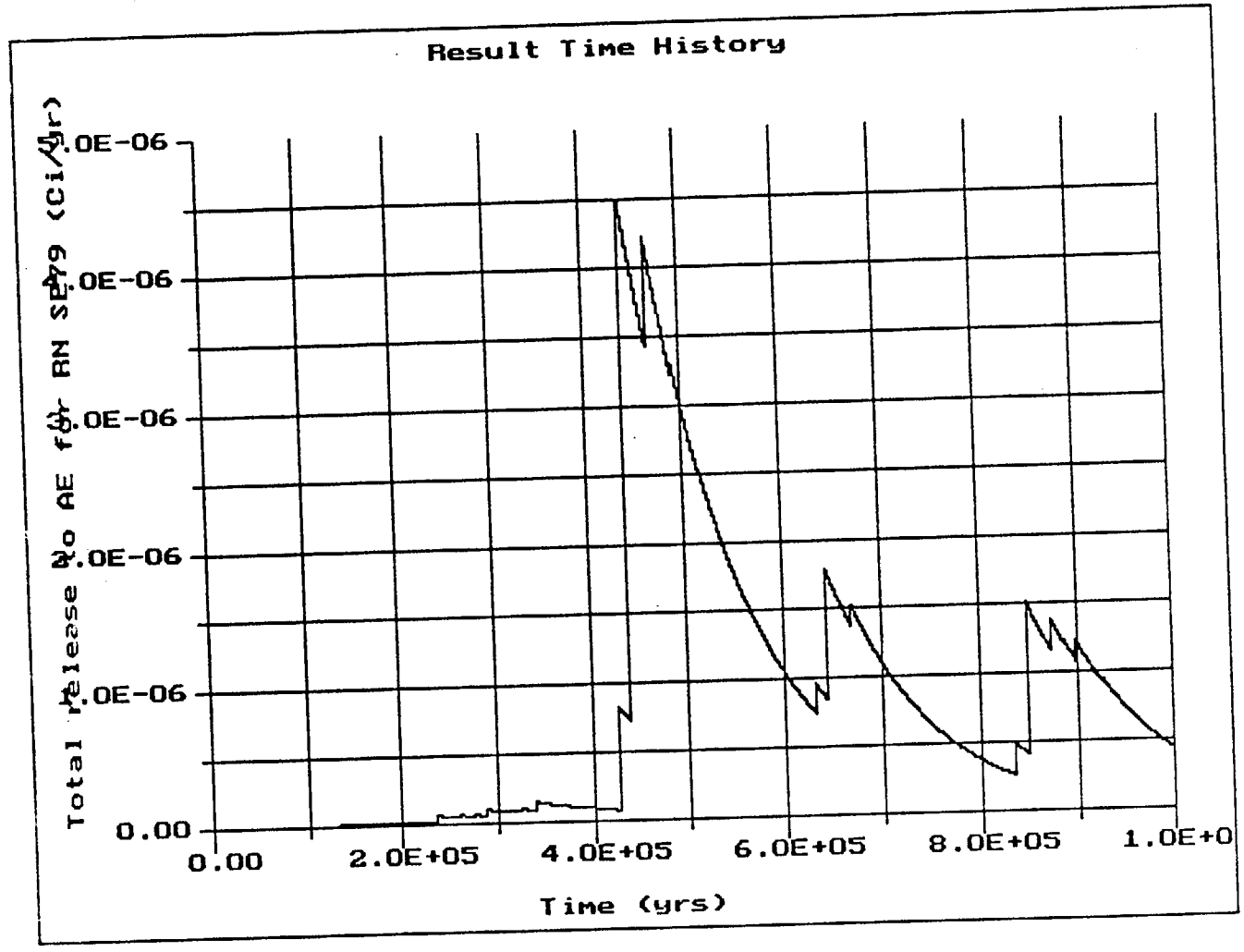

Figure 3-10e. Time History of Release Rate to Accessible Environment for ^{79}Se

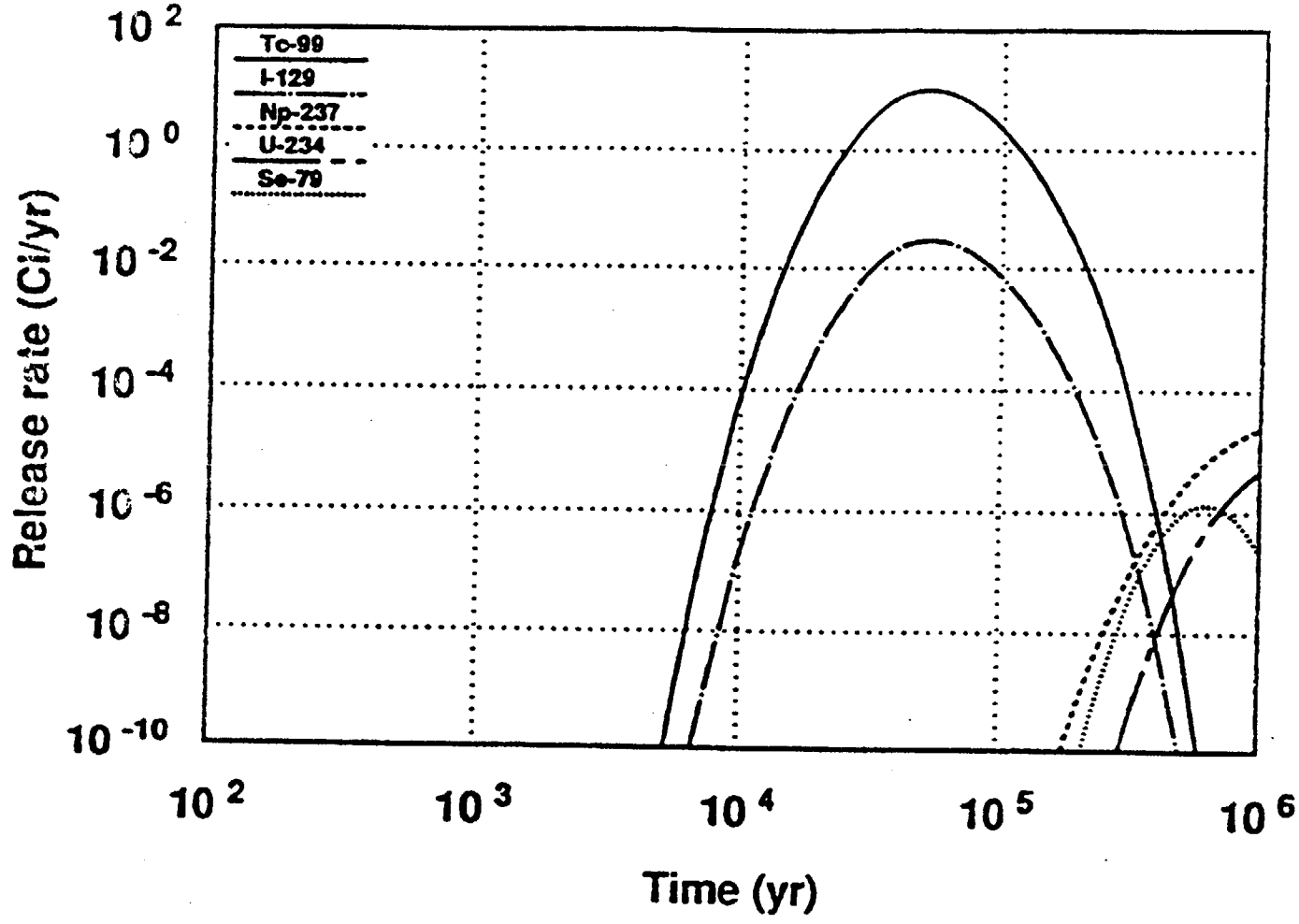

Figure 3-11. Release Rates to Accessible Environment for Radionuclides Released Using Composite Porosity Flow Model (taken from Barnard et al., 1992)

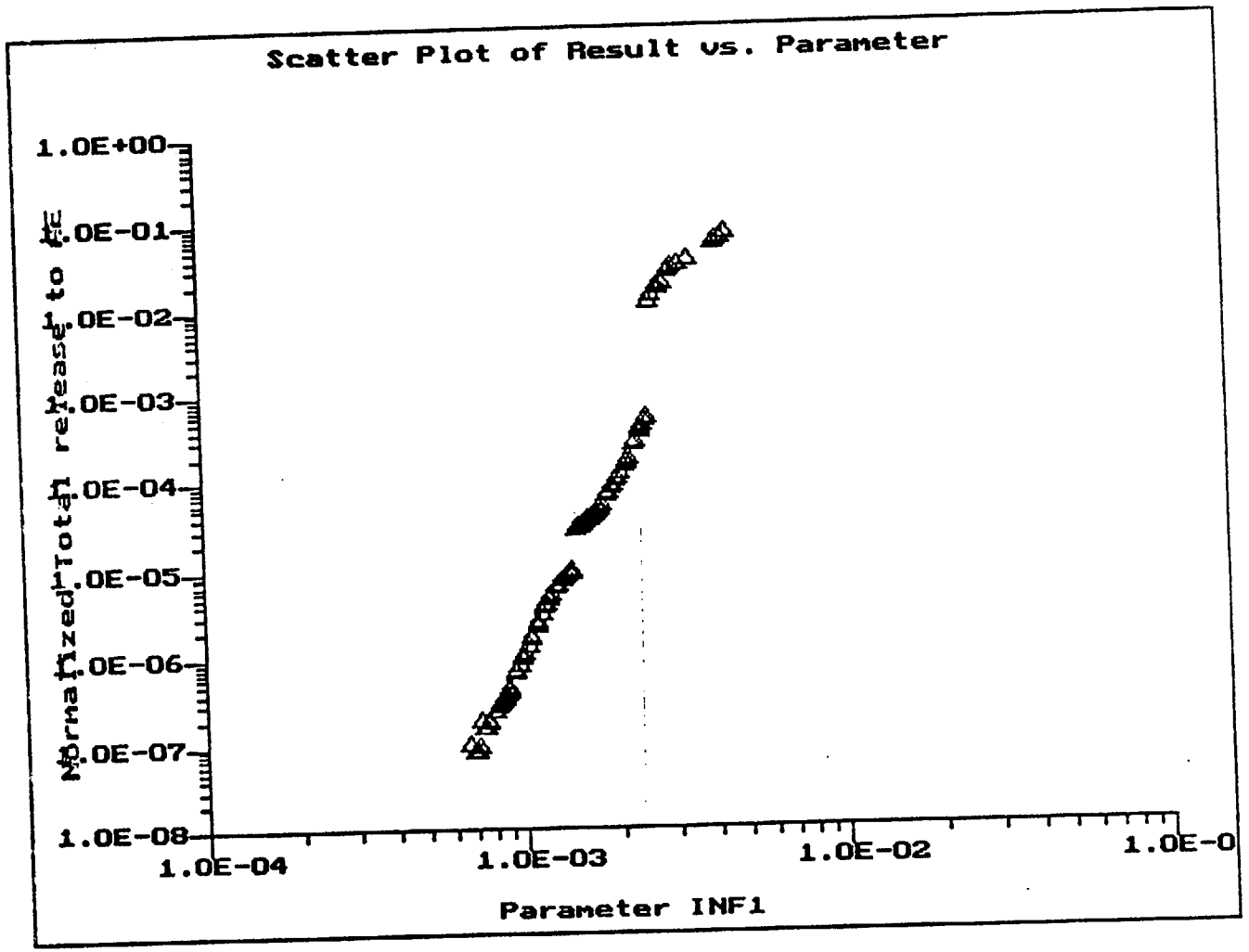

Figure 3-12. Scatter Plot of EPA Sum versus Infiltration Rate (all other parameters at mean value)

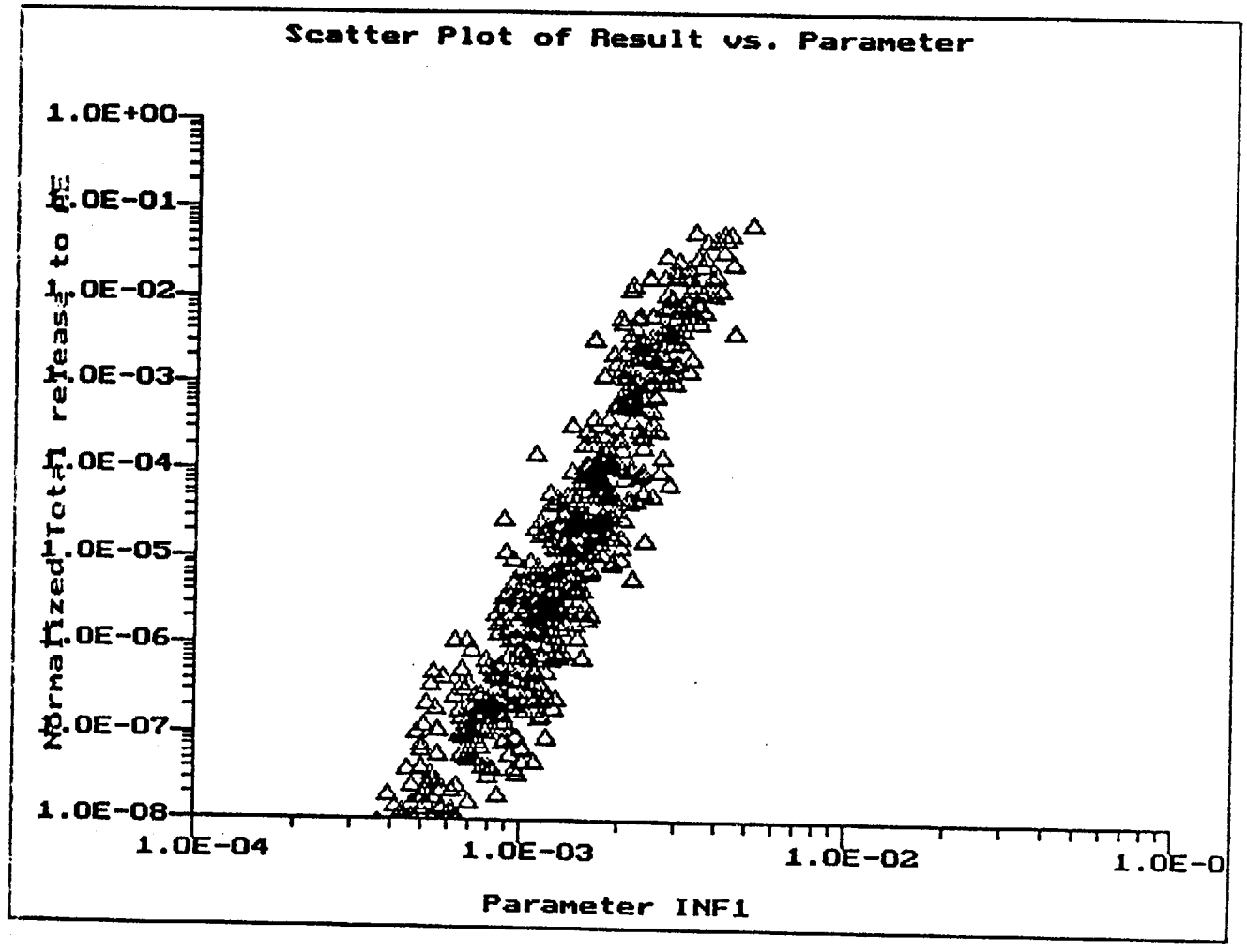

Figure 3-13. Scatter Plot of EPA Sum v[illegible] Infiltration Rate (all parameters are sampled)

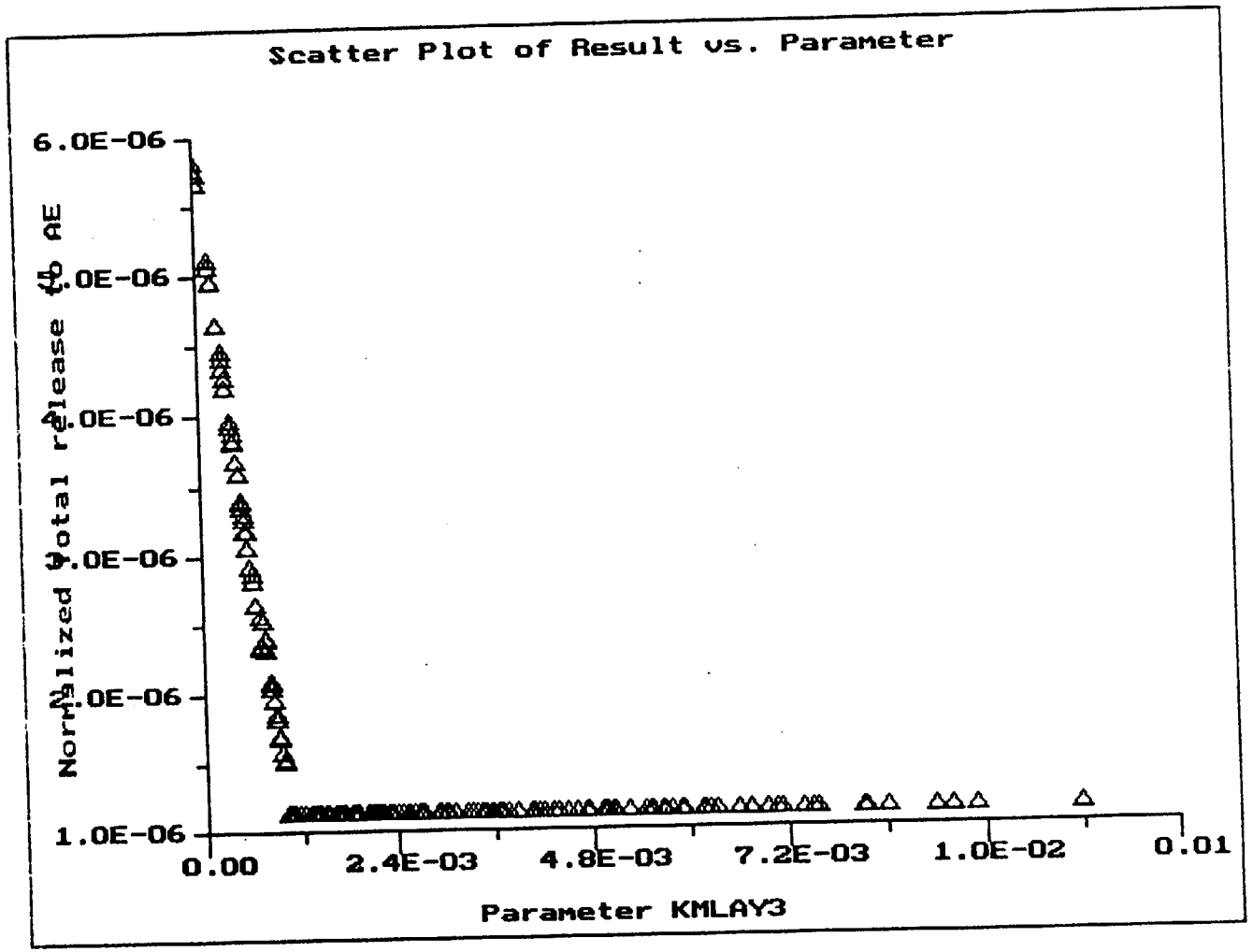

Figure 3-14. Scatter Plot of EPA Sum versus Matrix Hydraulic Conductivity of Layer 3

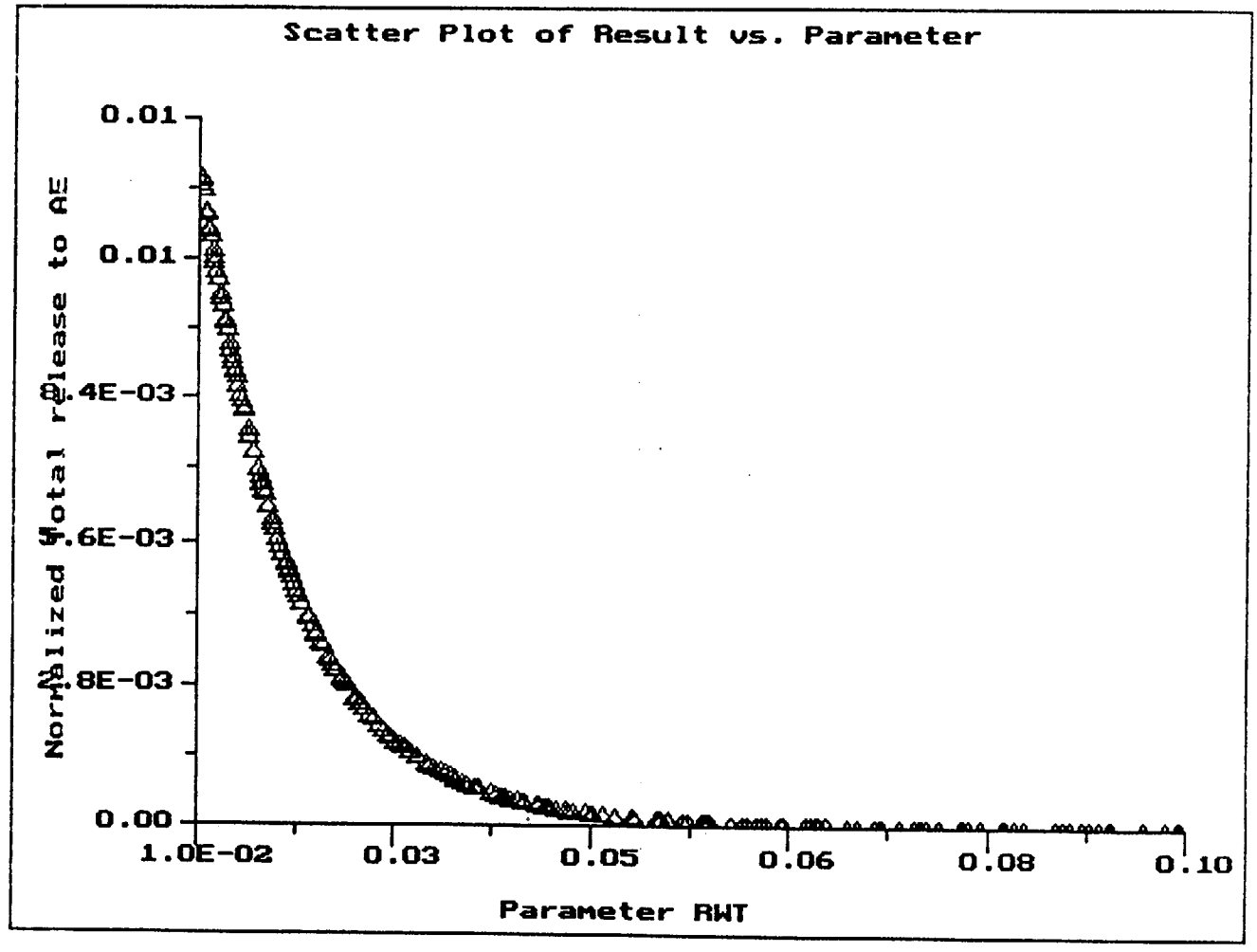

Figure 3-15. Scatter Plot of EP. Sum versus Poisson Transition Rate

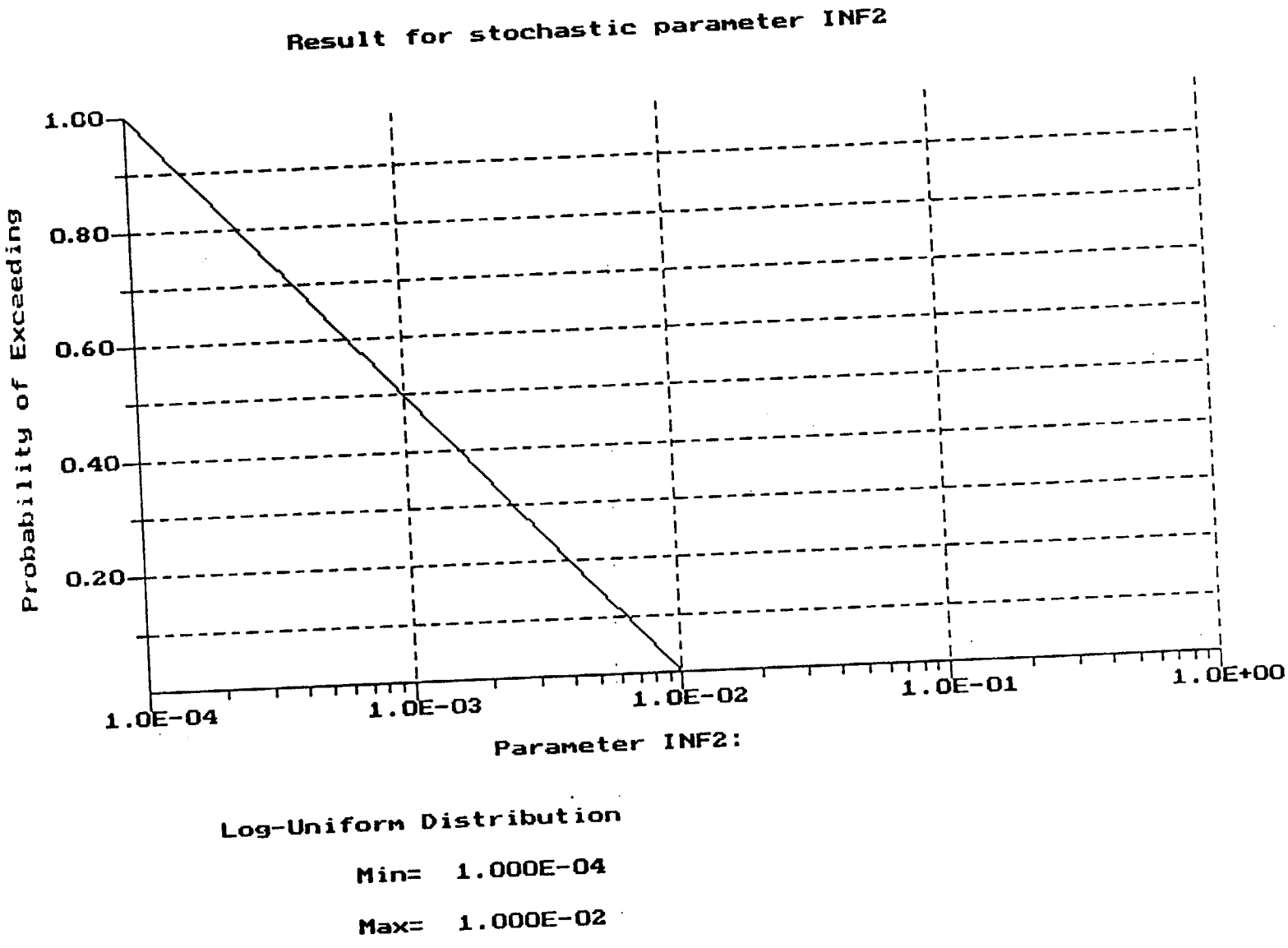

Figure 3-16a. CCDF for Infiltration — Run 3.2

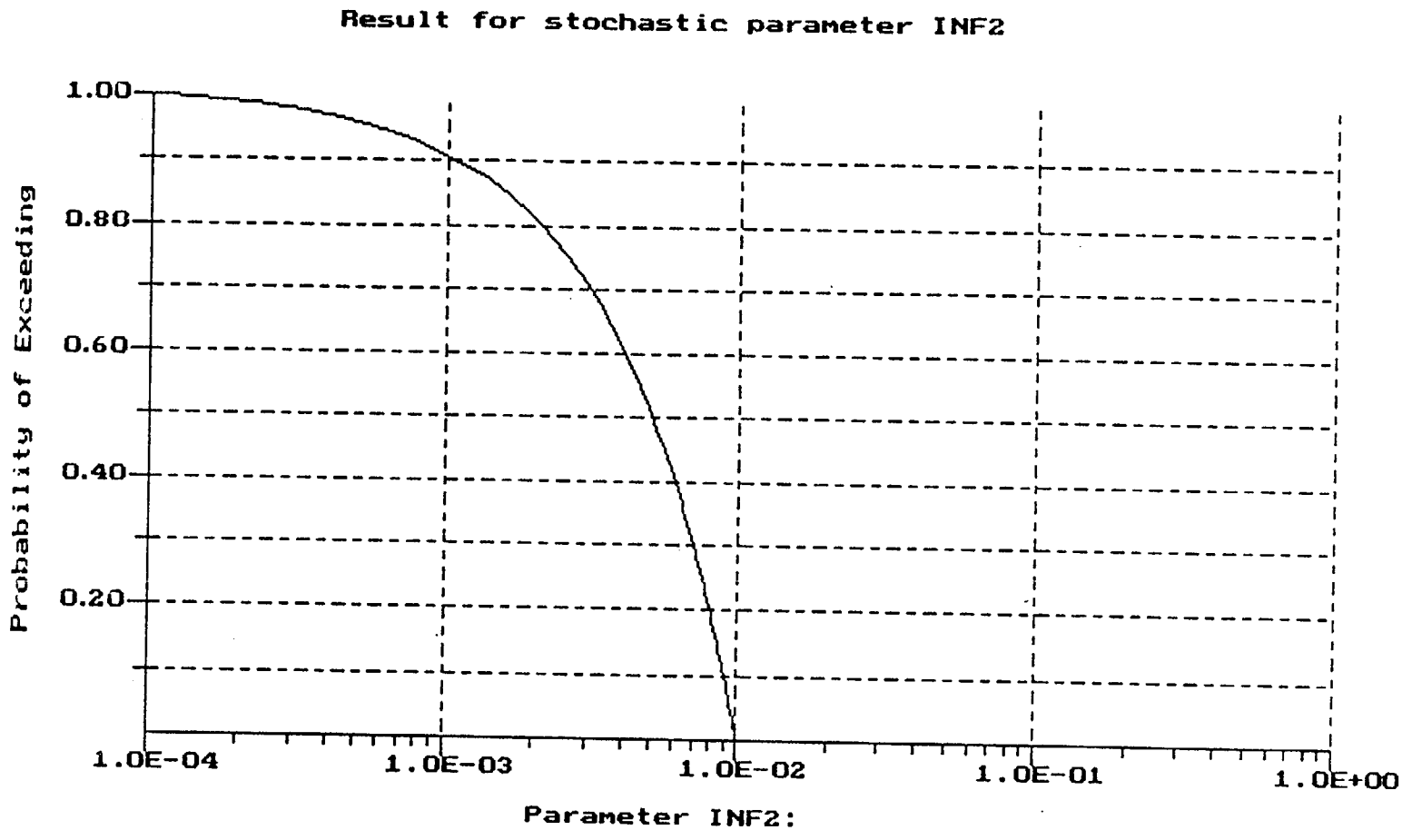

Figure 3-16b. CCDF for Infiltration — Run 3.3

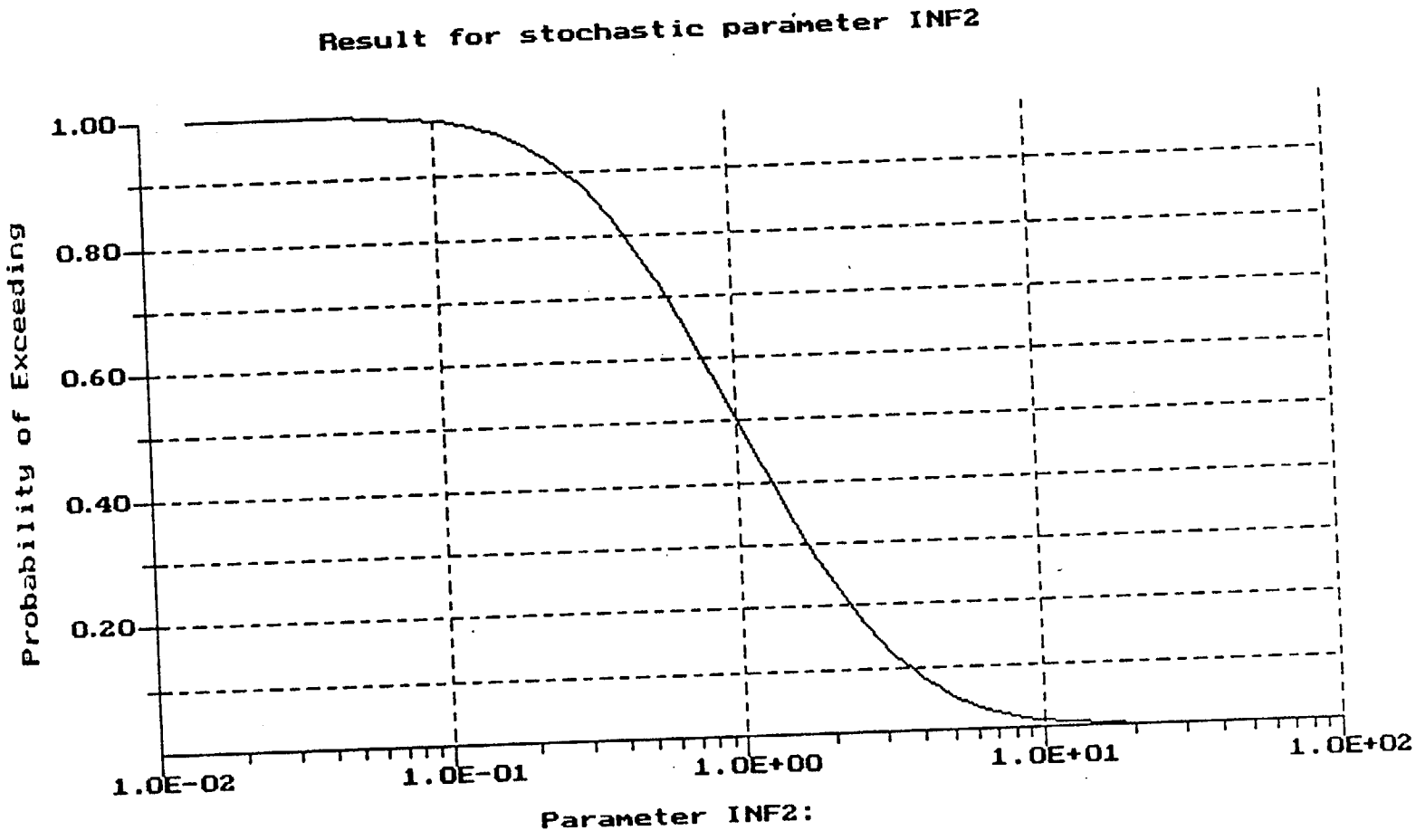

Figure 3-16c. CCDF for Infiltration — Run 3.4

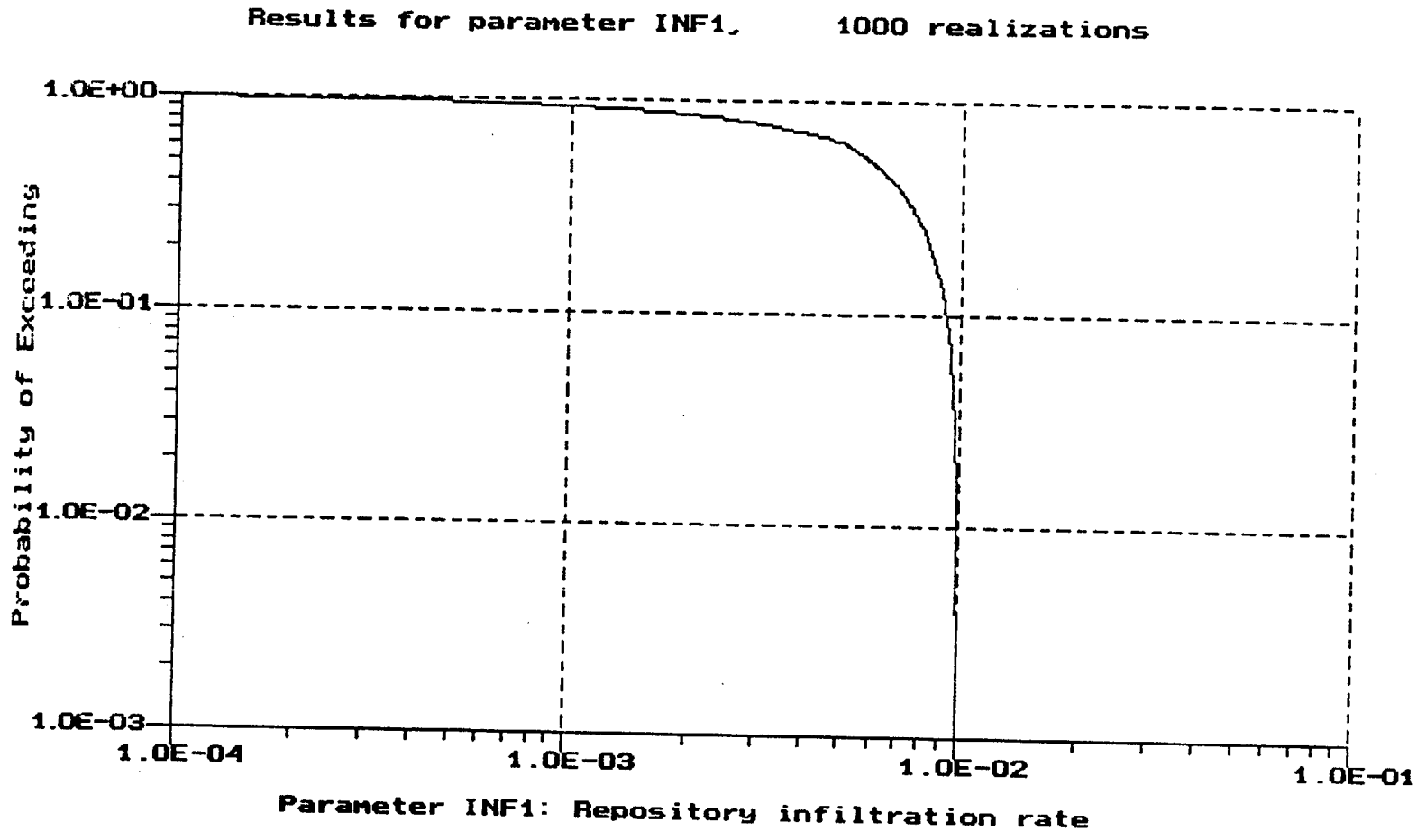

Distribution of Results

Mean= 5.701E-03

S.D.= 2.803E-03

Kurtosis= 2.021E+00

Skewness= -3.669E-01

Figure 3-16d. CCDF for Infiltration — Run 3.5

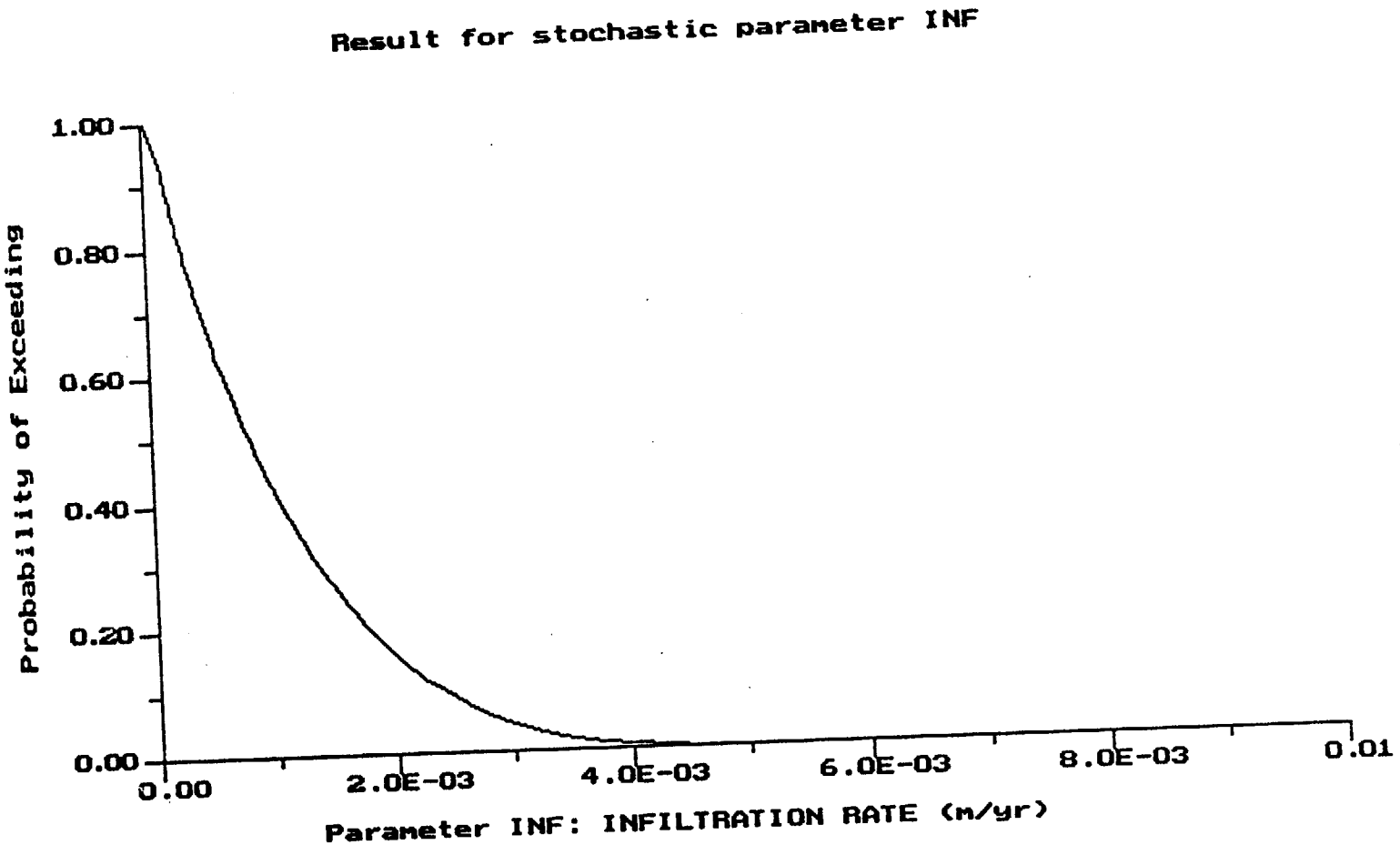

Figure 16e. CCDF for Infiltration — Run 3.1

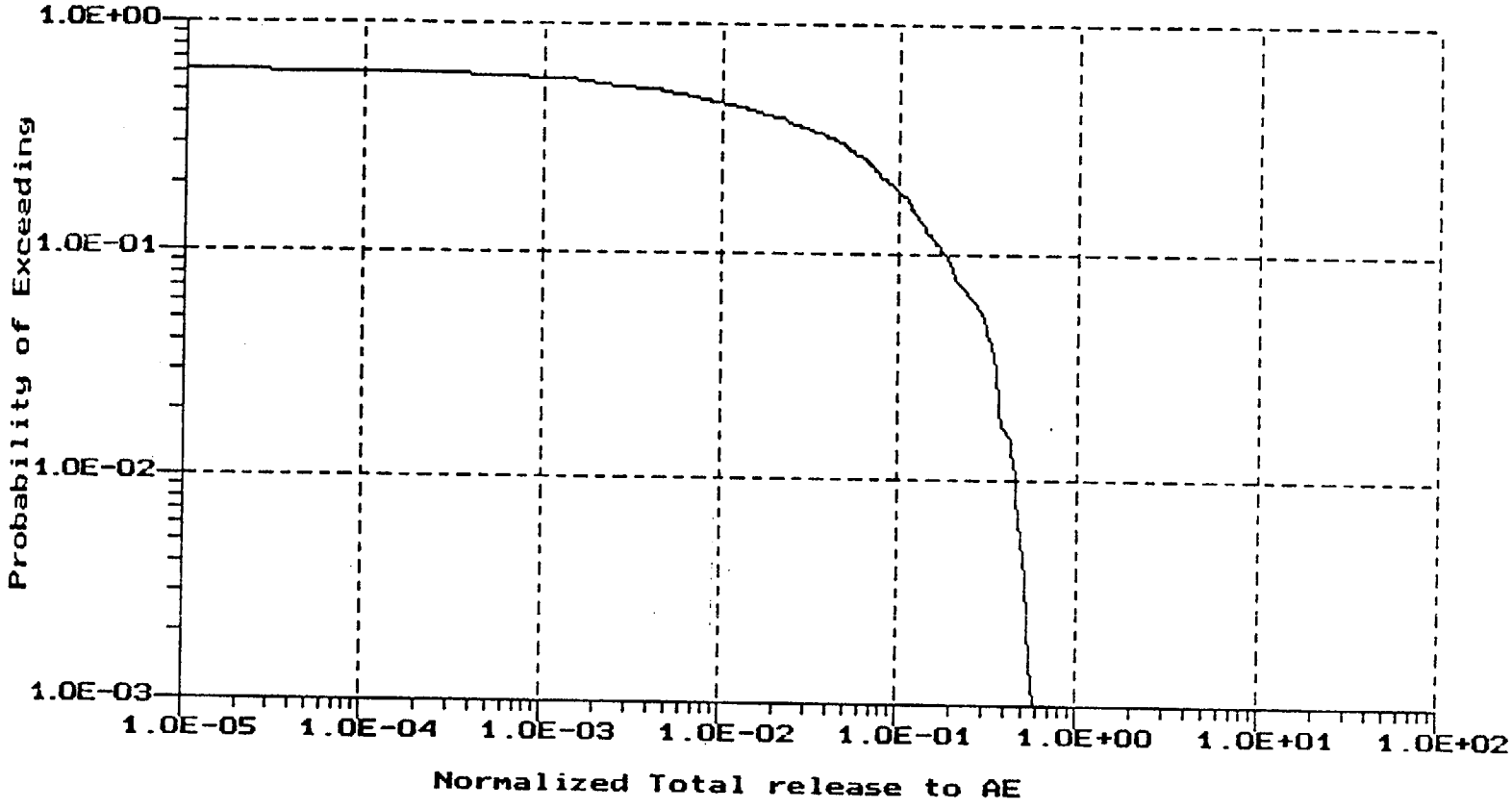

Distribution of Results

Mean= 5.484E-02

S.D.= 9.855E-02

Kurtosis= 9.324E+00

Skewness= 2.474E+00

Figure 3-17a. CCDF for EPA Sum — Run 3.2

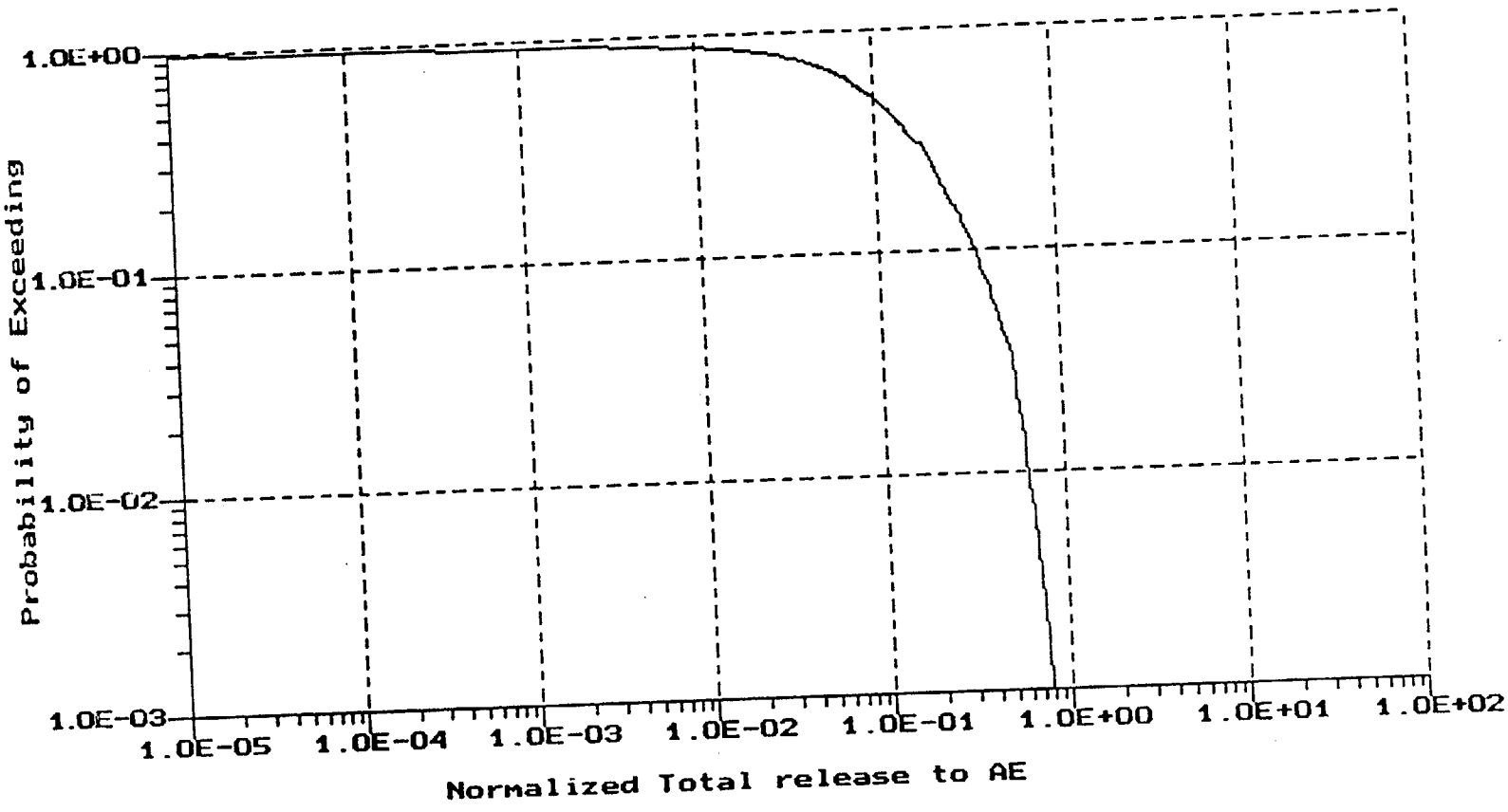

Figure 3-17b. CCDF for EPA Sum — Run 3.3

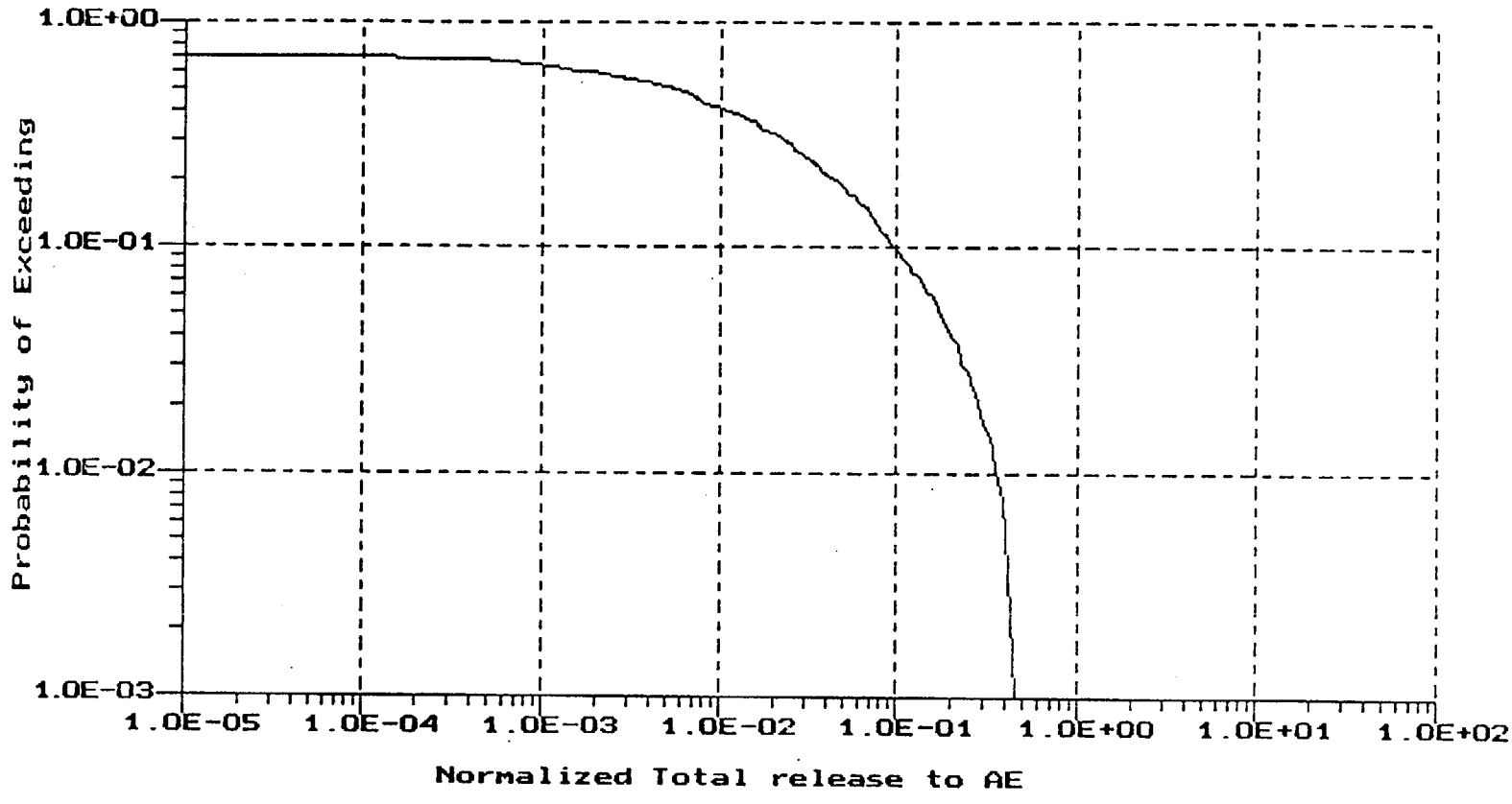

Distribution of Results

Mean= 3.333E-02

S.D.= 6.818E-02

Kurtosis= 1.518E+01

Skewness= 3.304E+00

Figure 3-17c. CCL ..or EPA Sum — Run 3.4

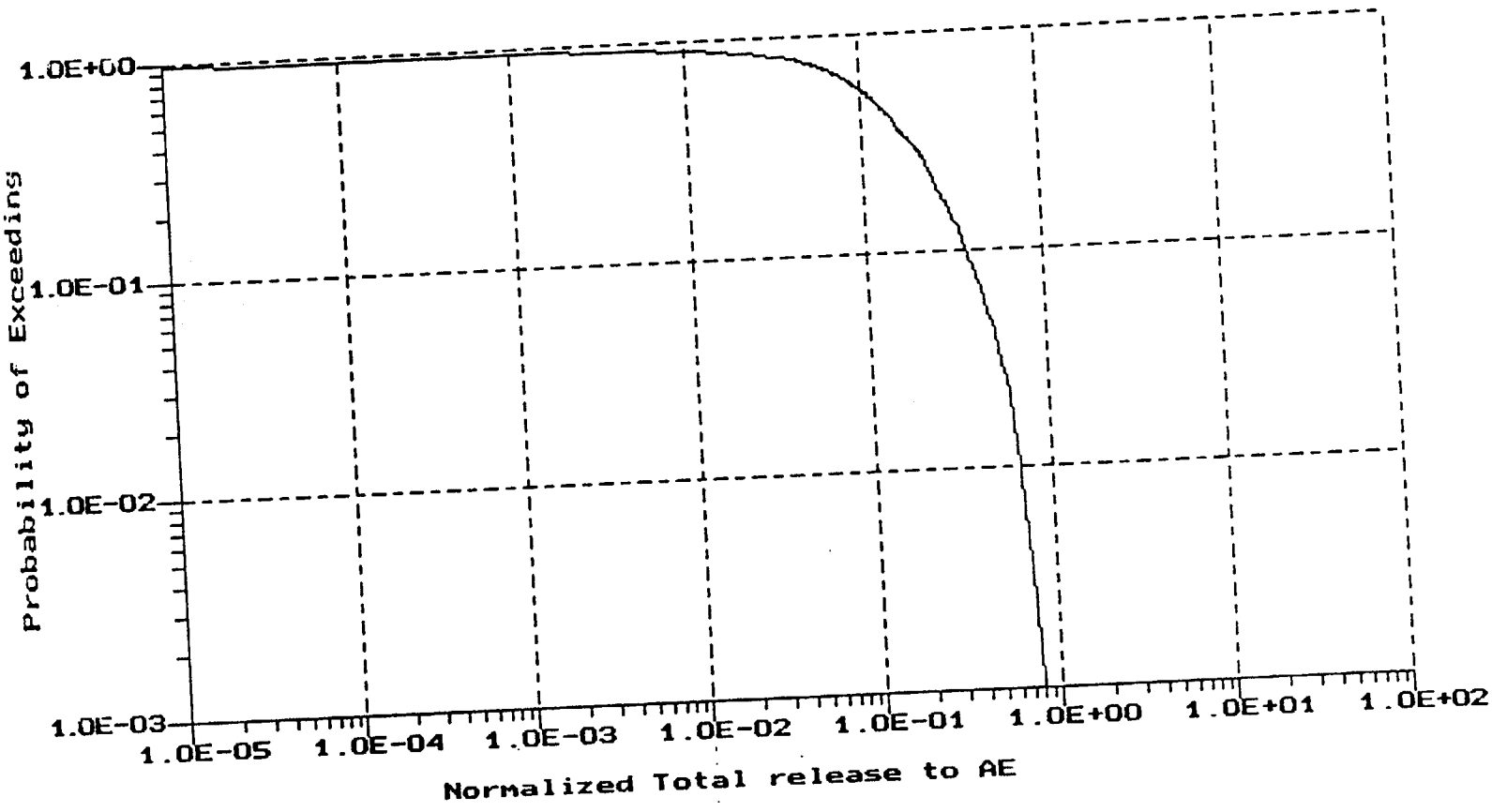

Distribution of Results

Mean= 1.613E-01

S.D.= 1.497E-01

Kurtosis= 5.022E+00

Skewness= 1.438E+00

Figure 3-17d. CCDF for EPA Sum — Run 3.5

Table 3-1. Hydrostratigraphy Used for Unsaturated-Zone Aqueous Problems (after Barnard et al., 1992)

Layer	Dominant Lithology
1	Moderately welded
2	Vitrophyre
3	Vitric, non- to partially welded
4	Zeolitic, non- to partially welded
5	Partially to moderately welded

Table 3-2. Elevations of Layers at Selected Locations in Geohydrologic Problem Domain (after Barnard et al., 1992)

Layer No. or Feature	Lithology	USW H-5 (m)*	West Boundary of Ghost Dance Fault (m)*	USW G-4 (m)*	UE-25 a#1 (m)*	500 m East of UE-25 a#1 (m)*
Surface		1478	1309	1270	1199	1175
Repository		1030	966	956	(870)	(831)
1	Welded tuff	996	875	869	811	781
2	Vitrophyre	974	863	860	798	771
3	Vitric tuff	905	832	836	784	759
4	Zeolitic tuff	885	734	723	637	596
5	Partially welded tuff/ water table boundary	770	731	731	729	730

* Elevation above sea level of the feature, or in the case of an individual layer, to the base of that layer. (Values in parentheses are projections.)

Table 3-3. Elevations[1] Used for the Composite-Porosity Model of the UZ (after Barnard et al., 1992)

Location	Elevation at Top of Layer						
	1	Re.[2]	2	3	4	5	Water Table
USW H-5	1478[3]	1035	996	974	905	885	770
120 m E (Col. 1)	1038[4]	1028	983	962	897	869	766
420 m E (Col. 2)	1021[4]	1011	950	932	877	827	755
660 m E (Col. 3)	1007[4]	997	923	907	861	794	747
940 m E (Col. 4)	990[4]	980	893	879	843	756	737
1099 m E Ghost Dance	1309[3]	971	875	863	832	734	731
1280 m E Ghost Dance	1309[3]	971	889	877	846	748	731
1280 m E (Col. 5)	966[4]	956	877	864	836	--[5]	731
1313 m E USW G-4[6]	1270[3]	961	869	860	836	--[5]	731
1700 m E (Col. 6)	930[4]	920	848	835	813	--[5]	730
UE-25a #1	1199[3]	(875)	811	798	784	--[5]	729

1 In meters
2 The repository is modeled as a 5-meter-thick layer
3 Ground surface
4 Top of simulated column
5 Below the water table
6 Not used in the linear interpolation

Table 3-4. Matrix Hydraulic Conductivity Distributions Used in TSPA-1991 and RIP (after Barnard et al., 1992)

Layer	Matrix Hydraulic Conductivity (m/yr): Beta Distribution			
	Mean	Standard Deviation	Minimum	Maximum
1	6.30×10^{-4}	6.10×10^{-4} (6.30×10^{-4})	0	2.50×10^{-2}
2	9.49×10^{-5}	6.00×10^{-5} (9.49×10^{-5})	9.40×10^{-6} (0)	4.00×10^{-3}
3	2.50×10^{-3}	2.30×10^{-3} (2.50×10^{-3})	0	9.78×10^{-2}
4	9.49×10^{-5}	6.00×10^{-5} (9.49×10^{-5})	9.40×10^{-6} (0)	4.00×10^{-3}
5	4.40×10^{-1}	4.30×10^{-1} (4.40×10^{-1})	0	1.71×10^{1}

( ) TSPA-1991 values

Table 3-5. Matrix Porosity Distributions Used in TSPA-1991 and RIP (after Barnard et al., 1992)

Layer	Matrix Porosities: Beta Distribution			
	Mean	Standard Deviation	Minimum	Maximum
1	0.11	0.022	0.044	0.197
2	0.09	0.018	0.037	0.161
3	0.209	0.042	0.001	1.0
4	0.41	0.082	0.001	1.0
5	0.24	0.048	0.001	1.0

Table 3-6. Fracture Porosity Distributions Used in TSPA-1991 and RIP

Layer	Fracture Porosity: Beta Distribution			
	Mean	Standard Deviation	Minimum	Maximum
1	5.94×10^{-3}	5.20×10^{-3} (5.94×10^{-3})	5.00×10^{-4} (0)	0.22 (0.42)
2	7.48×10^{-3}	7.20×10^{-3} (7.48×10^{-3})	1.00×10^{-4} (0)	0.3 (0.528)
3	4.20×10^{-4}	3.90×10^{-4} (4.20×10^{-4})	1.00×10^{-5} (0)	0.019 (0.0298)
4	3.36×10^{-4}	2.90×10^{-6} (3.36×10^{-4})	0 (0)	0.013 (0.024)
5	9.24×10^{-5}	8.00×10^{-5} (9.24×10^{-5})	1.00×10^{-4} (0)	0.038 (0.065)

( ) TSPA-1991 values

Table 3-7. Infiltration Rate Distribution Used in TSPA-1991 and RIP

Infiltration Rate (m/yr): Beta Distribution			
Mean	Standard Deviation	Minimum	Maximum
0.001	0.0009 (0.001)	0	0.039

( ) TSPA-1991 values

Table 3-8. Parameters Used to Model the Saturated Zone in TSPA-1991 and RIP (after Barnard et al., 1992)

Model Parameter	Distribution	Distribution Parameters[1]	Mean Value
Ground-water velocity, v (m/yr)	Beta	3.2, 5.9, 0.84, 2.87	4.07
Bulk porosity, ϕ_b	Beta	0.09, 0.29, 0.738, 1.37	0.175

[1] Parameters for the distribution are min, max, α, and β.

Table 3-9. Geohydrologic Units for Geochemistry in TSPA-1991 and RIP (after Barnard et al., 1992)

Geohydrologic Unit	Rock Type for K_d Definition
Welded	Devitrified
Vitrophyre	Vitric
Vitric	Vitric
Zeolitic	Zeolitic
Partially welded	Devitrified
Tuff saturated zone	Devitrified

Table 3-10. K_d Probability Density Distributions Used in TSPA-1991 and RIP (after Barnard et al., 1992)

Parameter	E[x]	C_v[x]	Min[x]	Max[x]	α	β
Beta Distributions						
K_d*, Cs Devitrified, or Vitric Tuff	50	0.20	20	100	4.25	7.75
K_d, Cs Zeolitic Tuff	2000	0.25	0	6000	9.33	19.67
K_d, Np Devitrified Tuff	2	1.00	0	50	-0.08	21.08
K_d, Np Vitric Tuff	0.5	1.00	0	12.5	-0.08	21.08
K_d, Np Zeolitic Tuff	4	1.00	0	100	-0.08	21.08
K_d, U (or Se) Devitrified Tuff	2.5	0.577	0	5	0.0	0.0
K_d, U (or Se) Vitric Tuff	2	0.577	0	4	0.0	0.0
K_d, U (or Se) Zeolitic Tuff	10	0.30	5	21	0.59722	2.51389
Constant Values						
K_d, C (all rocks)	0					
K_d, Tc (all rocks)	0					
K_d, Sn (all rocks)	100					
K_d, I (all rocks)	0					
K_d, Pu (all rocks)	100					
K_d, Am (all rocks)	100					

K_ds for all entries in table are in ml/g.

α, β are exponents in the Beta probability density function given below

E[x] = expected value

C_v[x] = coefficient of variation

$f(x) = C \cdot (x - a)^{\alpha} (b - x)^{\beta}$ = probability density

C = normalizing constant

a = Min[x]

b = Max[x]

Table 3-11. Additional Infiltration Distributions

Simulation	Type of Distribution	Infiltration (m/yr)	Figure	Reference
Run 3.2	Log-uniform	Range: 0.0001 to 0.01	3016a	--
Run 3.3	Uniform	Range: 0.0001 to 0.01	3-16b	--
Run 3.4	Log-normal	Mean = 0.001 s.d. = 0.00043	3-16c	--
Run 3.5	Discrete	36% probability LU: 0 - 0.005 3-16d 64% probability LU: 0.005 - 0.010	3-16d	NRC-DOE Technical Exchange, December 14, 1992
Run 3.1	Beta	Beta: min: 0.0 max: 0.039 mean: 0.001	3-16e	Barnard et al. (1992)